EFFECT OF EARLY ODORANT EXPOSURE ON THE STRUCTURE AND OUTPUT OF THE GLOMERULUAR MODULE

by

Annie Liu

BA, Northwestern University, 2011

Submitted to the Graduate Faculty of

The School of Medicine in partial fulfillment

of the requirements for the degree of

Doctor of Philosophy

University of Pittsburgh

2017

UNIVERSITY OF PITTSBURGH

School of Medicine

This dissertation was presented

by

Annie Liu

It was defended on

May 30, 2017

and approved by

Marcel Bruchez, Ph.D.

Sandra Kuhlman, Ph.D.

Stephen Meriney, Ph.D.

Katherine Nagel, Ph.D.

Anne-Marie Oswald, Ph.D.

Dissertation Advisor: Nathaniel N. Urban, Ph.D.

EFFECT OF EARLY ODORANT EXPOSURE ON THE STRUCTURE AND OUTPUT OF THE GLOMERULUAR MODULE

Annie Liu, PhD

University of Pittsburgh, 2017

Early sensory experience has the capacity to dramatically shape the final anatomy and function of a sensory circuit. Both sensory deprivation and enrichment have major impacts on the development and maintenance of sensory circuit structure. The olfactory system lacks the stimulus-based topography seen in the visual or auditory sensory systems, a consequence of the high dimensionality of odorant stimuli. However, it possesses a highly stereotyped organization, making it an ideal model system in which to study the processing of sensory stimuli in a systematic and specific manner. Axons from olfactory sensory neurons that express the same odorant receptor converge into glomeruli, spherical structures in the olfactory bulb (OB). Glomeruli and their post-synaptic targets, including principal projection neurons, the mitral and tufted cells, form the basis of the glomerular module, which is the basic odor coding unit of the OB. In this dissertation, we leverage this specific structure to study how early odorant experience changes the composition of a glomerular module and impacts the odor-evoked activity of mitral cells. In Chapter 2, we use an *in vivo* dye labeling technique to examine how prenatal and early postnatal odorant exposure impacts the number of primary projection neurons connected to activated glomeruli. We find that significantly more mitral and tufted cells become associated with activated glomerular modules, suggesting that sensory input plays a major role in modulating OB circuit refinement in early development. In Chapter 3, we investigate how odor-evoked mitral cell activity across the dorsal OB is impacted following the same exposure paradigm used in Chapter 2. Using 2-photon calcium imaging of mitral cell somata, we find that

early odorant exposure increases the number, amplitude, and reliability of excitatory odor-evoked mitral cell responses, potentially due to sensory enrichment during a developmental critical period. Together, these findings demonstrate that early odorant experience dramatically impacts OB anatomy and output, which may have significant implications on odor representation in the OB and olfactory perception. These changes may also influence olfactory-guided behavior, such as odor discrimination and preference.

TABLE OF CONTENTS

LIST OF TABLES

LIST OF FIGURES

PREFACE

The work presented in this dissertation is based on two manuscripts.

Chapter 2 is based on:

Liu A, Savya S, Urban NN. (2016). Early odorant exposure increases the number of mitral and tufted cells associated with a single glomerulus. *Journal of Neuroscience* **36**(46):11646-53. PMID: 27852773.

Chapter 3 is based on:

Liu A, Urban NN. Prenatal and early postnatal food-based odorant exposure heightens mitral cell odor-evoked responses. (submitted).

All of the experiments presented in this thesis were conducted by Annie Liu.

ACKNOWLEDGEMENTS

None of this work would have been possible without many individuals and organizations that have supported me during my training. First, I am sincerely grateful to my advisor, Dr. Nathaniel Urban, whose patience, encouragement, and support have been instrumental in my growth as a scientist. His thoughtfulness and intellectual curiosity are a constant source of inspiration. In addition, thank you to the past and present members of the Urban lab for their help and camaraderie. I would also like to thank my committee, Drs. Marcel Bruchez, Sandra Kuhlman, Anne-Marie Oswald, my committee chair Dr. Stephen Meriney, and my outside examiner, Dr. Katherine Nagel. I greatly appreciate their insight and dedication to my training. Special thanks to Dr. Claire Cheetham, whose humor, encouragement, and technical expertise were immensely helpful in the face of equipment malfunction.

Thank you to the NIDCD for funding throughout my training. In addition, thank you to the CNUP, the MSTP, and the CNBC for providing excellent programmatic support and professional development. Thank you to the Allen Institute and University of Washington for training opportunities in data analysis, which have proven invaluable and broadly applicable. Thank you to Dr. Paula Clemens, my career advisor, and Dr. Richard Steinman, the MSTP director, for their continued guidance. Sincere thank you to my wonderful, supportive family for teaching me resilience and persistence. Finally, thank you to Drs. Camilla and Joshua “JJ”

Sturm, Eric and Dr. Caroline Zimmerman, and Dr. Kaveh Ardalan for bringing so much joy to my life in Pittsburgh.

1.0 INTRODUCTION

Sensory systems transform information about environmental stimuli into meaningful neural representations that can be used by the brain to understand the outside world and help organisms gauge the importance and relevance of experienced stimuli. Organisms must detect sensory cues, extract and combine relevant features, add contextual information, and store experiences in memories – all of which allow them to respond to and interact with the world (Decharms and Zador, 2000). Thus, sensory systems do not function to exactingly describe the external environment through patterns of neural activation, but rather to drive behavior through communicating information about relevant cues (Churchland et al., 1994). Experience modulates these neural representations and contributes directly to the development and maintenance of sensory system circuitry. In this dissertation, we focus on understanding how early sensory experience influences the structure and output of the olfactory bulb (OB), which is responsible for early processing of olfactory stimuli.

We leverage the unique and distributed organization of the OB to examine how experience with specific odorant ligands changes the OB. The visual, somatosensory, and auditory systems are organized topographically, such that the spatial organization of neural activity in these areas mirrors the organization of stimulus space. There are retinotopic maps in the visual system, a cortical homunculus in the somatosensory system, and tonotopic maps in the auditory system. However, there is no clearly identifiable stimulus-based topographic map

within the olfactory system (Belluscio and Katz, 2001; Meister and Bonhoeffer, 2001; Soucy et al., 2009) because the structure of olfactory stimulus space is not easily organized by stimulus type, molecular characteristics, or percept. Despite this, the olfactory system exhibits a high level of stereotypy and specificity, for example in the projections from nose to brain, making it an ideal system in which to study how specific wiring patterns or stimulus-evoked responses change during development and following a perturbation (Buck and Axel, 1991; Belluscio and Katz, 2001). In this thesis, we examine how experience during development shapes the olfactory bulb. Specifically, we investigate how early odorant exposure changes the anatomy and output of the mouse main OB. Our results indicate that the anatomy and output of the olfactory bulb are highly plastic during the prenatal and early postnatal period and subject to dramatic modification following sensory experience.

1.1 OLFACTORY SYSTEM CIRCUITRY

An odorant is an airborne molecule that can bind to an odorant receptor (OR). In the mouse, the basic flow of information in the olfactory system begins in the nasal turbinates, where odorants bind to ORs expressed by olfactory sensory neurons (OSNs) whose cell bodies are located within the olfactory epithelium (OE). Information is relayed from OSNs to the olfactory bulb and from there to cortical areas. At every step of processing, the odorant representation is transformed by local circuits and long-ranging connections originating from cortical or mid-brain structures (Boyd et al., 2012; Markopoulos et al., 2012; Padmanabhan et al., 2016). In this thesis, we focus on the representation of odorants at the level of the OB; thus, the following sections describe general OB structure.

1.1.1 Nose to bulb

Odorant molecules contact and bind to ORs expressed on the cell bodies and cilia of mature OSNs within the OE, a mucosal layer that lines the nasal cavity (Menco, 1984; Falk et al., 2015). OSNs are bipolar cells whose cell somata are found within the center zone of the OE; these cells extend a single ciliated dendrite along the superficial mucosa and an unbranched axon that targets the glomerular layer of the olfactory bulb (OB) (Menco, 1984). The ends of each OSN dendrite forms a ciliated olfactory knob – each OSN has 10-30 immotile cilia which express ORs (Falk et al., 2015). OSNs are continually replaced throughout both development and adulthood through the maturation of globose basal cells located near the basal lamina of the OE, with sensory experience contributing to the rate of turnover (Caggiano et al., 1994). Estimates of the turnover period range from 30 days to several months and may depend on sensory experience or enrichment (Moulton, 1974; Kondo et al., 2010; Morrison et al., 2015). Severe trauma to the epithelium, in which OSNs and non-neuronal cells of the OE are destroyed, may induce another population of cells near the basal OE lamina, the horizontal basal cells, to differentiate into OSNs (Leung et al., 2007; Schwob et al., 2017).

Each OSN only expresses one odorant receptor (OR) type, which are G-protein coupled receptors (Buck and Axel, 1991). In mice, there are ~1200 genes that code for different ORs, the majority of which are mammalian olfactory receptors (mORs) and the minority of which are trace amine-associated receptors (TAARs) (Liberles and Buck, 2006; Johnson et al., 2012). Contrastingly, humans possess ~400 genes for ORs. The binding of an odorant molecule to an OR initiates a signal cascade within the OSN resulting in the opening of cyclic nucleotide gated ion channels (CNG), which leads to OSN depolarization and initializes action potential generation, the first step in neural odorant representation. Each OR has multiple different odorant

ligands, with different binding affinities for each ligand, and most ligands also bind to several different ORs – these features provide the olfactory system with the ability to use combinatorial strategies to describe a large number of stimuli using activation of combinations of ORs with varying affinity (Malnic et al., 1999; Hallem and Carlson, 2006). While there is no discrete clustering of OSNs within the epithelium based on OR type and no spatial organization based on genetic similarity or similarity of ligands, a rough zonal organization of OSNs does exist, with OSN cell bodies located within the spatial bounds of one of four OE zones (Ressler et al., 1993; Vassar et al., 1993; Strotmann et al., 1994). The axons of mature OSNs project through the cribiform plate to the OB where axons for OSNs expressing a given OR coalesce into spherical structures called glomeruli (Vassar et al., 1994). There are usually two glomeruli per bulb corresponding to each OR for a total of four glomeruli per animal associated with each OR, although exact fidelity of axon convergence into two discrete glomeruli varies slightly between glomeruli corresponding to different ORs (Strotmann et al., 2000; Schaefer et al., 2001; Bressel et al., 2015). OSN location within the olfactory epithelium corresponds with glomerulus location within the bulb, with dorsal zone OSNs expressing NQO-1 sending axons to the dorsal OB and ventral zone OSNs expressing OCAM sending axons to the ventral OB (Astic et al., 1987; Yoshihara et al., 1997; Gussing and Bohm, 2004; Miyamichi et al., 2005; Eerdunfu et al., 2017). These differences in positional targeting may also reflect innate behavioral correlates – for example, ablation of dorsally targeting OSNs disrupts innate aversive fear conditioning (Cho et al., 2011). In addition, OR identity influences OSN axon targeting, specifically along the dorsal-ventral axis of the OB. Because each OSN only expresses one OR type and each glomerulus is made up of axons from OSNs that express the same OR type (Treloar et al., 2002), there is a high

level of specificity and organization based on OR type within the peripheral olfactory circuit, which also informs the topography of the OB.

1.1.2 The olfactory bulb

The OB is the first structure in the olfactory system that integrates information about odorant stimuli. Local circuits within the bulb transform information from OSNs at the periphery of the olfactory system and transmit signals to higher cortical areas. The basic odor-coding circuit of the OB, the glomerular module, is centered around the glomerulus. Each glomerular module is a spherical microcircuit comprised of: 1) a convergence of the axons of OSNs expressing a single odorant receptor type, 2) the processes of excitatory and inhibitory local juxtaglomerular interneurons, and 3) the dendrites of excitatory projection neurons, the mitral and tufted cells (M/TCs), that send input from the bulb to other areas of the brain (Mombaerts, 1996; Mombaerts et al., 1996; Potter et al., 2001; Treloar et al., 2002; Chen and Shepherd, 2005; Kikuta et al., 2013). The main output neurons of the olfactory bulb, the M/TCs, receive excitatory input via axodendritic synapses with OSNs and external tufted cells (ETCs) within discrete glomeruli as well as inhibitory input from populations of interneurons, periglomerular cells (PGs) in the glomerular layer and granule cells (GCs) located in the GC layer (Price and Powell, 1970; De Saint Jan et al., 2009) (**Figure 1**). These M/TCs each have one apical dendrite projecting to one glomerulus as well as multiple lateral dendrites that course along the external plexiform layer (EPL) and contact the dendrites of inhibitory GCs via reciprocal dendrodendritic synapses (Pinching and Powell, 1971; Kosaka and Kosaka, 2011). MC lateral dendrites are unique from dendrites of cell types such as cortical pyramidal neurons in that they release neurotransmitter and thus serve as both pre- and post- synaptic structures to GCs. They extend radially up to 1

mm and can non-decrementally propagate action potentials, suggesting that each MC recruits a very extensive spatial network of inhibitory GCs (Price and Powell, 1970; Bischofberger and Jonas, 1997; Xiong and Chen, 2002; Debarbieux et al., 2003; Migliore and Shepherd, 2008).

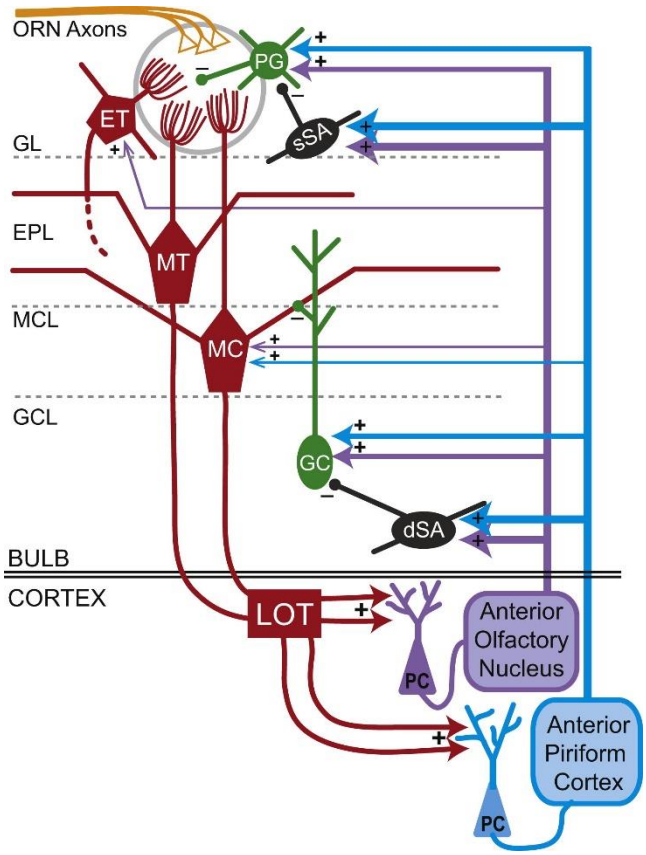

Figure 1. Basic circuitry of the olfactory bulb and cortical feedback projections. From Oswald and Urban, 2012. Olfactory sensory neuron (ORN) axons converge into spherical glomeruli in the glomerular layer (GL) of the OB, where they contact post-synaptic cells such as external tufted (ET) and periglomerular (PG) cells, as well as primary projection neurons – middle tufted cells (MT) in the external plexiform layer (EPL) and mitral cells (MC) in the mitral cell layer (MCL). Superficial short axon (sSA) cells provide inhibitory input in the GL, while granule cells (GC) and deep short axon cells (dSA) with cell bodies in the granule cell layer (GCL) modulate inhibitory input in the GCL, MCL, and EPL. MTs and MCs send axons via the lateral olfactory tract (LOT) to cortical areas such as the anterior olfactory nucleus and anterior piriform cortex. Pyramidal neurons (PC) from these regions send projections back to the OB, where they excite

inhibitory interneurons – sSAs, dSAs, GCs, PCs, and also provide some excitatory input to ETs and MCs.

Complex networks of lateral inhibition in the glomerular and granule cell layers modulate M/TC output. These work in concert to modulate the output of M/TCs and to mediate interglomerular signaling, which has important network and behavioral implications. In the glomerular layer, M/TCs form dendrodendritic synapses with PGs, which release GABA onto M/TCs in a glomerular module specific manner and provide lateral inhibition onto these primary neurons (Arruda et al., 2013; Najac et al., 2015). Superficial short axon cells in the glomerular layer form interglomerular connections and mediate ETC responsiveness (Hayar et al., 2004; De Saint Jan et al., 2009). In the granule cell layer, M/TCs provide glutamatergic excitatory input onto GCs, which then provide local recurrent GABA mediated inhibition, as well as widespread lateral inhibition onto additional connected M/TCs (Chen et al., 1997, 2000; Egger et al., 2003; Egger and Urban, 2006). Deep short axon cells comprise yet another class of inhibitory interneurons that coordinate glomerular output (Liu et al., 2013; Burton et al., 2016). As in other sensory systems, inhibition functions to sharpen odorant representations through contrast enhancement and modulating M/TC correlation (Urban, 2002; Arevian et al., 2008; Gschwend et al., 2015; Geramita et al., 2016). These circuits mediate crucial steps in olfactory processing such as MC synchrony, inter-glomerular communication, and odorant discrimination (Price and Powell, 1970; Shepherd et al., 2007; Koulakov and Rinberg, 2011; Lepousez and Lledo, 2013; Nunez-Parra et al., 2013).

1.1.3 Cortical and cortico-bulbar circuitry

M/TCs integrate and relay information about olfactory stimuli to higher cortical areas such as the piriform cortex, the amygdala, and the olfactory tubercle (Sosulski et al., 2011). Each odorant evokes a response from a set of glomeruli in a specific spatial arrangement and also evokes a

response from a population of neurons within the piriform cortex, yet there is no intuitive map of activation that is consistent between the OB and piriform cortex (Stettler and Axel, 2009; Wilson and Rennaker, 2010). Rather, odorants activate a spatially distributed set of piriform cortical neurons with no evidence of a spatial map. To add an additional level of complexity, the OB in turn receives feedback projections from olfactory cortical areas that modulate both the glomerular and the granule cell layers, in turn influencing M/TC activity and subsequent OB output (Boyd et al., 2012; Markopoulos et al., 2012; Oswald and Urban, 2012). It is unclear if these feedback projections have any spatial specificity once they reach the bulb – the existence of such a map may have important implications on odorant representation.

1.2 ODORANT REPRESENTATION IN THE OLFACTORY BULB

The olfactory system tackles the difficult problem of representing a large, high-dimensional set of stimuli that lacks an intuitive, simple organization. A single odorant ligand produces a perceptible, distinct odor, yet most encountered environmental odors are comprised of odorant combinations. Currently, it is not possible to reliably predict whether a molecule is an odorant or what olfactory percept a molecule will elicit (Keller et al., 2017). Despite only possessing ~400 distinct ORs, humans may still be able to discriminate millions of odors, which speaks to the immense capacity of combinatorial coding in the olfactory system (Bushdid et al., 2014; Meister, 2015). Such a coding schema is achieved through the sparse and spatially distributed representations of odorants within the olfactory bulb and higher olfactory cortical areas. Other sensory systems have stimulus-dependent contiguous organizations of cortical areas – a remarkable example is the somatosensory system and the cortical homunculus, where adjacent

cortical areas are dedicated to processing input from adjacent body parts. A rough chemotopy exists within the OB, where glomeruli and associated M/TCs within specific regions respond to odorants that share molecular features such as carbon chain length or functional groups (Imamura et al., 1992; Katoh et al., 1993; Johnson et al., 1998; Johnson and Leon, 2000, 2007; Meister and Bonhoeffer, 2001). However, this organization is not observed at the level of single glomeruli – a single odorant does not activate a contiguous, adjacent group of glomerular modules. Rather, a single odorant activates a set of spatially distributed glomerular modules, and neighboring glomeruli may not have OR identities that are genetically similar or have similar ligand sets (Soucy et al., 2009). Discriminations between odorants rely upon the ability of the system to distinguish between glomerular activation patterns – the distributed coding used by the olfactory system significantly increases the number of stimuli that can be represented and interpreted. Incredibly, rats can use slight differences in glomerular activation patterns and the amplitudes of glomerular activation to distinguish between pairs of odorant enantiomers (Rubin and Katz, 2001).

Although the olfactory "map" is not intuitively organized, there is remarkable stereotypy of anatomy within the olfactory system. As described above, OSN cell bodies organize in the OE within four rough spatial domains that translate into a general topography of corresponding glomeruli along the dorsal-ventral axis within the OB. OSN axons reliably form glomeruli in a relatively spatially invariant location, with the magnitude of positional variability dependent on OR identity with an inter-animal variance on the order of 100-200 microns (Mombaerts, 1996; Strotmann et al., 2000; Schaefer et al., 2001; Zapiec and Mombaerts, 2015). Interestingly, if OSNs are ablated during a critical period following an initial stage of glomerular map formation, newborn OSNs will target their previously defined locations and reform the original glomerular

map, suggesting that there are elements within the OB separate from OSNs that impart a level of permanence to the glomerular map following an early critical period (Gogos et al., 2000; Ma et al., 2014; Tsai and Barnea, 2014). This glomerular map is maintained throughout adulthood, with continually regenerating OSNs integrating within the circuit with high specificity of glomerular targeting.

1.3 PLASTICITY OF THE OLFACTORY BULB

General OB structure is mostly finalized during the prenatal period, with circuit refinement such as glomerular coalescence and development of inhibitory connections occurring during the first few postnatal weeks (Vassar et al., 1994; Potter et al., 2001; Dietz et al., 2011). During both development and adulthood, several elements of olfactory circuit anatomy are highly plastic and can be influenced by many types of olfactory experience, ranging from passive exposure to fear conditioning (Meisami and Safari, 1981; Benson et al., 1984; Kerr and Belluscio, 2006; Johnson et al., 2013; Dias and Ressler, 2014; Morrison et al., 2015). It is known that olfactory experience and the mechanisms allowing for experience-dependent plasticity are critical for the correct development and maintenance of the olfactory map. However, many of the functional and behavioral implications of the experience-dependent anatomical changes to olfactory circuitry are still unclear.

1.3.1 Timeline of circuit refinement

Gross OE and OB structure emerges during the prenatal period, with the OE appearing by embryonic day (E) 9 and the precursor to the OB appearing by E10. Mature OSNs begin expressing single ORs by E12 and start sending axons to the OB by E16, with glomerular formation occurring soon after (Mombaerts et al., 1996; Royal and Key, 1999). The timeline of glomerular coalescence is closely associated with OR identity. For example, glomeruli containing the axons of M72-receptor expressing OSNs form a single cohesive mature glomerulus by postnatal day (P) 5, while P2-receptor associated glomeruli have finalized coalescence by birth (Vassar et al., 1994; Mombaerts et al., 1996). OR identity is also correlated with OSN number and final glomerular volume (Bressel et al., 2015).

The formation of the glomerular module occurs a few days after OSNs begin organizing within the OE. Migration of M/TCs to their position and orientation in the MC layer and external plexiform layer, respectively, can be observed between E11-E15 (Hinds, 1973; Blanchart et al., 2006). Initially, these cells extend apical dendrites to multiple glomeruli. MCs are observed to have significant radially extending lateral dendrites by P5, indicating that the establishment of the MC and GC mediated network of lateral inhibition has a component of postnatal circuit development (Blanchart et al., 2006), which has also been supported by electrophysiology data indicating a postnatal refinement of MC-GC synapses between P15 and P30 (Dietz et al., 2011). By P10, these apical dendrites and a population of MCs have been pruned away such that each mitral and tufted cell only projects a single apical dendrite to a single glomerulus (Malun and Brunjes, 1996; Matsutani and Yamamoto, 2000; Blanchart et al., 2006). The mechanisms by which these projection neurons choose a final glomerulus to target are unclear, with some work

suggesting that sensory-evoked activity of OSNs may play a role (Lin et al., 2000), but we aim to address elements of this question in this thesis.

While MCs decrease slightly in population between birth to P20, the population of GCs expands substantially following birth, achieving adult numbers by P30 and with GC-MC and MC-GC synapse density also increasing substantially following birth at a similar rate (Hinds and Hinds, 1976). PGCs, which provide inhibitory input to projection neurons at the level of the glomerular layer, are present by E17 and are almost all incorporated within the glomerular circuit by the end of the first postnatal week (Kosaka et al., 1987). Adult-born GCs and PGCs continually integrate functionally within the OB circuit throughout life (Luskin, 1993; Lois and Alvarez-Buylla, 1994; Carleton et al., 2003).

Genetically determined factors influence the timing and specific organization of olfactory system development, including OR expression, OSN domain within the OE, chemical gradients directing axon OSN targeting, and OR-dependent axon sorting mechanisms (Vassar et al., 1994; Treloar et al., 2002; Feinstein and Mombaerts, 2004; Komiyama and Luo, 2006; Imai et al., 2009). However, substantial development of the OB circuit occurs postnatally, such as finalization of glomerular coalescence and formation of the glomerular synaptic network, M/TC targeting, and the formation of the lateral inhibitory network (Malun and Brunjes, 1996; Kim and Greer, 2000; Matsutani and Yamamoto, 2000; Blanchart et al., 2006; Dietz et al., 2011). These elements thus have the potential to be modulated or modified by early sensory experience. In addition, adult born neurons such as PGCs and GCs continually incorporate into the OB circuit throughout adulthood, providing a highly valuable source of circuit plasticity. Below, we outline the major known ways in which sensory experience influences elements of the glomerular module.

1.3.2 Experience and activity-dependent changes to olfactory sensory nerve projections to the olfactory bulb

OSN axon guidance from the OE to the OB and subsequent glomerular coalescence are primarily governed by OR identity and intrinsic OSN activity, which is crucial for the formation of the glomerular map (Lin et al., 2000; Yu et al., 2004). However, maintenance of the glomerular map requires both spontaneous activity and sensory experience (Zhao and Reed, 2001; Yu et al., 2004). In addition, sensory experience plays a central role in influencing how axons achieve final glomerulus convergence. Disruption of the olfactory CNG channel through targeted deletion of subunit-encoding genes Cnca or OCNC1 prevents sensory-evoked OSN activity. When all OSNs lack functional CNG channels, glomeruli undergo normal convergence (Lin et al., 2000). However, when select populations of OSNs lack functional CNG channels, survival of affected OSNs decreases, and axons from those OSNs form more supernumerary glomeruli and are less reliable with regards to glomerular position targeting, suggesting that activity-dependent competition may be important to OSN axon targeting (Zheng et al., 2000; Zhao and Reed, 2001). Postnatal aversive odorant conditioning using a paradigm where the nipples of nursing dams are painted with an odorant accelerates the rate of convergence of an activated glomerulus in pups (Kerr and Belluscio, 2006) – interestingly, odor exposure alone does not have the same effect. The deletion of Kv1.3, an important potassium ion channel expressed in MCs, results in poor glomerular convergence and the formation of supernumerary, heterogeneous glomeruli, suggesting that MC activity also plays a crucial role in axon guidance and final glomerular convergence (Fadool and Levitan, 1998; Fadool et al., 2004; Biju et al., 2008). Thus, intrinsic OSN activity, sensory-evoked OSN activity, and MC activity are all necessary for correct OSN axon targeting and glomeruli convergence.

Different types of prenatal and postnatal odorant conditioning can also change final glomerular volume. Todrank et al., 2011 used a food-based odorant exposure paradigm during the prenatal and early postnatal period and found that in pups subject to odorant exposure, activated glomeruli were larger in volume. Exposed pups also demonstrated a preference for food scented with conditioned odorant. Experience-dependent changes in glomerular volume are observed throughout adulthood as well – aversive fear conditioning in adult mice selectively increased the number of OSNs activated by ligands used for conditioning and the volume of associated glomeruli (Morrison et al., 2015). Extinction of this conditioned fear response resulted in a concomitant decrease in OSN number and glomerulus size. This type of anatomical change can be passed onto subsequent generations – following fear conditioning of the parental generation, the F1 generation also displayed increased OSN number and glomerulus size, as well as increased behavioral sensitivity to the conditioned odorant (Dias and Ressler, 2014). A different type of early odorant conditioning using chronic passive exposure to a vial of odorant placed in the cages of nursing mouse litters resulted in the formation of supernumerary glomeruli by P20, although total glomerular volume remained the same between control and exposed litters (Valle-Leija et al., 2012). Glomerular formation can thus be modulated by multiple types of passive and active odorant experience, including conditioning early in development and later in adulthood.

1.3.3 Experience dependent changes to mitral and tufted cells

Odorant experience is necessary for development of M/T cells. Some studies show that early postnatal sensory deprivation through nares occlusion results in poor formation of the MC layer and a reduction in M/TC soma size and number (Meisami and Safari, 1981; Maher et al., 2009).

However, an additional study found that while early postnatal nares occlusion decreased olfactory bulb volume and MC soma size, such an intervention did not change MC number (Benson et al., 1984). Sensory deprivation from other means, specifically through the elimination of sensory evoked OSN activity through deletion of the OCNC1 gene, appears to not change MC number, but does slow pruning of extraneous MC apical dendrites. This suggests that sensory-evoked OSN input is important for the targeting of mature MCs to single glomeruli (Lin et al., 2000). Odor enrichment through a month-long protocol exposing mice to odorants over five daily sessions also decreases MC density and soma size, while disruption of MC excitability by deletion of Kv1.3 channels increases MC number (Johnson et al., 2013). As noted above, the deletion of Kv1.3 channels in MCs also disrupts glomerular convergence, suggesting that MC activity is an important modulator of glomerular module formation during development. These results, while sometimes not easily reconciled between studies, suggest that both deprivation and odor enrichment can have profound effects on the anatomy of the MC layer.

Odorant experience also has the capacity to change MC responsiveness to odorants. Odor deprivation via immediate postnatal nares occlusion until P60 and P90 increases both excitatory and inhibitory odor-evoked responses in MCs, and also increases the number of odor stimuli that evoke responses in individual MCs (Rodríguez et al., 2013). Depending on context, prolonged odor exposure can either increase or decrease M/TC responsiveness. In adult rats, brief 20-minute bouts of passive odorant exposure over six-days leads to a decrease in excitatory odor-evoked activity of M/TCs (Buonviso and Chaput, 1999). Aversive odorant conditioning in adult mice has been shown to increase the amplitude of odor-evoked M/TC responses (Fletcher, 2012). A similar functional change is also observed in neonatal rats following positive associative odorant conditioning – this paradigm results in a greater percentage of excitatory responses to the

conditioned odorant while leaving the percentage of excitatory responses to an unconditioned odorant unchanged (Wilson et al., 1985). Activity of M/TCs can also be transiently modulated during learned tasks, as shown by Doucette and Restrepo, 2008, who determined that during an odor discrimination task, responses of single MCs to rewarded and non-reward odorants diverged significantly, potentially the result of changing centrifugal input. The use of these several different odorant exposure and conditioning paradigms to effect different anatomical and functional changes to M/TCs suggests that the context and type of odorant exposure may differentially modulate OB circuits.

1.3.4 Experience dependent changes to periglomerular and granule cells

The interneurons that mediate inhibitory networks in the OB, the PGCs and GCs, are also significantly impacted by odorant experience. These interneurons are continually generated and integrated into the OB throughout life, providing an important source of OB plasticity. In addition, there are large early developmental changes to the interneuron population that demonstrate the importance of sensory experience in mediating the development of OB inhibitory networks. Olfactory deprivation via nares occlusion selectively changes newborn GCs while preserving existing GCs and proliferation rate – deprivation decreases newborn GC number and survival as well as the cumulative lengths of the primary dendrite and dendritic tree (Frazier-Cierpial and Brunjes, 1989; Corotto et al., 1994; Saghatelyan et al., 2005; Yamaguchi and Mori, 2005). This olfactory deprivation also increases the excitability of newborn GCs.

Deprivation via nares occlusion does not change newborn PGC number, but rather selectively decreases TH expression in the OB and decreases the number of PGCs that express tyrosine hydroxylase (TH) (Bovetti et al., 2009). This decrease in TH expressing PGCs is

reversed following reversal of nares occlusion (Sawada et al., 2011). In addition, nares occlusion does not impact the number of calbindin-(CB) or calretinin-(CR)+ PGCs (Bovetti et al., 2009; Bastien-Dionne et al., 2010). Interestingly, enrichment has the opposite effect, significantly increasing the number of new TH-positive PGCs, demonstrating a very straightforward way in which activity or lack of activity modulates specific cell types and TH expression within the OB (Bonzano et al., 2014).

Olfactory enrichment through constant passive odorant experience also differentially affects PGCs and GCs, most notably through prolonging a higher survival rate of GCs several weeks following a period of olfactory enrichment while promoting a higher survival rate of PGCs during the enrichment period (Bovetti et al., 2009). This increase in adult-born GC survival following olfactory enrichment is accompanied by a significant behavioral effect, an increase in short term odor memory evaluated using an odor investigation task (Rochefort et al., 2002). Thus, odorant experience can significantly change the number of newborn PGCs and GCs that integrate into the postnatal OB, which has important behavioral implications. These experience-dependent changes may have an especially large impact on the inhibitory network during the early postnatal period, during which PGCs finalize integration in the OB circuit and the population of GCs rapidly expands before later decreasing.

1.4 TOOLS TO STUDY OLFACTORY BULB CIRCUIT ORGANIZATION

The stereotypic organization of glomerular modules within the OB by OR identity allows for targeted study of the effects of odorant experience. A number of ORs have been identified, sequenced, and deorphanized, meaning that a subset of odorant ligands has been identified for

these ORs (Buck and Axel, 1991; Xie et al., 2000; Zhang et al., 2012; Jiang et al., 2015). In addition, several mouse lines exist in which OSNs expressing a single OR type are labeled (Potter et al., 2001; Feinstein and Mombaerts, 2004; Feinstein et al., 2004). As a result, we are able to visually identify these particular OSNs and their respective glomeruli *in vivo* and use their known odorant ligands to provide stimulation. This combination also allows for targeted study of how odorant experience can change the structure and output of genetically identified glomerular modules. In Chapter 2 of this dissertation, we leveraged these tools to examine one well-defined structure, the glomerular module corresponding to OSNs expressing the M72 OR.

The M72 OR has been the subject of substantial study. Several ligands have been identified for the M72 OR, including perceptually distinct odorants such as acetophenone (fake cherry), methyl salicylate (wintergreen/mint), and ethyl tiglate (fruity). Each ligand varies significantly in the level of M72 glomerulus activation elicited, as measured by Zhang et al., 2012. The M72 glomerulus is located on the dorsolateral aspect of the OB, and neatly coalesces into a single glomerulus per aspect of the OB by P5, for a total of 2 glomeruli per OB. In addition, multiple mouse lines exist that allow for the visualization of M72-associated glomeruli *in vivo.* The wealth of knowledge about the M72 OR, including the position of M72-associated glomeruli in the OB and the identity of several M72-OR ligands, make the M72 glomerular module an ideal candidate with which to study how odorant exposure can change the structure of a specific, activated glomerular module. In Chapter 2, we build upon previous studies of the M72 glomerulus and examine how exposure to an M72-OR ligand changes the structure of the M72 glomerular module.

1.5 GOALS OF THE DISSERTATION

Sensory experience, whether prenatal, early postnatal, or during adulthood, can dramatically shape both anatomical and functional elements of olfactory circuitry. Many studies have sought to characterize the time-course and extent of these activity-dependent changes, although the heterogeneity of conditioning paradigms between studies has made it difficult to infer how experience-dependent anatomical changes inform odor-evoked activity in the bulb. Previous studies have produced conflicting results regarding the effects of odorant experience on anatomy or odorant representation, although these differences in result can potentially be explained by differences in study design, specifically regarding odorant exposure timing and methodology. This suggests that the context of odorant experience is an important factor in the modulation of OB circuitry. In this dissertation, we examine how one specific early odorant exposure paradigm (Todrank et al., 2011) may shape the anatomy and the function of the olfactory bulb, specifically focusing on the connectivity and odor-evoked responses of primary projection neurons.

Many studies examine how sensory enrichment through passive odorant exposure or active odorant conditioning changes change olfactory bulb anatomy (Kerr and Belluscio, 2006; Johnson et al., 2013; Dias and Ressler, 2014; Morrison et al., 2015). These studies focus on glomerular convergence or on the gross structure of the OB and OB layers. But, glomeruli are the foci of glomerular modules, microcircuits involving many different cellular subtypes that may also be modified by odorant experience. Todrank et al., 2011 found that a food-based prenatal and early postnatal odorant exposure paradigm significantly increases the volume of glomeruli activated by the exposure odorant ligand. In Chapter 2 of this dissertation, we used this same odorant exposure paradigm to investigate changes to a different component of the glomerular module, the mitral and tufted cells. We used *in vivo* electroporation of the M72

glomerulus to label components of the M72 glomerular module. We assessed glomerular volume, M/TC number, and attempted to understand the behavioral impact of these anatomical changes by measuring food preference. In addition, we provided the first study determining how many M/TCs are connected to a single glomerulus, a fundamental question of OB circuitry previously not addressed.

We determined that this type of odorant exposure significantly changes both glomerular volume and M/TC number. Dramatic changes to circuit structure such as these might have a significant impact on odorant representation in the OB. Thus, we sought to examine how the activity of MCs might be affected by early odorant exposure. In Chapter 3, we apply the same odorant exposure paradigm as Chapter 2. Using 2-photon calcium imaging, we determine how prenatal and early postnatal odorant exposure changes the odor-evoked responses of MCs in adult mice. In Chapter 4, we discuss the implications of these anatomical and functional changes on odorant representation in the OB and reconcile these results with findings from previous studies. These studies offer insight into the large impact of early odorant experience on fundamental characteristics of M/TCs in the OB, and contribute to a framework by which to consider how experience-dependent circuit changes may change both odorant representation and behavioral elements of odorant experience such as odor valence.

2.0 EARLY ODORANT EXPOSURE INCREASES THE NUMBER OF MITRAL AND TUFTED CELLS ASSOCIATED WITH A SINGLE GLOMERULUS

2.1 INTRODUCTION

The structure of the mouse OB demonstrates remarkable regularity from animal to animal. OSNs expressing the same OR coalesce into ~two glomeruli per OB with relatively low positional variance across animals, the amplitude of which is related to OR identity (Mombaerts et al., 1996; Strotmann et al., 2000; Schaefer et al., 2001; Feinstein and Mombaerts, 2004; Zapiec and Mombaerts, 2015). While location is determined by OR identity, odorant conditioning increases the rate of coalescence and the precision of axonal targeting (Kerr and Belluscio, 2006; Dias and Ressler, 2014), suggesting both genetic and experience-dependent mechanisms govern the development of reliable OB glomerular patterns. However, the role of experience-dependent mechanisms in shaping other components of olfactory circuitry is unknown.

OSN axons reach a targeted location in the OB by approximately embryonic day 15 (E15), and the formation of early glomerular structures is observed by E16-20 (Royal and Key, 1999; Blanchart et al., 2006), but other glomeruli may form in early postnatal days (Potter et al., 2001). Mitral cell (MC) apical dendrites infiltrate the glomerular layer by E17, with some neurons initially sending apical dendrites to multiple glomeruli (Blanchart et al., 2006). Pruning of these apical dendrites occurs by P10, at which point each cell has one branched apical dendrite

receiving OSN input in a single glomerulus (Malun and Brunjes, 1996; Matsutani and Yamamoto, 2000; Blanchart et al., 2006) and may be influenced by activity (Lin et al., 2000). Thus, the assignment of M/TCs to specific glomerular modules is determined early in development through a pruning process. **Figure 2D** depicts a very basic schematic of multiple glomeruli and a few of their post-synaptic targets, including periglomerular cells located in the glomerular layer, TCs in the external plexiform layer (EPL), and MCs in the mitral cell layer (MCL). Both OR identity and activation play major roles in glomerular development (Wang et al., 1998) - prenatal and early postnatal odorant exposure increases the volume of activated glomeruli, increases the incidence of supernumerary glomeruli, and biases odorant preference towards the exposed ligand (Todrank et al., 2011; Valle-Leija et al., 2012). As a result, early odorant exposure may also influence the development of other OB neurons, such as by increasing the number of projection neurons connected to activated glomeruli.

Whether the same glomerular module consistently recruits a specific number of M/TCs across animals has not been explored but may be an important feature for odor coding. The number of M/TCs associated with a specific glomerulus could affect the coding capacity of glomerular modules and alter the functional relevance of particular glomeruli. Glomerular modules with more M/TCs may exert more lateral inhibition (Egger and Urban, 2006) and provide more output to olfactory cortical areas. Understanding the influence of experience on M/TC number and glomerular module composition will provide insight into how experience affects odorant representation in the OB.

Here, we use *in vivo* electroporation to label and quantify the M/TCs connected to the M72 glomerulus (M72 M/TCs). We use the M72-IRES-tauGFP mouse line, in which M72-OR expressing OSNs also express GFP, allowing for the targeting of a single genetically identified

glomerulus across animals (Potter et al., 2001). Following prenatal and early postnatal odorant exposure with methyl salicylate, a strong M72 ligand (Zhang et al., 2012), we analyze M72 M/TC number and location, as well as glomerulus volume as defined by the spread of M72-expressing OSN axons, and food preference as measured by sniffing time. We show that, in addition to increasing the size of the M72 glomerular module and the preference for methyl salicylate-scented food, the number of M72 M/TCs can be increased by prenatal and early postnatal methyl salicylate exposure.

2.2 MATERIALS AND METHODS

2.2.1 Subjects

Homozygote male and female M72-IRES-tauGFP mice were used for the majority of experiments except for one control behavior experiment, where heterozygote male and female M72-IRES-ChR2-YFP mice were used. Control and methyl salicylate-exposed mice completed the methyl salicylate-scented vs. control food behavior task at P24 and were sacrificed at P25 for anatomical studies. Two additional groups of mice (control and odor-exposed) also completed the methyl salicylate-scented vs. control food behavior task between P24-26 and were used for *in vivo* electroporation studies from P25-P40. There was no effect of age or sex on these measured parameters, therefore data were pooled. A third cohort of animals was exposed to hexanal-scented food, completed the hexanal-scented vs. control food behavior task at P24, and was sacrificed at P25-P35 for anatomical studies. A fourth cohort of M72-ChR2-YFP mice that had

not undergone odorant-exposure completed the hexanal-scented vs. control food behavior task between P26-P36.

2.2.2 Prenatal and postnatal odorant exposure

Prenatal and postnatal odorant exposure was performed on M72-IRES-tauGFP mice as described by Todrank et al., 2011. Briefly, food was mixed with either methyl salicylate or hexanal (1% by volume) and dried for three days in a glass dish under a fume hood. Breeding pairs were fed exclusively with scented food immediately after establishment, as well as following litter birth throughout nursing until litters were weaned at P22-24. Odorant-exposed litters were continuously fed with methyl salicylate or hexanal-odorized food until being sacrificed for anatomical studies at (P25-P53) or having their OBs electroporated at P25-40. Another cohort of methyl-salicylate exposed litters was weaned onto control unscented food until anatomical studies at P53. Mice were weighed for the first three days of odorant exposure to ensure normal growth while on the scented food.

2.2.3 *In vivo* electroporation

The *in vivo* electroporation procedure was adapted from the procedures detailed in (Nagayama et al., 2007; Hovis et al., 2010; He et al., 2012). Briefly, P25-P40 mice were anesthetized using a ketamine/xylazine intraperitoneal injection, and one craniotomy 0.75 mm in diameter was made above each OB. Target glomeruli were visualized using two-photon microscopy. Monopolar glass electrodes (5-7MΩ resistance) were back-filled with dye-containing solutions, comprised of Alexa Fluor 594 Hydrazide or Alexa Fluor 594 Dextran in PBS (for theta-glass double label

experiments, dyes used were Alexa Fluor 594 Dextran and Alexa Fluor 488 Dextran in PBS, and electrodes were pulled using theta capillary glass). Following electrode placement in the center of the target glomerulus, 150 current pulses were delivered (0.01 mA in amplitude, 500 ms in duration, interpulse interval of 1.5 s). Following electroporation, mice were sacrificed using cardiac perfusion with cold 4% paraformaldehyde. Criteria for successful electroporation were as follows: 1) glomerulus boundaries as defined by GFP-expressing OSN axons were completely filled by dye, 2) perimeter of labeled JGCs surrounded the targeted glomerulus, and 3) apical dendrites of filled M/T cells could be clearly followed back to targeted glomerulus.

2.2.4 Tissue processing for *in vivo* electroporation

Following fixation, tissue was cryoprotected (30% sucrose solution) and cut into 100µm-thick sections. While targeting of GFP glomeruli was performed under two-photon imaging *in vivo*, confocal imaging was performed on sectioned, fixed OB tissue to enable the clearest identification of M/TC apical dendrites targeting the M72 glomerulus. Z-stacks (2 µm optical sections) were obtained for each tissue section using a Zeiss LSM 510 Meta DuoScan Spectral Confocal Microscope. Image analysis and measurements were performed in FIJI (RRID:SCR_002285) and Matlab (RRID: SCR_001622).

2.2.5 Food preference assessment

Mice were tested for food preference as described by Todrank et al., 2011 after P24. Mice were placed into a 38.1 cm diameter circular arena, with two different food pellets placed into wire mesh containers at opposite sides of the arena. Behavior was recorded for three minutes starting

from time mouse began exploring the arena. Food preference was assessed by comparing time spent sniffing a scented food pellet versus a control food pellet. Mice were excluded from analysis if they climbed on top of and became entangled with the wire mesh containers (n=3).

2.2.6 Mitral/tufted cell identification

Post-electroporation, the number of M72 M/TCs was counted through the z-stack of each OB section, avoiding double counting of cell bodies that span physical sections (data presented as mean±SD, p-values determined by unpaired t test). Labeled cells with cell somata larger than >10 μm and located >50% within the MCL were counted as MCs; labeled cells with cell somata larger than >10 μm and located within the EPL were counted as tufted cells (TCs). External tufted cells were not analyzed. The locations of M/TCs were mapped on a coordinate system determined by anatomical landmarks (the M72 glomerulus center and the MCL below the glomerulus) to create a glomerulus-centric 3-dimensional (3D) map of M/TC spatial distribution that can be compared across animals. For each cell, we measured: 1) A=the absolute distance from the center of the soma to the glomerulus center and 2) B=the angle between the perpendicular line from the MCL to the glomerulus center and the line formed by the glomerulus center and the soma center. X and Y cartesian coordinates were obtained by: x=-A*sin(B); y=A*cos(B). The z cartesian coordinate was the distance of the cell from the optical section that contained the maximum glomerular diameter. The distance from the MCL to the glomerular layer was used to normalize measurements between physical sections and animals. Glomerular volume was measured by tracing the outline of the GFP-expressing axons in the glomerular layer within each optical Z-stack section.

2.2.7 Acute odorant exposure

To examine activation of the M72 odorant by ligands and non-ligands, we used an acute odorant exposure paradigm. 4 cohorts of 4 animals each were used: one of animals exposed to 2-OH acetophenone, one of animals exposed to piperonal, and one cohort of control animals for each exposure group. Each cohort was placed into a glass rectangular aquarium. Room air was circulated continuously through the aquarium for 1 hour. Then, 30 minutes of intermittent odorant exposure was initiated, consisting of 3 sequences of [5 minutes odorized air, 5 minutes no air]. 2-OH acetophenone and piperonal odorants were prepared as 2% odorant by volume in mineral oil, while control odorized air was solely mineral oil. Following odorant exposure, room air was again circulated through the aquarium for 1 hour. Mice were then removed from the aquarium and sacrificed using cardiac perfusion with cold 4% paraformaldehyde. Following fixation, tissue was cryoprotected (30% sucrose solution) and cut into 25 µm sagittal sections.

2.2.8 Immunostaining and cFos quantification

25 µm sections from acute odorant exposure animals were washed 3 times for 5 minutes each with phosphate buffer (PB). Each section was then blocked and permeabilized with 2% normal donkey serum and 0.1% Triton X-100 at room temperature for 1 hour with oscillation. Following another set of 3 5-minute washes with PB, sections were incubated overnight at 4°C with primary antibody (1:5000, rabbit anti-cFos, Calbiochem #PC38) in 2% normal donkey serum and 0.05% Tween 20 in PB. Primary antibody was removed, and sections were washed 3 times for 5 minutes each with PB. Then, sections were incubated for 1 hour in the dark with secondary antibody (1:600, AlexaFluor 594 donkey anti-rabbit, Invitrogen #A-10040) with 2% normal

donkey serum, 0.05% Tween 20, and 1:40000 Hoechest in PB. Following removal of secondary antibody, sections were washed 3 times for 5 minutes each with PB. Sections were then mounted in Gelvatol mounting medium and imaged at 10x and 20x using an epifluorescence microscope.

To quantify cFos+ cells, we imaged tissue sections containing the GFP-expressing M72 glomerulus. Images were blinded and cells were manually counted by two observers using FIJI software. A square with side length 150 μm was drawn centered on the M72 glomerulus. All cFos+ JG cells (as determined by cell body placement within the glomerular layer) within this box around the M72 glomerulus were counted as "center" in **Figure 7A,D**. The box was moved 150 μm rostrally and 150 μm caudally to the M72 glomerulus to quantify cFos expression at non-M72 glomeruli – these counts are referred to as "rostral" and "caudal" in **Figure 7A,D**.

2.3 RESULTS

2.3.1 Early methyl salicylate exposure increases M72 glomerulus volume and changes food preference

When mice were fed food odorized with methyl salicylate (mint), a strong M72 ligand, the size of the M72 glomerulus increased in M72-IRES-GFP mice (**Figure 2**). This confirms previous work showing that similar exposure to isopropyl tiglate, another strong M72 ligand with a mint-like smell, also increases M72 glomerulus volume (Todrank et al., 2011). We used methyl salicylate because it more selectively activates M72 compared to other nearby glomeruli (Zhang et al., 2012). Methyl salicylate exposure (from E0 to P25) increased the volume of both the medial and lateral glomeruli (**Figure 2A-B**; one-way ANOVA with Tukey's multiple

comparisons test; ctrl vs. mint; mean±SD; lateral - 0.89±0.34 vs. 1.93±0.30 10^5 μm^3, n=9 vs. 10, adjusted p<0.0001; medial – 0.86±0.19 vs. 1.60±0.68 10^5 μm^3, n=10 vs. 10, adjusted p=0.0062). At P24-26, these same odor-exposed mice showed a preference for mint-scented food as opposed to control food (**Figure 2C**; Kruskal-Wallis test with Dunn's multiple comparisons test; ctrl | m vs. mint | m; mean±SD of ratio of time spent sniffing mint-scented food to total time spent sniffing food: 0.39±0.15 vs. 0.57±0.09, n=15 vs. 22, adjusted p=0.0170).

To examine the specificity of these anatomical and behavioral changes, we performed food-based odorant-exposure on a third cohort of animals using hexanal, which is known to not activate M72 receptors. Prenatal and early postnatal hexanal exposure did not increase the volume of either the medial or lateral glomeruli as compared to control animals (**Figure 2A-B**; one-way ANOVA with Tukey's multiple comparisons test; ctrl vs. hexanal; mean±SD; lateral - 0.89±0.34 vs. 1.08±0.39 10^5 μm^3, n=9 vs. 7, adjusted p=0.9633(n.s.); medial – 0.86±0.19 vs. 1.05±0.58 10^5 μm^3, n=10 vs. 7, adjusted p=0.9544(n.s.)). Comparing mint and hexanal-exposed glomeruli revealed a significant difference between the volumes of mint-exposed and hexanal-exposed glomeruli (one-way ANOVA with Tukey's multiple comparisons test, adjusted p=0.0038), but not between mint-exposed and hexanal-exposed medial glomeruli (one-way ANOVA with Tukey's multiple comparisons test, adjusted p=0.1337(n.s.)). Hexanal-exposed animals also showed a preference for hexanal-exposed food as opposed to control food (**Figure 2C**; Kruskal-Wallis test with Dunn's multiple comparisons test; ctrl | h vs. hexanal | h; mean±SD of ratio of time spent sniffing hexanal-scented food to total time spent sniffing food: 0.23±0.25 vs. 0.65±0.11, n=10 vs. 9, adjusted p<0.0001). Mint-exposed animals and hexanal-exposed animals did not demonstrate a significant difference in time spent sniffing scented food (Kruskal-Wallis test with Dunn's multiple comparisons test; adjusted p>0.9999 (n.s.)). There was also no

significant difference in odorant preference between the cohort of control animals subject to the test of mint-scented vs. control food (ctrl | m) and the cohort subject to the test of hexanal-scented vs. control food (ctrl | h) (Kruskal-Wallis test with Dunn's multiple comparisons test; adjusted p=0.7072 (n.s.)).

We established that early odorant exposure with methyl salicylate, a known M72 ligand, increases M72 glomerular volume and changes food preference. Use of a non-M72 ligand, hexanal, for odorant exposure did not increase M72 glomerular volume but did change food preference. We next chose to investigate whether methyl salicylate odorant exposure induced additional anatomical changes to the M72 glomerular module. Specifically, we used *in vivo* electroporation to label and compare the population of M/TCs contained within the M72 glomerular module (**Figure 2E**).

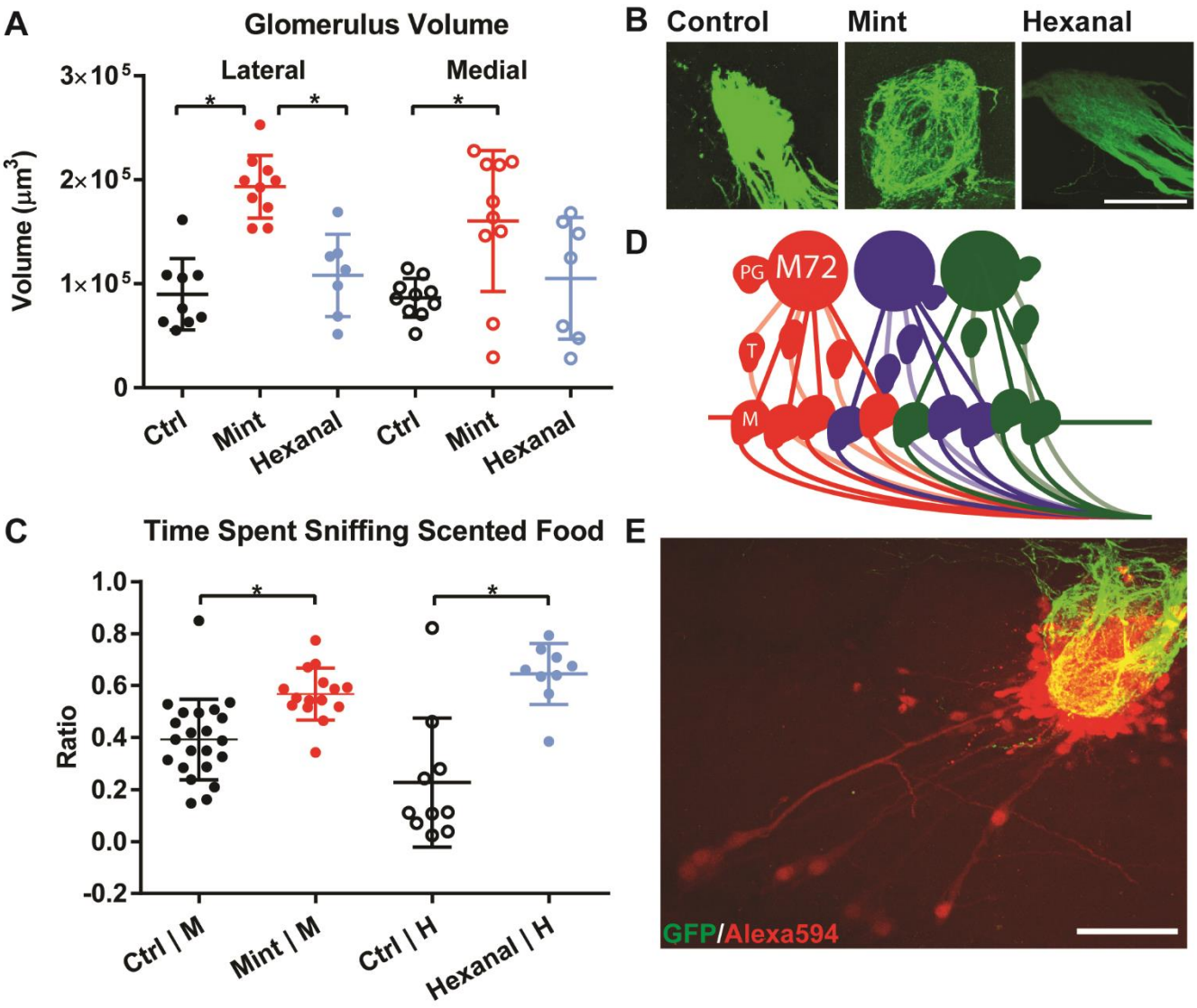

Figure 2. Prenatal and early postnatal methyl salicylate exposure increases M72 glomerulus volume and changes food preference. **A.** Prenatal and early postnatal odorant exposure using food odorized with methyl salicylate (mint, 1% by volume) increases the size of the lateral and medial M72 glomeruli but food odorized with hexanal (hexanal, 1% by volume) has no effect. *p<0.01 **B.** Max projection images of example glomeruli of control and odor-exposed (mint and hexanal) animals at P25-35. Scale bar: 50 µm. **C.** Prenatal and early postnatal odorant exposure using food odorized with methyl salicylate (mint, 1% by volume) or hexanal (hexanal, 1% by volume)

increases ratio of time spent sniffing scented food to total time spent sniffing food, Ctrl | M: control mice in preference test between methyl salicylate-scented and control food; Mint | M: methyl salicylate-exposed animals in preference test between methyl salicylate-scented and control food; Ctrl | H: control mice in preference test between hexanal-scented and control food; Hexanal | H: hexanal-exposed animals in preference test between hexanal-scented and control food. *$p<0.05$ **D.** Schematic of three glomeruli with basic post-synaptic targets comprising three glomerular modules. Example M72 glomerulus is labeled, along with periglomerular cells (PG), tufted cells (T), and mitral cells (M). **E.** Example max projection image of electroporation labeled M72 glomerulus (control) showing GFP expressing OSN axons coalescing into single glomerulus and Alexa Fluor 594 Hydrazide filled JGCs and M/TCs. Scale bar: 50 μm.

2.3.2 Early odorant exposure with an M72 ligand increases number of M/TCs in the M72 glomerular module

We used *in vivo* electroporation to label the post-synaptic targets of the M72 glomerulus in both control M72-IRES-GFP mice and in mice that had been pre and postnatally exposed to methyl salicylate. This type of odorant exposure caused a remarkable increase in the number of M/TCs connected to the glomerulus (unpaired t test; ctrl vs. mint; mean±SD; 6.82 ± 1.08 vs. 10.0 ± 1.07 MCs; 2.91 ± 0.94 vs. 6.63 ± 1.41 TCs; n=8 vs. 11, $p<0.0001$ for both cell types), which demonstrates that early odorant exposure has a profound impact on OB circuit structure beyond affecting glomerulus volume (**Figure 3A**). The ratio of TCs to MCs within a single M72 glomerular module also increased, showing that odorant exposure increased TC number more than MC number, suggesting that chronic early odorant exposure may have differential impacts on these two parallel pathways (unpaired t test; ctrl vs. mint, mean±SEM; TC:MC number; 0.43±0.04 vs. 0.66±0.03; n=11 vs. 8, p=0.0011). In these mice, early odorant exposure also increased glomerulus size (data not shown) and food preference for methyl salicylate-scented food (data pooled in with behavioral study), corroborating the findings shown in **Figure 2**.

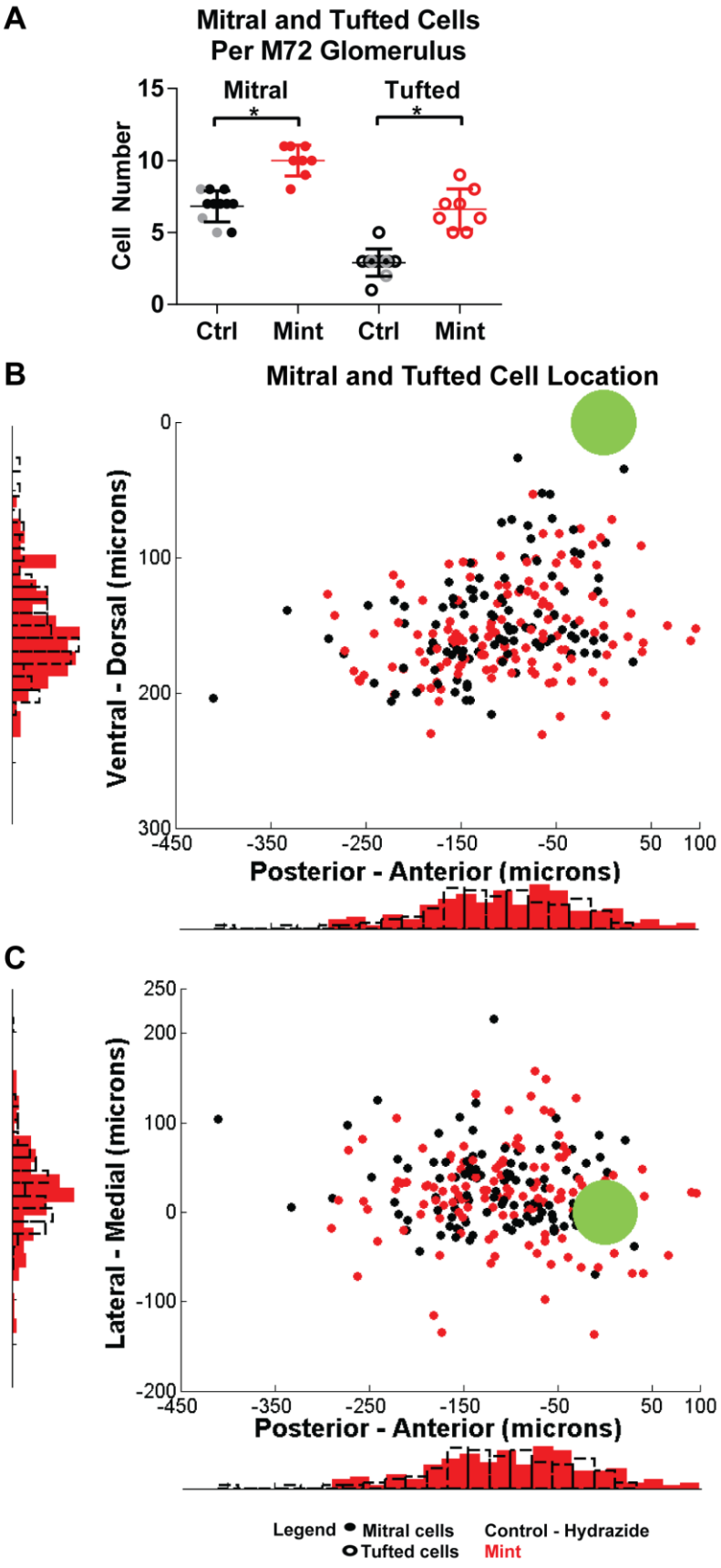
A
Mitral and Tufted Cells
Per M72 Glomerulus
Mitral
Tufted
*
*
Cell Number
15
10
5
0
Ctrl
Mint
Ctrl
Mint
B
Mitral and Tufted Cell Location
Ventral - Dorsal (microns)
0
100
200
300
-450
-350
-250
-150
-50
50
100
Posterior - Anterior (microns)
C
Lateral - Medial (microns)
250
200
100
0
-100
-200
-450
-350
-250
-150
-50
50
100
Posterior - Anterior (microns)
Legend
Mitral cells
Tufted cells
Control - Hydrazide
Mint

Figure 3. Prenatal and early postnatal methyl salicylate exposure increases the number of M72 M/TCs. **A.** Number of M/TCs connected to the lateral M72 glomerulus increases following methyl salicylate exposure (Black filled and open circles – electroporation of control animals with Alexa Fluor 594 Hydrazide, gray filled and open circles – electroporation of control animals with Alexa Fluor 594 Dextran, red filled and open circles – electroporation of methyl salicylate-exposed animals with Alexa Fluor 594 Dextran; mean±SD, *$p<0.0001$). **B-C.** Spatial distribution of mitral and tufted cells corresponding to control (black circles, 11 animals, 74 total MCs, 32 total TCs) and odor-exposed (mint) (red circles, 8 animals, 80 total MCs, 51 total TCs). Green circle denotes M72 glomerulus location. Histograms of cell position next to corresponding axes (Black outline bars – control; red solid bars - mint). **B.** Sagittal view. **C.** Horizontal view. Comparison of median spatial locations n.s.

2.3.3 Odorant exposure does not change the spatial distribution of M/TCs post-synaptic to the M72 glomerulus

In addition to examining the numbers of M/TCs connected to the M72 glomerulus, we also analyzed the location of M/TC somata relative to the M72 glomerulus. An increase in M72 M/TCs distributed over a larger area in the OB may predict a broader range of lateral inhibition. Therefore, we measured the spatial distribution of principal neurons by plotting the locations of the labeled M/TCs relative to the location of the M72 glomerulus (**Figure 3B-C**). M/TCs from control and odor-exposed groups were located in similar areas around the M72 glomerulus. All MCs from both groups were found in an area within the MCL described by an ellipse with length 450 μm and width 300 μm. Previous measurements indicate that MC density in the dorsal OB is ~56 MCs per mm (Richard et al., 2010), so an ellipse of this size contains a total ~345 MCs. TCs from both groups were found at a mean distance of 126 μm below the glomerular layer in an area within the EPL with all cells located in an ellipse with length 350 μm and width 300 μm. There was no statistical difference between control and odor-exposed mean MC and TC location in all three coordinates (Kolmogorov-Smirnov test to compare distribution in each dimension separately resulted in a significant p-value of 0.045 when comparing the Y-dimension coordinates for MCs (mean±SD; ctrl vs. mint; 164 ± 21.8 vs. 170.6 ± 23.6), but a Kruskal-Wallis test with a Dunn's multiple comparisons test yielded no significant differences between the median locations of MCs and TCs from control and odor-exposed groups). Thus, we conclude that odorant exposure increases the number of recruited M72 M/TCs but does not meaningfully affect their locations relative to the M72 glomerulus.

2.3.4 Glomerulus volume persists following removal of odorized food

Here, we used two cohorts of animals to investigate whether the changes in glomerular volume persist after removal of odorized food. One cohort, Mint to Control (M → C) animals were fed methyl salicylate-scented food throughout gestation and nursing. They were weaned onto control food until P53, when the volume of the M72 glomerulus was measured. Mint to Mint (M → M) animals were fed methyl salicylate-scented food throughout gestation, nursing, and post-weaning until P53. The timeline of exposure is shown in **Figure 4**. There were no significant differences between the lateral and medial M72 glomeruli of either M → C or M → M mice (**Figure 4B**; Kruskal-Wallis test with Dunn's multiple comparisons test: all adjusted p-values >0.9999). Thus, early odorant exposure causes an increase in glomerular volume that persists for at least 30 days following removal of odorized food.

Food preference as measured by sniff time does not persist following removal of odorized food. Rather, M → C and M → M mice spent significantly different time investigating methyl salicylate food, with M → C spending more time sniffing control food (**Figure 4C**; Mann-Whitney test; p=0.0381). We find that food preference reflects the more recently fed food, with M → C mice preferring control food and M → M mice preferring methyl salicylate-scented food.

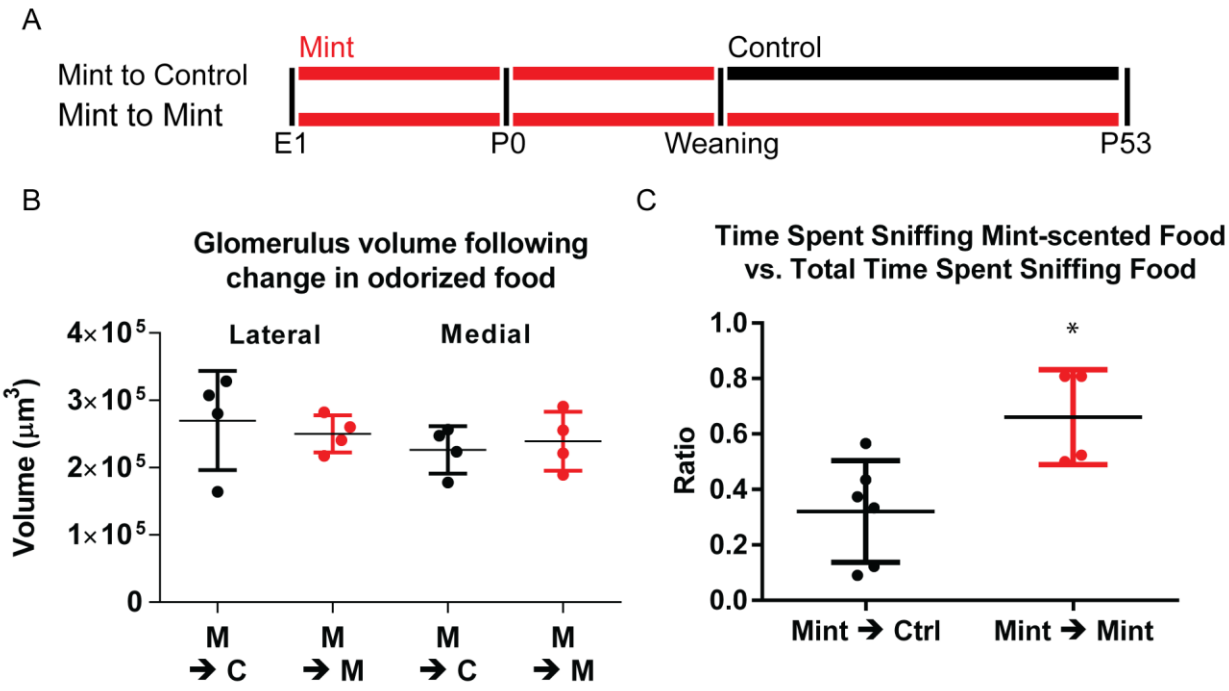

Figure 4. Glomerulus volume persists for at least 30 days after removal of odorized food. A. Odorant exposure timeline. Mint to Control (M → C) animals are fed methyl salicylate odorized food throughout gestation and nursing, then weaned onto control unscented food. Mint to Mint (M → M) animals are fed control unscented food throughout gestation, nursing, and weaned onto control food. **B.** Glomerulus volume is not significantly different between M → C and M → M groups at P53. **C.** M → C and M → M spend significantly different time sniffing methyl salicylate.

2.3.5 Odorant exposure, not age or sex, is correlated with increased M/TC number and glomerular volume

Glomerulus volume is not correlated with MC or TC number, within either control or exposed groups (**Figure 5A**; Spearman's correlation: glomerulus volume vs. control TC: r=-0.034, 95%CI: -0.634 to 0.591, p=0.9257; gv vs. control TC: r=-0.162, 95%CI: -0.705 to -.501, p=0.640; gv vs. exposed MC: r=-0.501, p=0.218; gv vs. exposed TC: r=-0.388, p=0.339). However, when MC and TC count data are combined between the two groups, there is a significant correlation between MC and TC number and glomerulus volume (Spearman's correlation; gv vs. MC: r=0.68, 95%CI: 0.316 to 0.871, p=0.001; gv vs. TC: r=0.686, 95%CI: 0.323 to 0.8726; p=0.0012). These results indicate that the correlation between glomerulus volume and M/TC number is likely due to the increase in both metrics following odorant exposure rather than a difference in M/TC number due to intrinsic variability in M72 glomerulus size.

Sex and age differences also do not account for the differences in glomerular volume or M/TC number seen after odorant exposure. There was no significant difference in MC or TC number between male and female mice within control and conditioned groups (**Figure 5B**; Male vs. female; control MC: adjusted p=0.3669; control TC: adjusted p=0.9996; conditioned MC: adjusted p>0.9999; conditioned TC: adjusted 0.9962). Age is not significantly correlated with MC or TC number in either control or exposed groups (**Figure 5C**; Spearman's correlation; age vs. control MC: r=0.26321, 95%CI: -0.417 to 0.754, p=0.433; age vs. control TC: r=0.169, 95%CI: -0.495 to 0.754, p=0.623; age vs. exposed MC: r=0.038, p=0.956; age vs. exposed TC: r=0.140, p=0.735). Combining groups also does not reveal a correlation between age and MC or TC number (Spearman's correlation; age vs. all MC: r=0.128, 95% CI: -0.359 to 0.560, p=0.601;

age vs. all TC: r=0.263, 95% CI: -0.231 to 0.649; p=0.277). Age is also not significantly correlated with glomerulus volume in control, conditioned, or M → C groups (**Figure 5D**; Spearman's correlation; age vs. control: r=-0.0323, p=0.866; age vs. mint: r=0.0942, p=0.634; age vs. M → C: =-0.5494, p=0.0653). These data indicate that during the time period in which we make our observations, glomerulus volume does not significantly increase with age, but instead reflects odorant experience.

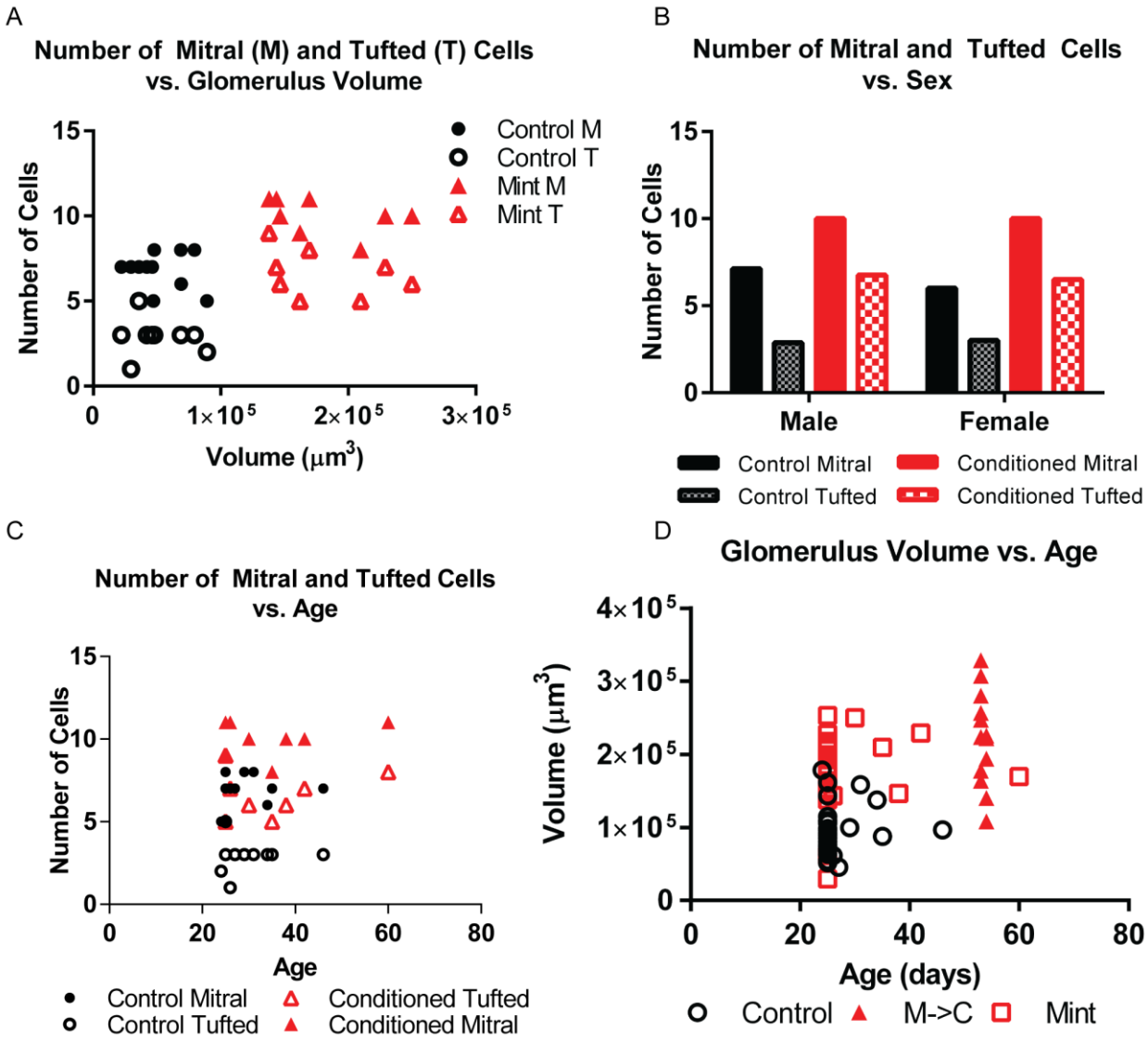

Figure 5. Odorant exposure, not age or sex, is correlated with mitral/tufted cell number or glomerular volume. **A.** There is no correlation between glomerulus volume and M/TC number within group, but there is a correlation when data are combined. **B.** There is no significant difference in M/TC number between control and conditioned animals of either sex. **C.** There is no significant correlation between MTC number and age. **D.** There is no significant difference correlation between glomerulus volume and age.

2.3.6 *In vivo* electroporation reliably labels the post-synaptic targets of a single glomerulus

In vivo electroporation has been previously used to label the complement of JGCs and principle projection neurons of a single glomerulus (Nagayama et al., 2007; Sosulski et al., 2011; He et al., 2012; Ke et al., 2013). To interpret these experiments, it is important to confirm that this approach reliably and specifically labels cells associated with a single glomerulus (**Figure 6**). To test labeling consistency, we performed sequential electroporations in control M72-IRES-GFP mice (n=7) with two colors of dye and using three separate electroporation protocols. **Figure 6A** shows example physical sections (**Figure 6A1**, z-stack images) and optical sections (**Figure 6A2**) of an M72 glomerulus and labeled cells following dual-color electroporation using a stationary theta glass electrode. In this first method, two sequential electroporations were performed using a single theta glass electrode, in which a glass septum forms two isolated compartments into which two dyes (Alexa Fluor 594 Dextran and Alexa Fluor 488 Dextran) were backfilled, one in each compartment. A separate silver electrode wire was placed in each compartment, allowing for isolated single-color electroporations. The electrode tip position remained constant between the two electroporations. **Figure 6B-C** shows example optical sections of M72 glomeruli from two different animals following dual-color electroporation using a repositioned theta glass electrode. In this second method, two sequential electroporations were performed, again with a single theta glass electrode and two dyes, but here we moved the electrode tip ~20 µm between each single-color electroporation, a substantial distance within the M72 glomerulus, which is 75-100 µm at its longest diameter. Finally, **Figure 6D** shows example optical sections of an M72 glomerulus following dual-color electroporation using two separate electrodes made from plain capillary glass, each backfilled with either Alexa Fluor 594 Dextran

or Alexa Fluor 488 Dextran. Electroporation pulse parameters for all three approaches were kept constant as described in the Methods section. In all of these experiments, we observed that 1) both dyes filled the entirety of the glomerulus and 2) identical populations of JGCs, M/TCs, and neuronal processes are labeled by both dyes, demonstrating reliable and complete labeling by the two electroporations. All dual-color electroporation experiments yielded labeled M/TC numbers within the range of labeled M/TCs reported in **Figure 3**. In addition, these data demonstrate that exact replication of electrode tip position within the glomerulus between electroporations is not necessary to label the same cohort of cells and cell processes. This evidence allows us to use *in vivo* dye electroporation to compare numbers of labeled M/TCs connected to the M72 glomerulus between animals and odor-exposure conditions.

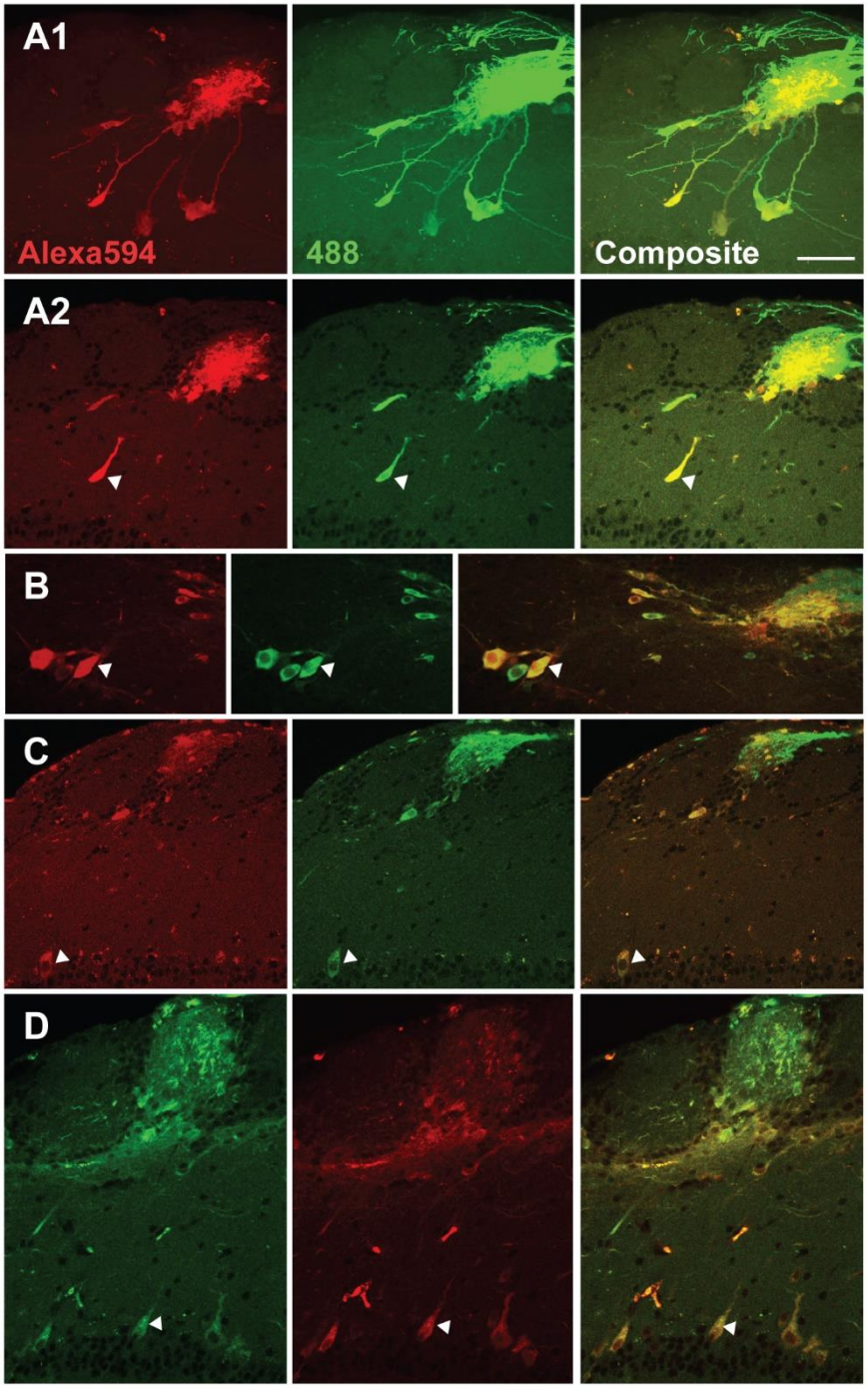

Figure 6. ***In vivo*** **electroporation reliably labels the post-synaptic targets of a single glomerulus.** A. Sequential dual-color electroporation of control M72 glomerulus using theta glass electrode and no change in electrode tip position between sequential single-color electroporations of Alexa

Fluor 594 Dextran and Alexa Fluor 488 Dextran. **A1.** Max projection image of one physical section containing the M72 glomerulus and dual-labeled JGCs and M/TCs. **A2.** Optical section from physical section from **A1.** White arrowhead corresponds to dual-labeled TC soma. **B-C.** Optical sections from separate sequential dual-color electroporations of two control M72 glomeruli using theta glass electrode and ~20 µm movement of electrode tip position between single-color electroporations of Alexa Fluor 594 Dextran and Alexa Fluor 488 Dextran. White arrowheads correspond to dual-labeled MC somata. **D.** Optical section from dual-color electroporation of control M72 glomerulus using two separate electrodes backfilled with either Alexa Fluor 594 Dextran or Alexa Fluor 488 Dextran. White arrowhead corresponds to dual-labeled MC. Scale bar: 50 µm

2.3.7 cFos staining reveals strong activation of the M72 glomerulus by an M72 ligand

We find that methyl salicylate odorant exposure increases the volume of the M72 glomerulus, while hexanal odorant exposure does not change the volume of the M72 glomerulus. We attribute these effects to the activation of the M72 glomerulus by methyl salicylate, a known ligand, while hexanal is a known non-M72 ligand. Methyl salicylate, a known strong activator of the M72 glomerulus, also activates a number of additional glomeruli across the dorsal OB. Recent data from the Rinberg lab show that 2-OH acetophenone may be a more selective, strong activator for the M72 glomerulus (Arneodo et al., 2017). We use this odorant to examine an alternative way to measure glomerulus activation by putative ligands. Here, we use cFos staining to compare the relative activation of the M72 glomerulus by 2-OH acetophenone and piperonal, an odorant known to not activate M72. We find that acute exposure to 2-OH acetophenone dramatically increases the number of cFos+ periglomerular cells near the M72 glomerulus, while leaving the number of cFos+ PGCs 225-375 μm rostral or caudal to the M72 glomerulus unchanged (**Figure 7A-B**; n=4 OB from 2 animals per group; Kruskal-Wallis with Dunn's multiple comparisons test; control vs. exposed caudal: adjusted $p>0.9999$; control vs. exposed center: adjusted $p=0.0005$; control vs. exposed rostral: adjusted $p=0.2914$). Acute piperonal exposure does not change cFos+ expression in cells around the M72 glomerulus, or in cells 225-375 μm rostral or caudal to the M72 glomerulus (**Figure 7B-C**; n=4 OB from 2 animals per group; Kruskal-Wallis with Dunn's multiple comparisons test; all adjusted $p>0.9999$). Unfortunately, 2-OH acetophenone is a highly unpleasant odorant, which makes it a poor candidate for a food-based exposure paradigm. However, this method can be used to test potential odorant ligands for genetically identified glomeruli.

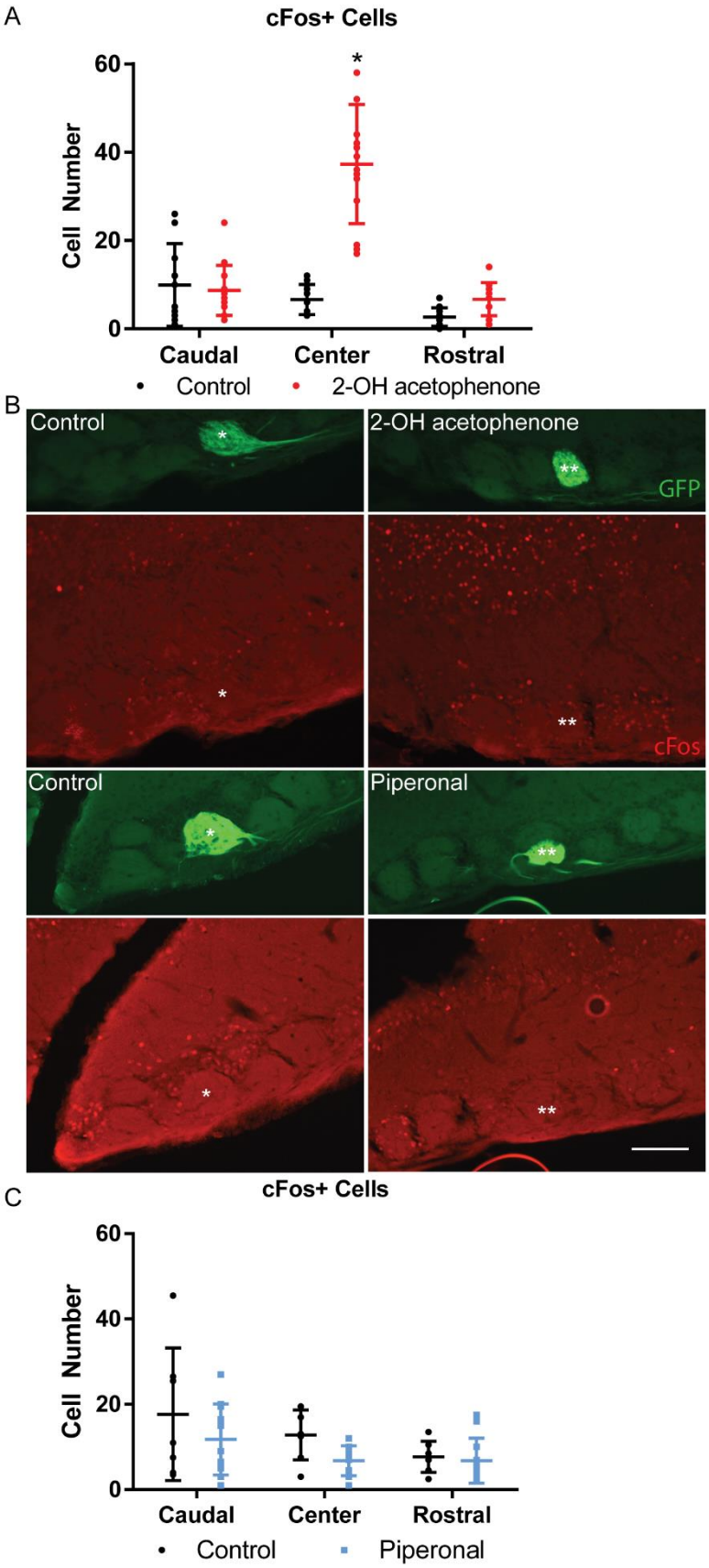
A
cFos+ Cells
Cell Number
60
40
20
0
Caudal
Center
Rostral
Control
2-OH acetophenone
B
Control
2-OH acetophenone
GFP
cFos
Control
Piperonal
C
cFos+ Cells
Cell Number
60
40
20
0
Caudal
Center
Rostral
Control
Piperonal

Figure 7. cFos staining reveals strong activation of the M72 glomerulus by an M72 ligand. A. Counting cFos positive periglomerular cells demonstrated a significant increase in cFos positive JGs around the M72 glomerulus following odorant exposure with 2-OH acetophenone, an M72 ligand. No significant increase in cFos positive cells was found in regions 225-375 μm rostral or caudal to the M72 glomerulus. **B.** Example images of sections from control, 2-OH acetophenone exposed, and piperonal mice. M72 glomerulus is shown in * denotes control glomerulus location; ** denotes odor-exposed glomerulus location. Scalebar: 100 μm. **C.** Counting cFos positive PGCs demonstrated no change in activation caudal, rostral, or around the M72 glomerulus following odorant exposure with piperonal, a non-M72 ligand.

2.4 DISCUSSION

2.4.1 Early odorant exposure profoundly changes the structure of a glomerular module

Here, we demonstrate that odorant exposure during the prenatal and early postnatal period has profound effects on the composition of the glomerular module. Namely, odorant exposure with methyl salicylate, an M72 ligand, increases the number of mitral and tufted cells connected to the M72 glomerulus by 40% and 100%, respectively.

The timing of our odorant exposure paradigm suggests that relevant early olfactory experience may specifically impact the process by which M/TC apical dendrites are pruned. Immature MCs extend multiple apical dendrites and innervate multiple nearby glomeruli (Pomeroy et al., 1990; Matsutani and Yamamoto, 2000). By P10, the majority of M/TCs complete dendritic pruning such that each M/TC projects a single apical dendrite to a single glomerulus (Malun and Brunjes, 1996; Matsutani and Yamamoto, 2000). There is some evidence that this maturation process is odor-dependent (Maher et al., 2009). Our odorant exposure paradigm begins prior to birth and continues through early postnatal development, encompassing this refinement period, and our data show that odorant exposure induces the addition of nearby M/TCs to the M72 glomerular module (**Figure 3**). Thus, specific odorant experience may stabilize the M72-glomerulus-projecting apical dendrite of M/TCs while the apical dendrites projecting to other neighboring glomeruli are eliminated. This would have the secondary effect of decreasing the number of M/TCs connected to neighboring glomeruli, although this likely represents a reduction of less than one cell per nearby glomerulus.

The dense local labeling of dendrites and axons in the glomerulus generated by *in vivo* electroporation precludes a robust analysis of the structural changes within the glomerulus itself.

The larger glomeruli produced following odorant exposure may be the product of increased OSN number or increased OSN axon branching, and odorant exposure could also increase the volume of intraglomerular processes from JGCs or M/TCs.

In this study, we specifically examine the M72 glomerulus, a dorsally located glomerulus with a number of known odorant ligands. These qualities allow for access to perform *in vivo* electroporation and also odorant exposure with an M72 ligand. However, we believe that these results will likely generalize to other glomeruli. The M72 glomerulus has been well characterized, and these analyses have been broadly applied to other glomeruli (Potter et al., 2001; Treloar et al., 2002; Feinstein and Mombaerts, 2004; Cavallin et al., 2010; Richard et al., 2010; Valle-Leija et al., 2012; Zapiec and Mombaerts, 2015). However, the relatively late development of the M72 glomerulus compared to other, more rostral glomeruli (Bailey et al., 1999; Potter et al., 2001) may mean that the effects that we observe may be more or less prominent than in glomeruli that develop earlier.

2.4.2 Anatomical changes to the M72 glomerular module are ligand-specific

Prenatal and postnatal odorant exposure to hexanal-scented food did not significantly increase M72 glomerular volume. As hexanal is not a high affinity ligand for the M72 odorant receptor, these data indicate that the structural changes induced by odorant exposure are not a result of global changes across the OB, but rather are specific to activated glomeruli. Both hexanal and methyl salicylate-exposed mice showed a preference for food odorized with the exposure odorant, suggesting that the lack of change in M72 glomerular volume of hexanal-exposed animals was not due to ineffective odorant exposure. Thus, we conclude that the observed changes in glomerulus volume are activation specific. Further analysis of the M/TC network of

the M72 glomerulus is necessary to investigate whether plasticity of the M/TC network is also activation-specific.

2.4.3 Generalizability of observed changes to a single glomerular module

In Chapter 2, we examined experience-dependent anatomical changes to a single glomerular module. Similar to what Todrank et al., 2011 described, we found that prenatal and postnatal exposure to an M72 ligand, which in our experiments was methyl salicylate, resulted in an increase in the volume of the M72 glomerulus. Todrank et al., 2011 observed that exposure to ethyl tiglate, another M72 ligand, increased the volume of the M72 glomerulus but did not increase the volume of the M71 glomerulus. Ethyl tiglate is not a known ligand of M71, suggesting that this type of odorant exposure only increases the glomerular volume of activated glomeruli. Similarly, we found that odorant exposure using a non-M72 ligand, hexanal, did not increase the volume of the M72 glomerulus. Since each odorant activates numerous glomeruli across the bulb, these experience-dependent changes may also affect other glomerular modules that are activated by methyl salicylate but which we did not examine.

2.4.4 Impact of increasing number of M/TCs connected to a specific glomerulus

Increasing the number of M/TCs connected to a single glomerulus may have several effects on odor processing. First, since M/TCs represent the output from the OB, increasing the cohort of cells specific to the M72 glomerular module will increase the representation of M72 glomerulus associated information in higher cortical areas, such as the piriform cortex. Second, increasing the number of M72 M/TCs may also increase the number of M72 M/TC lateral dendrites, and as

a result, the number of reciprocal synapses and recurrent inhibitory synapses up to 1 mm away from the M72 glomerulus (Egger and Urban, 2006). Increasing the number of M72 M/TCs could increase the strength and/or number of lateral inhibitory interactions that M72 ligands evoke in other glomerular modules.

Third, our data show that odorant exposure increases the number of M72-associated M/T cells in a spatially confined region within a few hundred microns of the M72 glomerulus. Thus, if we assume that all M/T cells extend lateral dendrites in a radially symmetric way (Mori et al., 1983), this would increase the density of lateral dendrites located close to the M72 glomerulus that are activated by M72 ligands. As these dendrites form reciprocal connections with nearby granule cells, activation of an odor-exposed M72 glomerulus would cause greater excitation of granule cells close to the M72 glomerulus, leading to increased granule cell mediated lateral inhibition between homotypic M72 M/TCs (Urban and Sakmann, 2002). Such homotypic lateral inhibition could also be modulated in the glomerular layer by periglomerular cells (Najac et al., 2015).

2.4.5 Number of M/TCs associated with a single glomerular module

Beyond the plasticity we observe following early odorant exposure, simply knowing the number of M/T cells for a given glomerulus is an important indication of the complexity of the olfactory system. Previous work using stereological estimates to assess the number of glomeruli and MCs in the OB suggest that on average, there are as many as 20-40 MCs/glomerulus in the mouse OB (Thamke et al., 1973; Benson et al., 1984; Pomeroy et al., 1990), a number and range that far exceeds any of the cell counts that we observe (maximum 11 MCs and 9 TCs). Estimates of MCs per single glomerulus also vary significantly in other species, ranging from 13-16

MCs/glomerulus in rats (Panhuber et al., 1985; Royet et al., 1998) to 9-23 MCs/glomerulus in rabbits (Allison and Warwick, 1949; Royet et al., 1998). These values were determined using estimates of the total number of glomeruli and MCs within the OB and therefore represent average MC number across all glomeruli. These estimates also vary significantly between observers, with the early mouse studies cited above reporting ~40,000 MCs and 1800 glomeruli (~21 MCs/glomerulus), while a more recent study, (Richard et al., 2010), reported 33000 MCs and 3600 glomeruli (~9 MCs/glomerulus). (Sosulski et al., 2011) also reported an average of ~9 MCs/glomerulus after using *in vivo* electroporation to label the post-synaptic targets of single glomeruli located on the dorsal and lateral OB. The M/TC counts reported by both Richard et al., 2010 and Sosulski et al., 2011 are more similar to our results (average across both groups: ~8 MCs/glomerulus and ~4.5 TCs/glomerulus), suggesting that the range of M/TCs per glomerulus may be larger than previously thought. Here, we use an approach similar to that used by Sosulski et al., 2011 that allows us to determine the number of M/TCs per glomerulus for a single, genetically identified glomerulus, with low animal-to-animal variability (**Figure 6**). Thus, although our M/TC counts are lower than some of those previously reported, we believe that this may reflect the relative sparsity of M72-expressing OSNs, and that the specificity and reliability of our approach allow us to make valid comparisons between animals about the number of M/TCs per glomerulus. Using *in vivo* electroporation, we show that early odorant exposure to a ligand odorant significantly changes the structure of both the glomerulus and the M/TC network of the activated M72 glomerular module.

3.0 PRENATAL AND EARLY POSTNATAL FOOD-BASED ODORANT EXPOSURE HEIGHTENS MITRAL CELL ODOR-EVOKED RESPONSES

3.1 INTRODUCTION

The olfactory bulb (OB) has a stereotyped structure, the organization of which is dictated in part by odorant receptor (OR) identity (Ressler et al., 1994; Vassar et al., 1994; Potter et al., 2001; Bozza et al., 2002; Treloar et al., 2002; Feinstein and Mombaerts, 2004; Komiyama and Luo, 2006). Olfactory sensory neurons (OSNs) send axons to the OB, where axons from OSNs expressing the same OR converge into roughly spherical structures called glomeruli. Each glomerulus contains dendrites of a cohort of juxtaglomerular and primary projection neurons, the mitral and tufted cells (M/TCs) – together, these make up a glomerular module, the basic odor-coding unit of the OB. Each glomerular module thus has a genetic identity based on OR expression as well as a cohort of activating odorant ligands for the corresponding OR.

This OR-identity based organization facilitates the investigation of how specific olfactory experiences change the OB. Anatomical studies demonstrate that the OB circuitry is highly plastic and subject to experience-dependent structural changes throughout both development and adulthood. Odor exposure using a number of different conditioning paradigms increases glomerular volume (Woo et al., 1987; Todrank et al., 2011; Dias and Ressler, 2014; Morrison et al., 2015). Combined prenatal and early postnatal odor exposure increases both glomerular

volume and associated M/T cell number (Todrank et al., 2011; Liu et al., 2016), while early aversive conditioning accelerates the rate of glomerular convergence (Kerr and Belluscio, 2006). Early postnatal passive odorant exposure has also been shown to decrease cell turnover in the glomerular and granule cell layers (Woo et al., 2006). In adult mice, aversive odorant conditioning increases OSN number and glomerular volume – these changes are reversed following the extinguishing of the learned aversive response (Morrison et al., 2015). These studies use different conditioning or exposure paradigms, yet they all have significant effects of OB circuitry, suggesting that several distinct mechanisms may influence the development and maintenance of OB structure. These large modifications to OB circuitry may in turn have significant effects on the representation and processing of odorants in the OB.

Odor-evoked activity in the rodent OB is also influenced by odorant experience and exposure. Rodents demonstrate both acute and chronic reductions in the amplitude and probability of odor-evoked excitatory M/TC responses following repeated odor presentation (Chaudhury et al., 2010; Kato et al., 2012). In rats, early postnatal odorant exposure paired with positive somatosensory stimuli decreases the number of excitatory M/TC responses elicited by the learned odorant while leaving responses to unassociated odorants unchanged (Wilson et al., 1985, 1987). However, the potential relationship between experience-dependent anatomical circuit changes and odor-evoked activity in the OB is not well understood.

Here, we use an odor exposure paradigm with a previously characterized anatomical correlate to understand how odor representation may be affected by these changes in circuit structure. Todrank et al., 2011, and Liu et al., 2016, found that food-based prenatal and early postnatal odorant exposure increases glomerulus volume and the number of M/T cells corresponding to activated glomerular modules, while increasing behavioral preference for the

odor that was paired with food. Given that a single odorant activates multiple glomeruli across the OB, these observed changes in glomerular volume and M/TC number could be generalized to many glomeruli and thus have a large distributed impact on odor representation in the OB. We use this odorant exposure paradigm to investigate how early chronic food-based odorant exposure, a paradigm known to effect anatomical changes, affects odor-evoked responses of MCs in the dorsal mouse OB. Surprisingly, we find that odor-evoked calcium transients in MCs are broadly enhanced rather than reduced in this food pairing paradigm.

3.2 MATERIALS AND METHODS

3.2.1 Animals and surgical methods

All experiments were done in male and female M72-IRES-tauGFP mice. Imaging was done on adult mice. During all surgical procedures, animals were anesthetized using a ketamine/xylazine mixture, provided analgesia using carprofen injections, and maintained at 37°C body temperature. Expression of GCaMP6s was achieved through injection of 1 µl of AAV-hsyn-GCaMP6s ~250 µm underneath the pial surface in the dorsal posterior OB surface. Animals were allowed to recover for 2 weeks, after which they were used for acute *in vivo* anesthesized imaging experiments. For acute imaging, a 2 mm diameter craniotomy was made over the dorsal posterior OB and covered with low melting point agarose. A coverslip was secured over the craniotomy using dental cement to minimize z-plane movement. Imaging was done in anesthetized animals maintained at 37°C body temperature.

3.2.2 Odorant exposure

Prenatal and early postnatal odorant exposure was performed on M72-IRES-tauGFP mice as detailed in Todrank et al., 2011, and Liu et al., 2016. Food was mixed with either methylsalicylate (mint) or hexanal (1% by volume) and dried under a fume hood for 3 days. Breeding pairs were fed with either control, mint-scented, or hexanal-scented food for the duration of gestation and nursing (**Figure 8A**). Litters were subsequently weaned onto and continuously fed with either control, mint-scented, or hexanal-scented food until acute calcium imaging experiments. Both male and female mice were used for imaging. Breeding pairs were weighed regularly to ensure that odorized food did not interfere with food consumption. Odorant-exposed litters were not of substantially different weights from control litters.

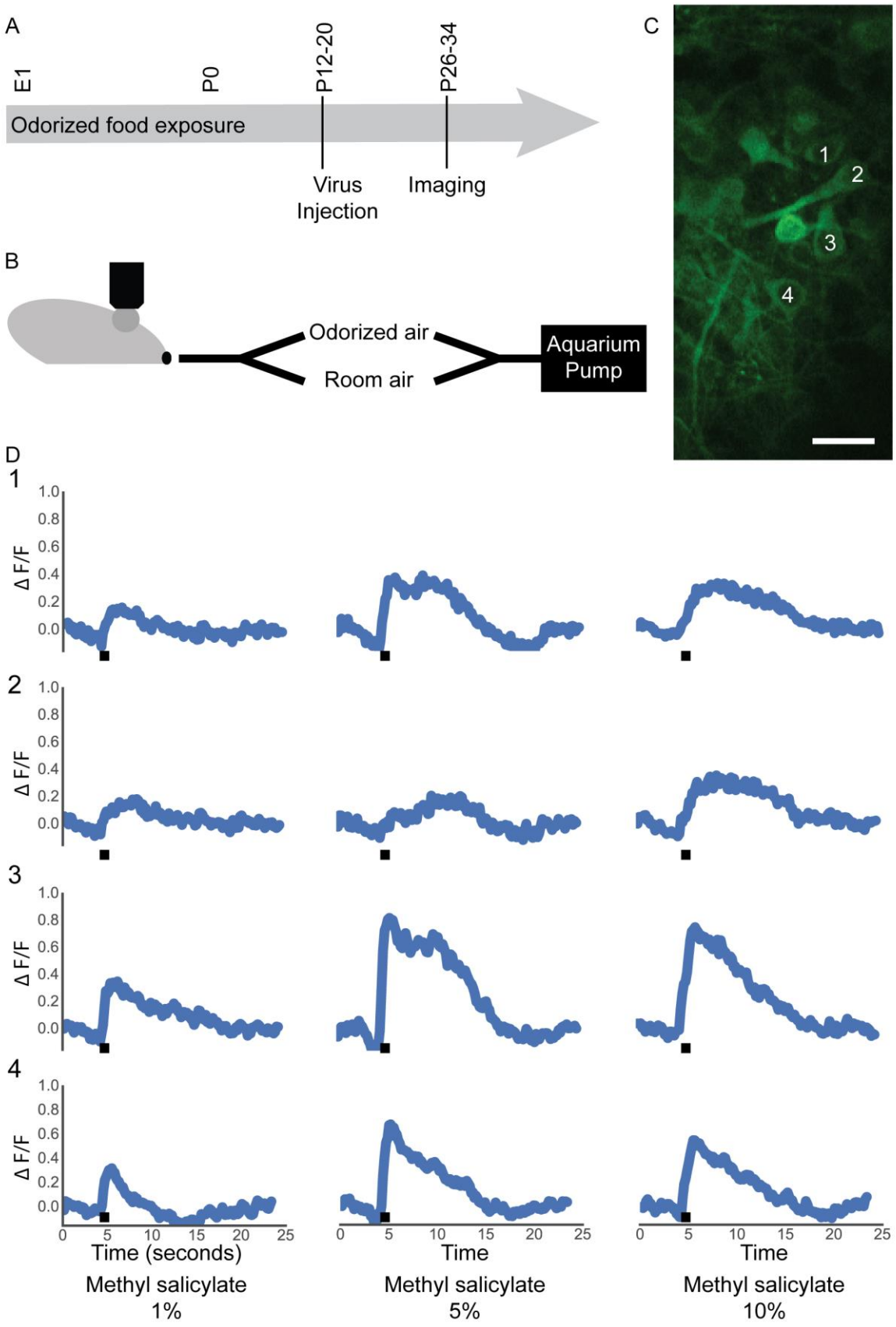
A
E1
P0
P12-20
P26-34
Odorized food exposure
Virus Injection
Imaging
B
Odorized air
Room air
Aquarium Pump
C
1
2
3
4
D
1
2
3
4
ΔF/F
1.0
0.8
0.6
0.4
0.2
0.0
0
5
10
15
20
25
Time (seconds)
Time
Methyl salicylate 1%
Methyl salicylate 5%
Methyl salicylate 10%

Figure 8. Odor-evoked calcium responses in the MC layer. **A.** Odorized food exposure lasted through the entirety of gestation and the postnatal period until imaging at P26-P34. Virus injection into the dorsal OB was done at P12-P20. Imaging was performed 2 weeks after virus injection. **B.** The dorsal OB was imaged during stimulus presentation using a custom-built 2-channel olfactometer with airflow provided by an aquarium pump. **C.** The MC layer was imaged with manual ROI selection. Four cells are labeled, with corresponding odor-evoked responses shown in **D.** White scale bar = 25μm. Black bar indicates 1 second odor stimulus.

3.2.3 Stimulus delivery

Each trial consisted of 4 seconds room air, 1 second odorized air, and 25 seconds room air. Each odorant was presented 4 times in pseudorandom stimulus order and with inter-trial interval length of at least 1 minute. Stimuli consisted of 8 odorants diluted in mineral oil at different concentrations (1%: isoamyl acetate (IAA), hexanal, methyl salicylate (MS), ethyl butyrate (EB), propionic acid (PA), hexanone, acetophenone (AP), and 2-OH acetophenone (THA); 5%: isoamyl acetate, hexanal, methyl salicylate; 10%: isoamyl acetate, hexanal, methyl salicylate). All odorants are known dorsal OB ligands. Odorants were delivered using a custom built olfactometer controlled via TTL input from a HEKA ITC-18 external DA/AD/TTL device run by IGOR Pro (RRID:SCR_000325; **Figure 8B**).

3.2.4 Imaging

Two-photon imaging was done in the MC layer ~150-225 microns under the pial surface using a VIVO 2-Photon system from 3I Intelligent Imaging Innovations and SlideBook Imaging software. Image capture rate was 6-9Hz.

3.2.5 Analysis

The dataset consists of 862 cells from 17 mice (5 control, 6 mint-exposed, and 6 hexanal-exposed; at least 200 cells in each odor-exposure group) for a total of 12945 cell-odor pairs. To select ROIs, cell somata in each field of view were traced manually using SlideBook software and avoiding intersecting cell processes as determined by Z-stacks of each field of view (**Figure**

8C). All detected GCaMP6 fluorescent cells were included; cell responsiveness was not a metric used to determine cell selection. Raw intensity values were calculated using SlideBook software. dF/F traces were calculated using the average baseline intensity from the frames prior to stimulus onset at 4s after start of the trial. Traces were detrended by subtracting a polynomial fit from the calculated dF/F trace (**Figure 8D**). Response threshold was set at 3 standard deviations away from baseline. All analysis and visualization was done using Python (RRID:SCR_008394; Code available at Github repository). Some statistical tests were performed using Graphpad Prism (RRID:SCR_002798).

3.3 RESULTS

3.3.1 Majority of MC odor-evoked responses were excitatory

MC odor-evoked responses were dominated by excitatory responses, constituting 11606 cell-odor pairs out of 12945 total cell-odor pairs or ~89% of all measured responses. Both peak and integral of odor-evoked response were calculated. Due to sparsity of inhibitory responses across three treatment groups and across the odor panel, there were not enough inhibitory responses per group to statistically measure differences in inhibitory responses. However, inhibitory responses are displayed in subsequent box plots. A strong correlation between peak and integral of individual responses was observed (pearson r = 0.97; **Figure 9C**), but there was no significant correlation between initial baseline intensity and either peak (pearson r = -0.0048) or integral of responses (pearson r = -0.018) (**Figure 9A-B**). Thus, all data were pooled regardless of initial baseline intensity. Given the strong correlation between peak and integral of odor-evoked

response, subsequent data regarding odorant-evoked responses are shown as peak values. The distribution of all responses to all odorants are visualized in **Figure 9D**, with significant statistical differences observed between the response density functions of MCs from control, hexanal-exposed, and mint-exposed animals (Kruskal-Wallis test with Tukey's multiple comparisons test; p=6.65E-199; Adjusted p-values between groups approximated 0).

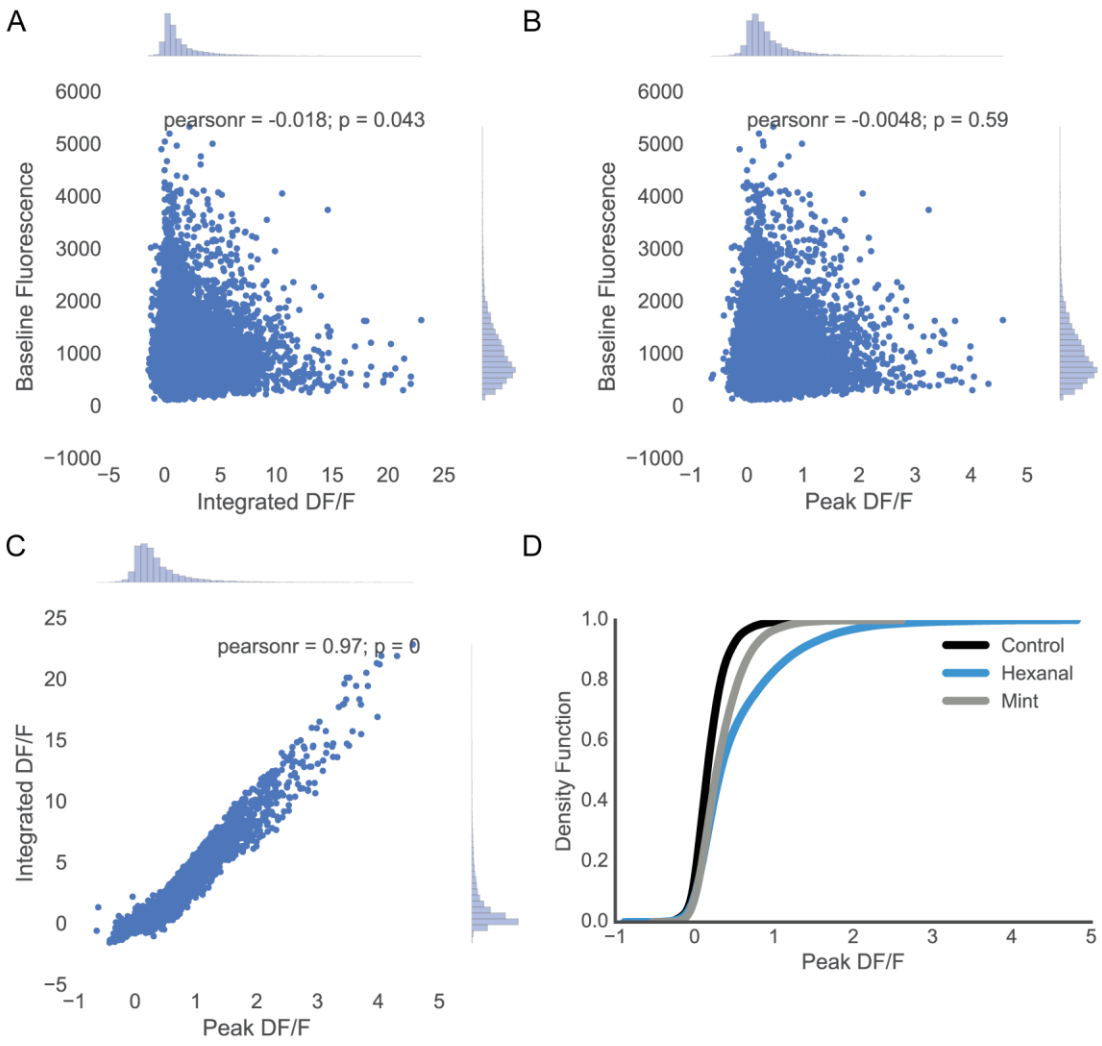

Figure 9. Response characteristics. **A.** Integral and baseline of response are not correlated. **B.** Peak and baseline of response are not correlated. **C.** Peak and integral of response are strongly correlated. **D.** KDE describing distribution of responses across all cells and odorants in control, hexanal-exposed, and mint-exposed mice (statistically significant distributions between groups).

3.3.2 Odorant exposure changes odor tuning

Two qualitatively distinct odorants were used for odor-exposure groups. Methyl salicylate has a wintergreen scent and activates both olfactory and trigeminal responses, while hexanal has a green grass scent and activates only olfactory receptors. Both odorants are strong activators of glomeruli on the dorsal OB surface in rats and mice, with different but overlapping activation areas (Glomerular Activity Response Archive, Michael Leon, *gara.bio.uci.edu/index.jsp,* Wachowiak and Cohen, 2001, 2003*).* Given the responses elicited by these two odorants, we investigated whether chronic early exposure with either odorant would shift the odor tuning of mice in each exposure group. We exposed animals to these odors by adding these odors to the food provided to these animals, as described previously (Todrank et al., 2011; Liu et al., 2016), a manipulation which results in altered preference for the conditioned food. To evaluate tuning across animals and cells in which differences in GCaMP expression, cell depth, and other factors would significantly complicate assessing average responses, we primarily examined the ranking of responses to different odors within individual cells. This ranking of responses to odorants should be largely independent of these factors that will likely vary from cell to cell and animal to animal. We assigned response ranks to each odorant on a within cell basis, using all measured odor-evoked responses. Ranks were assigned in ascending order, with the odor corresponding to the largest evoked response assigned the largest numerical rank (14). There were significant differences in the rank of specific odorants between control, mint-exposed, and hexanal-exposed groups **(Figure 10)**. We have listed these in table form in **Figure 10E**. For clarity, results of statistical comparisons and descriptive statistics are listed in **Table 1**. The control group (n=225 cells) differed from the mint-exposed group (n=269 cells) on 6 out of 14 possible odorant/concentration combinations (Kruskal-Wallis test followed by Dunn's multiple

comparisons test). The control group differed from the hexanal-exposed group (n=369 cells) on 10 out of 14 odorant/concentration combinations. Mint-exposed and hexanal-exposed groups differed on 8 of 14 odorant/concentration combinations. These data show that food-based prenatal and postnatal odorant exposure does change relative stimulus preference, as demonstrated by comparisons of individual odor ranks. There are also odor-specific differences between the mint-exposed and hexanal-exposed groups, suggesting that the identity of the conditioning odorant could impact resultant changes in odorant response ranking.

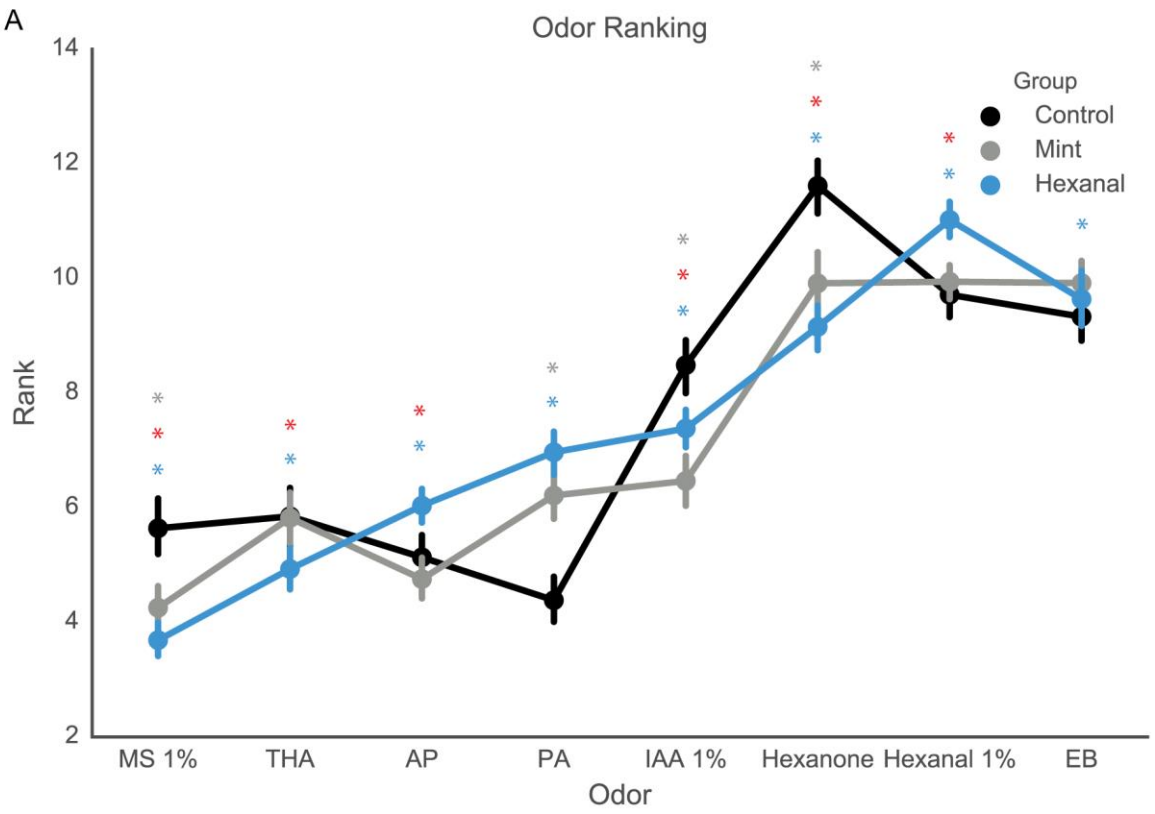

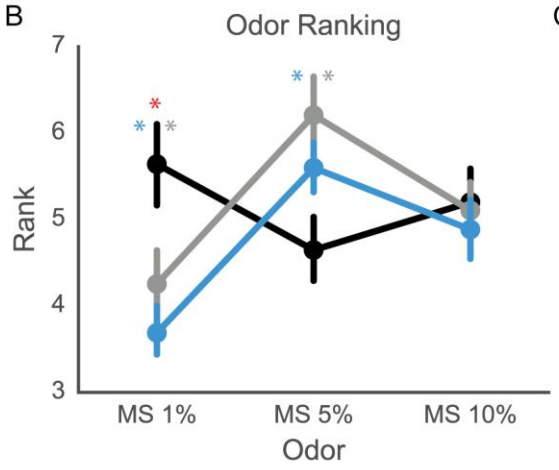

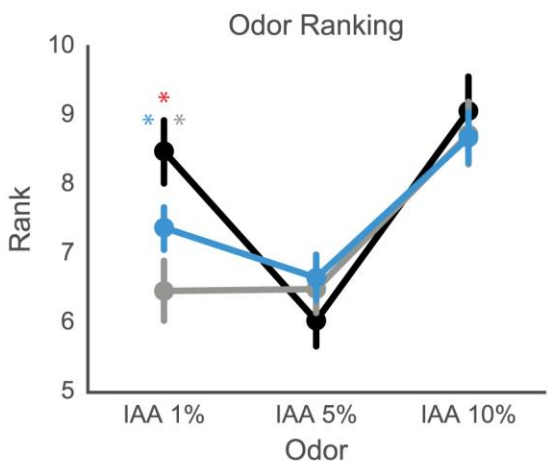

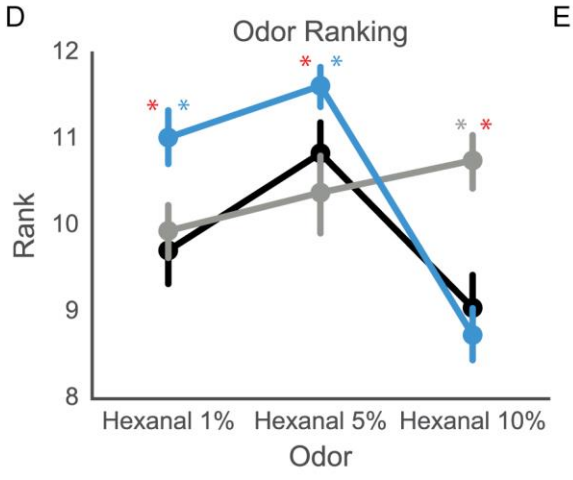

E

Significant Comparisons		
C vs. M	**C vs. H**	**H vs. M**
	AP	AP
	EB	
hexanone	hexanone	hexanone
PA	PA	
	THA	THA
hexanal, 10%		
	hexanal, 1%	hexanal, 1%
	hexanal, 5%	hexanal, 5%
IAA, 1%	IAA, 1%	hexanal, 10%
MS, 1%	MS, 1%	MS, 1%
MS 5%	MS, 5%	

Figure 10. Odor ranking changes for specific odorants following odor exposure. **A.** Response rank for each odor calculated on a cell-by-cell basis. Odorants at 1% concentration displayed. **B-D.** Response rank for multiple concentrations of methyl salicylate (**B.**), isoamyl acetate (**C.**), and hexanal (**D.**). **E.** Table of significant differences in odorant ranks for each group comparison. Gray *: significant difference between mint-exposed and control groups; blue *: significant difference between hexanal-exposed and control groups; red *: significant difference between mint- and hexanal-exposed groups.

Table 1. Comparison of odor ranks. Statistical test results of odor ranks between control, mint-, and hexanal-exposed groups. Data shown in **Figure 10.**

Comparison	Test	P-value	Significant	Median C	Median M	Median H
Response Rank				**C; N=225**	**M; N=268**	**H; N=369**
AP; all groups	**Kruskal-Wallis**	**<0.0001**	**Yes**	**5**	**4**	**6**
AP; C vs. M	Dunn's	0.417	No	5	4	
AP; C vs. H	**Dunn's**	**0.0002**	**Yes**	**5**		**6**
AP; H vs. M	**Dunn's**	**<0.0001**	**Yes**		**4**	**6**
EB; all groups	**Kruskal-Wallis**	**0.0176**	**Yes**	**10**	**10**	**11**
EB; C vs. M	Dunn's	0.2086	No	10	10	
EB; C vs. H	**Dunn's**	**0.0138**	**Yes**	**10**		**11**
EB; H vs. M	Dunn's	>0.9999	No		10	11
Hexanal 1%; all groups	**Kruskal-Wallis**	**<0.0001**	**Yes**	**10**	**10**	**12**
Hexanal 1%; C vs. M	Dunn's	>0.9999	No	10	10	
Hexanal 1%; C vs. H	**Dunn's**	**<0.0001**	**Yes**	**10**		**12**
Hexanal 1%; H vs. M	**Dunn's**	**<0.0001**	**Yes**		**10**	**12**
Hexanone; all groups	**Kruskal-Wallis**	**<0.0001**	**Yes**	**13**	**11**	**11**
Hexanone; C vs. M	**Dunn's**	**<0.0001**	**Yes**	**13**	**11**	
Hexanone; C vs. H	**Dunn's**	**<0.0001**	**Yes**	**13**		**11**
Hexanone; H vs. M	**Dunn's**	**0.0001**	**Yes**		**11**	**11**
IAA 1%; all groups	**Kruskal-Wallis**	**<0.0001**	**Yes**	**9**	**6**	**7**
IAA 1%; C vs. M	**Dunn's**	**<0.0001**	**Yes**	**9**	**6**	
IAA 1%; C vs. H	**Dunn's**	**0.0004**	**Yes**	**9**		**7**
IAA 1%; H vs. M	**Dunn's**	**0.0065**	**Yes**		**6**	**7**
MS 1%; all groups	**Kruskal-Wallis**	**<0.0001**	**Yes**	**5**	**3**	**3**
MS 1%; C vs. M	**Dunn's**	**<0.0001**	**Yes**	**5**	**3**	
MS 1%; C vs. H	**Dunn's**	**<0.0001**	**Yes**	**5**		**3**
MS 1%; H vs. M	**Dunn's**	**0.0391**	**Yes**		**3**	**3**
PA; all groups	**Kruskal-Wallis**	**<0.0001**	**Yes**	**4**	**5**	**7**
PA; C vs. M	**Dunn's**	**<0.0001**	**Yes**	**4**	**5**	
PA; C vs. H	**Dunn's**	**<0.0001**	**Yes**	**4**		**7**
PA; H vs. M	Dunn's	0.0908	No		5	7
THA; all groups	**Kruskal-Wallis**	**0.0028**	**Yes**	**5**	**5**	**4**
THA; C vs. M	Dunn's	>0.9999	No	5	5	
THA; C vs. H	**Dunn's**	**0.0234**	**Yes**	**5**		**4**
THA; H vs. M	**Dunn's**	**0.0071**	**Yes**		**5**	**4**
MS 5%; all groups	**Kruskal-Wallis**	**<0.0001**	**Yes**	**4**	**6**	**5**
MS 5%; C vs. M	**Dunn's**	**<0.0001**	**Yes**	**4**	**6**	

MS 5%; C vs. H	**Dunn's**	**0.0001**	**Yes**	**4**		**5**
MS 5%; H vs. M	Dunn's	0.4328	No		6	5
MS 10%; all groups	Kruskal-Wallis	0.0731	No	5	5	4
MS 10%; C vs. M	Dunn's	>0.9999	No	5	5	
MS 10%; C vs. H	Dunn's	0.1503	No	5		4
MS 10%; H vs. M	Dunn's	0.1864	No		5	4
IAA 5%; all groups	Kruskal-Wallis	0.1561	No	7	7	6
IAA 5%; C vs. M	Dunn's	0.3965	No	7	7	
IAA 5%; C vs. H	Dunn's	0.1912	No	7		6
IAA 5%; H vs. M	Dunn's	>0.9999	No		7	6
IAA 10%; all groups	Kruskal-Wallis	0.3245	No	10	9	9
IAA 10%; C vs. M	Dunn's	0.6739	No	10	9	
IAA 10%; C vs. H	Dunn's	0.4643	No	10		9
IAA 10%; H vs. M	Dunn's	>0.9999	No		9	9
Hex 5%; all groups	**Kruskal-Wallis**	**<0.0001**	**Yes**	**12**	**12**	**12**
Hex 5%; C vs. M	Dunn's	>0.9999	No	12	12	
Hex 5%; C vs. H	**Dunn's**	**0.0012**	**Yes**	**12**		**12**
Hex 5%; H vs. M	**Dunn's**	**<0.0001**	**Yes**		**12**	**12**
Hex 10%; all groups	**Kruskal-Wallis**	**<0.0001**	**Yes**	**9**	**12**	**9**
Hex 10%; C vs. M	**Dunn's**	**<0.0001**	**Yes**	**9**	**12**	
Hex 10%; C vs. H	Dunn's	0.7317	No	9		9
Hex 10%; H vs. M	**Dunn's**	**<0.0001**	**Yes**		**12**	**9**

3.3.3 Amplitude of excitatory response increases following early odorant exposure

Several additional features of the odor-evoked response change significantly following early odorant exposure. The amplitude of excitatory odor-evoked responses increases significantly for cells in both odor-exposed groups as compared to cells in the control animals (**Figure 11A**). **Figure 11B** shows clear differences in median DF/F across all odorants at 1% concentration for control vs. hexanal- and mint-exposed and for hexanal vs. mint-exposed. This increase in response amplitude is not odor-specific, but rather is observed for almost all odors and concentrations in the odor stimulus panel (**Figure 11, 12**). Descriptive and odor-specific group comparison statistics can be found in **Table 2**.

Within-group differences in responses to the same odorant were also observed across concentrations (**Figure 12**). However, these concentration differences were largely similar between the control, mint-exposed, and hexanal-exposed groups, suggesting that the increased responsiveness seen following odor exposure was not specific to a single concentration. There were 2 combinations of odorants and concentrations for which significant differences were observed in all 3 exposure groups, 2 additional combinations with significant differences observed in only the control group, 1 additional observed in the mint-exposed group, and 2 additional observed in the hexanal-exposed group (Kruskal-Wallis test followed by Dunn's multiple comparisons test). Full details about statistical comparisons available in **Table 3**.

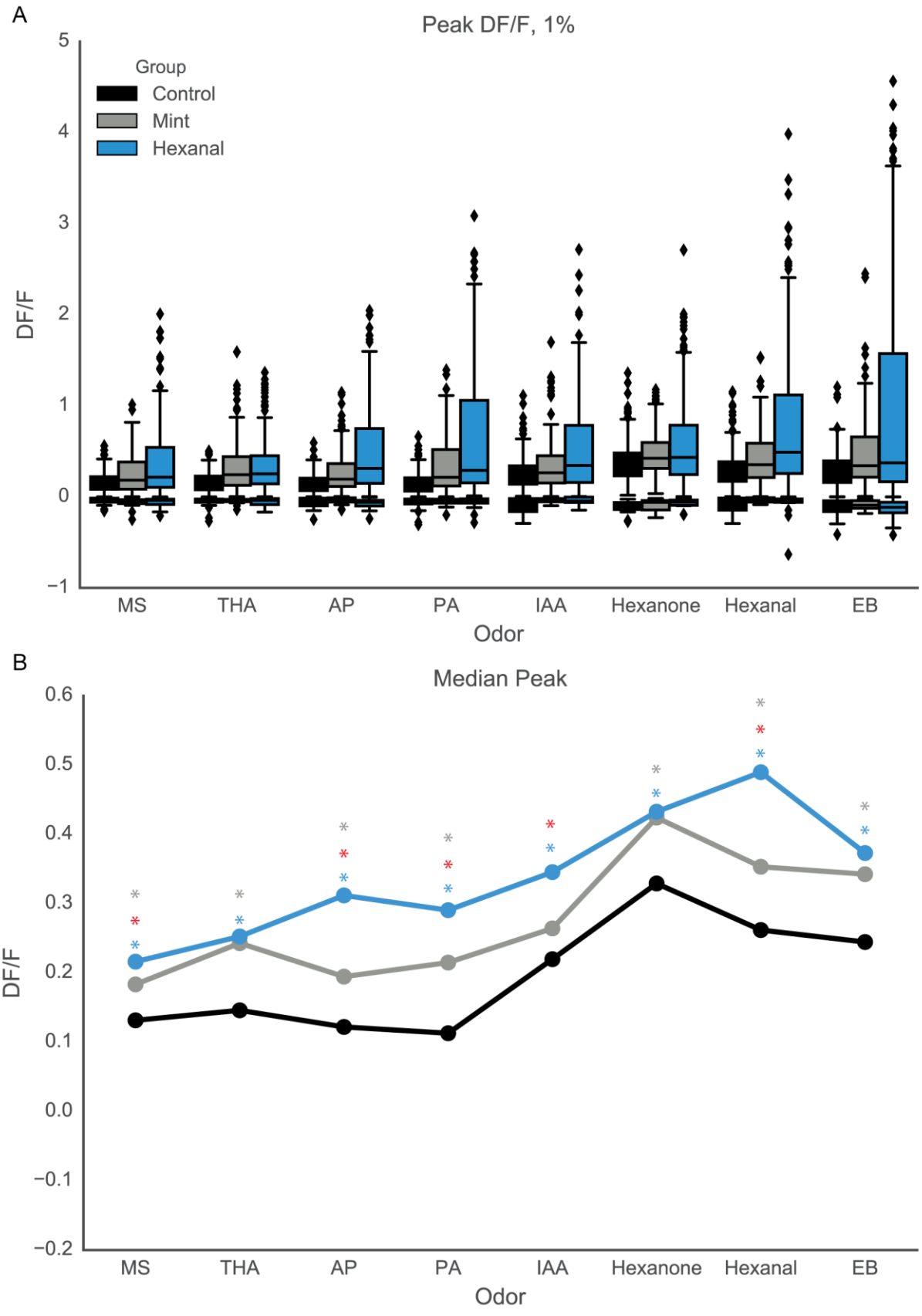
A
Peak DF/F, 1%
Group
Control
Mint
Hexanal
DF/F
5
4
3
2
1
0
−1
MS
THA
AP
PA
IAA
Hexanone
Hexanal
EB
Odor
B
Median Peak
DF/F
0.6
0.5
0.4
0.3
0.2
0.1
0.0
−0.1
−0.2
MS
THA
AP
PA
IAA
Hexanone
Hexanal
EB
Odor

Figure 11. Odor exposure increases median amplitude of MC response to odorants at 1% concentration by volume. **A.** Boxplot describing distribution of peak odor-evoked DF/F of MC response to odorants at 1% concentration by volume. (Abbreviations: MS – methyl salicylate, THA – 2-OH acetophenone, AP – acetophenone, PA – propionic acid, IAA – isoamyl acetate, EB – ethyl butyrate) **B.** Median peak DF/F across all odorants at 1% concentration by volume. Gray *: significant difference between mint-exposed and control groups; blue *: significant difference between hexanal-exposed and control groups; red *: significant difference between mint- and hexanal-exposed groups. For graphical clarity, significance was denoted on median graph (**B**) rather than on box plots as well. For detailed statistics, refer to **Table 2**.

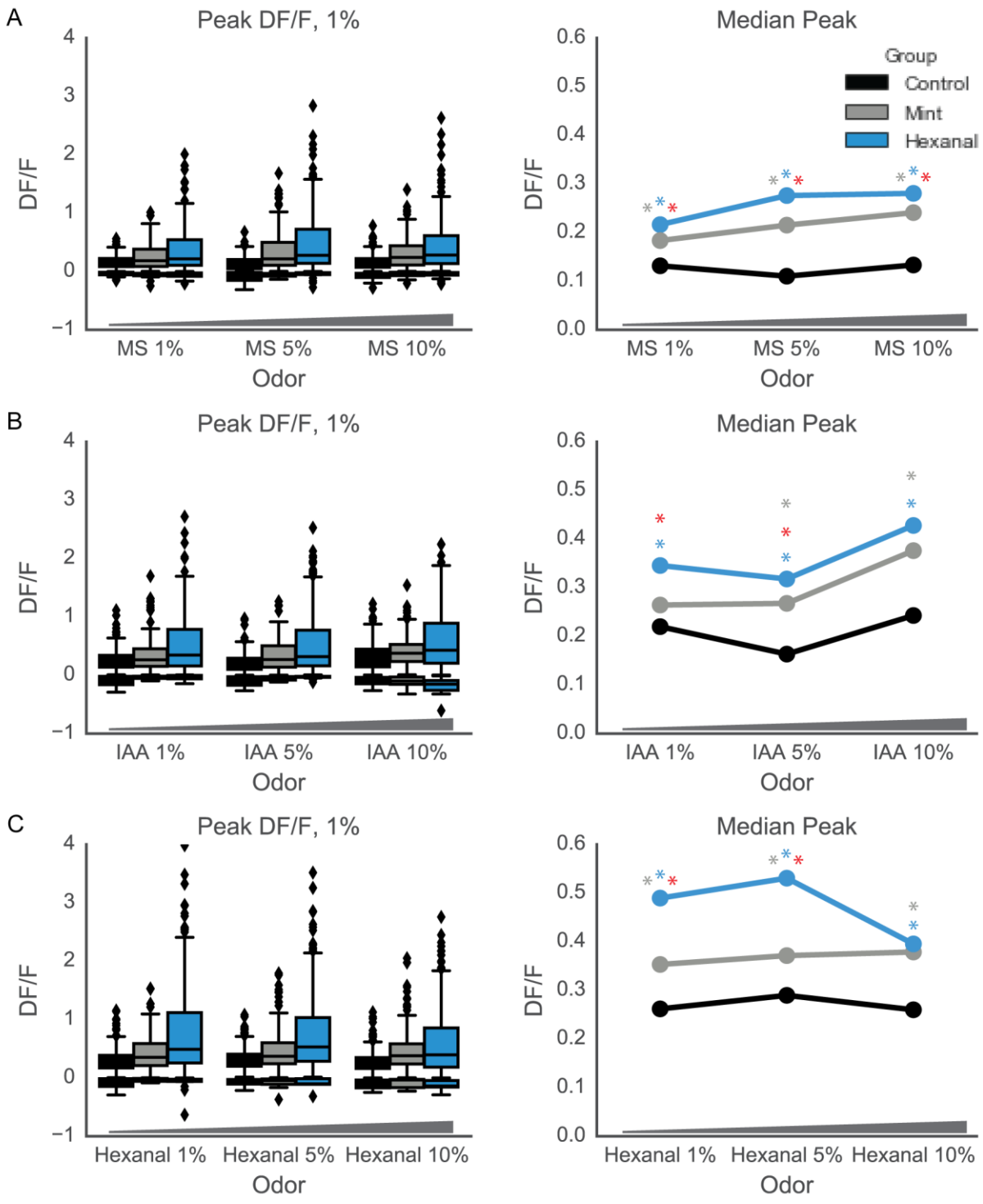

Figure 12. Odor exposure increases median amplitude of MC response to odorants across concentrations. Mint-exposed and hexanal-exposed MCs have higher medians of peak DF/F across all concentrations of methyl salicylate (**A.**), isoamyl acetate (**B.**), and hexanal (**C.**). Gray *:

significant difference between mint-exposed and control groups; blue *: significant difference between hexanal-exposed and control groups; red *: significant difference between mint- and hexanal-exposed groups. For graphical clarity, significance was denoted on median graphs rather than on box plots as well. We list significant within-group comparisons here: **Control**: IAA 1% vs. 5%; IAA 5% vs. 10%; Hexanal 5% vs. 10%; **Mint**: IAA 1% vs. 10%, IAA 5% vs. 10%; **Hexanal**: MS 1% vs. 5%; IAA 5% vs. 10%; Hexanal 1% vs. 10%; Hexanal 5% vs. 10%.

Table 2. Comparisons of excitatory response amplitude, 1% odorant concentration. Statistical test results of excitatory response amplitudes of cells from control, mint-, and hexanal-exposed groups in response to odorants at 1% concentration. Data shown in **Figure 11.**

Comparison	Test	P-value	Significant	Median C	Median M	Median H
Peak ΔF/F Amplitude				**C; N=225**	**M; N=268**	**H; N=369**
IAA 10%; all groups	**Kruskal-Wallis**	**<0.0001**	**Yes**	**0.216**	**0.3547**	**0.3697**
IAA 10%; C vs. M	**Dunn's**	**<0.0001**	**Yes**	**0.216**	**0.3547**	
IAA 10%; C vs. H	**Dunn's**	**<0.0001**	**Yes**	**0.216**		**0.3697**
IAA 10%; H vs. M	Dunn's	0.0967	No		0.3547	0.3697
IAA 1%; all groups	**Kruskal-Wallis**	**<0.0001**	**Yes**	**0.2018**	**0.2389**	**0.3306**
IAA 1%; C vs. M	**Dunn's**	**0.0745**	**No**	**0.2018**	**0.2389**	
IAA 1%; C vs. H	**Dunn's**	**<0.0001**	**Yes**	**0.2018**		**0.3306**
IAA 1%; H vs. M	**Dunn's**	**0.0001**	**Yes**		**0.2389**	**0.3306**
AP; all groups	**Kruskal-Wallis**	**<0.0001**	**Yes**	**0.1081**	**0.1837**	**0.2822**
AP; C vs. M	**Dunn's**	**<0.0001**	**Yes**	**0.1081**	**0.1837**	
AP; C vs. H	**Dunn's**	**<0.0001**	**Yes**	**0.1081**		**0.2822**
AP; H vs. M	**Dunn's**	**<0.0001**	**Yes**		**0.1837**	**0.2822**
MS 10%; all groups	**Kruskal-Wallis**	**<0.0001**	**Yes**	**0.1026**	**0.1961**	**0.2566**
MS 10%; C vs. M	**Dunn's**	**<0.0001**	**Yes**	**0.1026**	**0.1961**	
MS 10%; C vs. H	**Dunn's**	**<0.0001**	**Yes**	**0.1026**		**0.2566**
MS 10%; H vs. M	**Dunn's**	**0.0143**	**Yes**		**0.1961**	**0.2566**
IAA 5%; all groups	**Kruskal-Wallis**	**<0.0001**	**Yes**	**0.1404**	**0.2386**	**0.2973**
IAA 5%; C vs. M	**Dunn's**	**<0.0001**	**Yes**	**0.1404**	**0.2386**	
IAA 5%; C vs. H	**Dunn's**	**<0.0001**	**Yes**	**0.1404**		**0.2973**
IAA 5%; H vs. M	**Dunn's**	**0.0023**	**Yes**		**0.2386**	**0.2973**
Hexanal 1%; all groups	**Kruskal-Wallis**	**<0.0001**	**Yes**	**0.2409**	**0.3421**	**0.4718**
Hexanal 1%; C vs. M	**Dunn's**	**<0.0001**	**Yes**	**0.2409**	**0.3421**	
Hexanal 1%; C vs. H	**Dunn's**	**<0.0001**	**Yes**	**0.2409**		**0.4718**
Hexanal 1%; H vs. M	**Dunn's**	**0.0001**	**Yes**		**0.3421**	**0.4718**
EB; all groups	**Kruskal-Wallis**	**<0.0001**	**Yes**	**0.2262**	**0.3254**	**0.3204**
EB; C vs. M	**Dunn's**	**<0.0001**	**Yes**	**0.2262**	**0.3254**	
EB; C vs. H	**Dunn's**	**<0.0001**	**Yes**	**0.2262**		**0.3204**
EB; H vs. M	Dunn's	0.6847	No		0.3254	0.3204
MS 1%; all groups	**Kruskal-Wallis**	**<0.0001**	**Yes**	**0.1167**	**0.1641**	**0.1933**
MS 1%; C vs. M	**Dunn's**	**0.0028**	**Yes**	**0.1167**	**0.1641**	
MS 1%; C vs. H	**Dunn's**	**<0.0001**	**Yes**	**0.1167**		**0.1933**
MS 1%; H vs. M	**Dunn's**	**0.0026**	**Yes**		**0.1641**	**0.1933**
PA; all groups	**Kruskal-Wallis**	**<0.0001**	**Yes**	**0.0733**	**0.2004**	**0.2511**

PA; C vs. M	**Dunn's**	**<0.0001**	**Yes**	**0.0733**	**0.2004**	
PA; C vs. H	**Dunn's**	**<0.0001**	**Yes**	**0.0733**		**0.2511**
PA; H vs. M	**Dunn's**	**0.0244**	**Yes**		**0.2004**	**0.2511**
MS 5%; all groups	**Kruskal-Wallis**	**<0.0001**	**Yes**	**0.0777**	**0.1796**	**0.2503**
MS 5%; C vs. M	**Dunn's**	**<0.0001**	**Yes**	**0.0777**	**0.1796**	
MS 5%; C vs. H	**Dunn's**	**<0.0001**	**Yes**	**0.0777**		**0.2503**
MS 5%; H vs. M	**Dunn's**	**<0.0001**	**Yes**		**0.1796**	**0.2503**
Hexanone; all groups	**Kruskal-Wallis**	**<0.0001**	**Yes**	**0.3185**	**0.4161**	**0.421**
Hexanone; C vs. M	**Dunn's**	**<0.0001**	**Yes**	**0.3185**	**0.4161**	
Hexanone; C vs. H	**Dunn's**	**<0.0001**	**Yes**	**0.3185**		**0.421**
Hexanone; H vs. M	Dunn's	0.8052	No		0.4161	0.421
Hexanal 10%; all groups	**Kruskal-Wallis**	**<0.0001**	**Yes**	**0.2438**	**0.3768**	**0.3778**
Hexanal 10%; C vs. M	**Dunn's**	**<0.0001**	**Yes**	**0.2438**	**0.3768**	
Hexanal 10%; C vs. H	**Dunn's**	**<0.0001**	**Yes**	**0.2438**		**0.3778**
Hexanal 10%; H vs. M	Dunn's	0.9975	No		0.3768	0.3778
THA; all groups	**Kruskal-Wallis**	**<0.0001**	**Yes**	**0.1171**	**0.2183**	**0.2415**
THA; C vs. M	**Dunn's**	**<0.0001**	**Yes**	**0.1171**	**0.2183**	
THA; C vs. H	**Dunn's**	**<0.0001**	**Yes**	**0.1171**		**0.2415**
ThA; H vs. M	Dunn's	0.2795	No		0.2183	0.2415
Hexanal 5%; all groups	**Kruskal-Wallis**	**<0.0001**	**Yes**	**0.2758**	**0.3534**	**0.5212**
Hexanal 5%; C vs. M	**Dunn's**	**0.0001**	**Yes**	**0.2758**	**0.3534**	
Hexanal 5%; C vs. H	**Dunn's**	**<0.0001**	**Yes**	**0.2758**		**0.5212**
Hexanal 5%; H vs. M	**Dunn's**	**<0.0001**	**Yes**		**0.3534**	**0.5212**

Table 3. Comparisons of excitatory response amplitude, multiple concentrations. Statistical test results of excitatory response amplitudes of cells from control, mint-, and hexanal-exposed groups in response to odorants at 1%, 5%, and 10% concentration. Data shown in **Figure 12**.

Comparison	Test	P-value	Significant	Median C	Median M	Median H
Peak ΔF/F Amplitude				**C; N=225**	**M; N=268**	**H; N=369**
Control Group						
MS; all conc.	Kruskal-Wallis	0.0586	No	0.1167	0.0777	0.1026
MS; 1% vs. 5%	Dunn's	0.0508	Yes	0.1167	0.0777	
MS; 1% vs. 10%	Dunn's	0.4478	No	0.1167		0.1026
MS; 5% vs. 10%	Dunn's	0.4695	No		0.0777	0.1026
IAA; all conc.	**Kruskal-Wallis**	**<0.0001**	**Yes**	**0.2018**	**0.1404**	**0.216**
IAA; 1% vs. 5%	**Dunn's**	**0.0028**	**Yes**	**0.2018**	**0.1404**	
IAA; 1% vs. 10%	Dunn's	0.768	No	0.2018		0.216
IAA; 5% vs. 10%	**Dunn's**	**0.0001**	**Yes**		**0.1404**	**0.216**
Hexanal; all conc.	**Kruskal-Wallis**	**0.0214**	**Yes**	**0.2409**	**0.2758**	**0.2438**
Hexanal; 1% vs. 5%	Dunn's	0.1657	No	0.2409	0.2758	
Hexanal; 1% vs. 10%	Dunn's	0.8025	No	0.2409		0.2438
Hexanal; 5% vs. 10%	**Dunn's**	**0.0206**	**Yes**		**0.2758**	**0.2438**
Mint Group						
MS; all conc.	Kruskal-Wallis	0.206	No	0.1642	0.1796	0.1961
MS; 1% vs. 5%	Dunn's	0.0194	Yes	0.1642	0.1796	
MS; 1% vs. 10%	Dunn's	0.1692	No	0.1642		0.1961
MS; 5% vs. 10%	Dunn's	0.7856	No		0.1796	0.1961
IAA; all conc.	**Kruskal-Wallis**	**<0.000A1**	**Yes**	**0.2389**	**0.2386**	**0.3547**
IAA; 1% vs. 5%	Dunn's	0.9991	No	0.2389	0.2386	
IAA; 1% vs. 10%	**Dunn's**	**0.0001**	**Yes**	**0.2389**		**0.3547**
IAA; 5% vs. 10%	**Dunn's**	**0.0001**	**Yes**		**0.2386**	**0.3547**
Hexanal; all conc.	Kruskal-Wallis	0.3426	No	0.3421	0.3534	0.3768
Hexanal; 1% vs. 5%	Dunn's	0.7615	No	0.3421	0.3534	
Hexanal; 1% vs. 10%	Dunn's	0.3775	No	0.3421		0.3768
Hexanal; 5% vs. 10%	Dunn's	0.9178	No		0.3534	0.3768
Hexanal Group						
MS; all conc.	**Kruskal-Wallis**	**0.0184**	**Yes**	**0.1933**	**0.2503**	**0.2566**
MS; 1% vs. 5%	**Dunn's**	**0.0146**	**Yes**	**0.1933**	**0.2503**	
MS; 1% vs. 10%	Dunn's	0.2718	No	0.1933		0.2566
MS; 5% vs. 10%	Dunn's	0.5645	No		0.2503	0.2566
IAA; all conc.	**Kruskal-Wallis**	**0.0433**	**Yes**	**0.3306**	**0.2973**	**0.3697**
IAA; 1% vs. 5%	Dunn's	0.8326	No	0.3306	0.2973	

IAA; 1% vs. 10%	Dunn's	0.2488	No	0.3306		0.3697
IAA; 5% vs. 10%	**Dunn's**	**0.0425**	**Yes**		**0.2973**	**0.3697**
Hexanal; all conc.	**Kruskal-Wallis**	**<0.0001**	**Yes**	**0.4718**	**0.5212**	**0.3778**
Hexanal; 1% vs. 5%	Dunn's	0.3105	No	0.4718	0.5212	
Hexanal; 1% vs. 10%	**Dunn's**	**0.0137**	**Yes**	**0.4718**		**0.3778**
Hexanal; 5% vs. 10%	**Dunn's**	**<0.0001**	**Yes**		**0.5212**	**0.3778**

3.3.4 Early odorant exposure increases the number and reliability of excitatory responses

The proportion of excitatory responses increases following prenatal and early postnatal odorant exposure (**Figure 13A-D and Table 4**; ANOVA with Tukey's multiple comparisons test; $p<0.0001$; medians: control: 0.88; mint: 0.9235; hexanal: 0.9377; significant Tukey's tests for control vs. mint and control vs. hexanal). The mint-exposed and hexanal-exposed groups both had a significantly larger proportion of excitatory responses than the control group. In addition, MCs of odor-exposed animals exhibited excitatory responses to more odorants than MCs of control animals (**Figure 13E**; ANOVA with Tukey's multiple comparisons test; $p<0.0001$; medians: Control: 13; Mint: 14; Hexanal: 14; significant Tukey's tests for control vs. mint and control vs. hexanal). These measures indicate that odor exposure increases excitatory MC odor-evoked responses, both in number and in number of activating odors.

Excitatory responses to certain odorants were also more reliable following odor-exposure, as measured by the proportion of successful trial presentations of each odorant (**Figure 14A-D and Table 5**; data pooled across odorants; Kruskal-Wallis Test with Dunn's multiple comparisons test; $p<0.0001$; medians: 1 for each group). As detailed in the Methods section, an excitatory response is defined as a peak evoked $\Delta F/F$ at least 3 S.D. above average fluorescence intensity prior to stimulus onset. This increase in the reliability of MCs between control and odor-exposed groups (0.75 median control to 1 for each odor-exposed group) is significant for the following odorants: methyl salicylate 1% (Kruskal-Wallis test; $p=0.0139$), methyl salicylate 5% ($p<0.0001$), methyl salicylate 10% ($p<0.0001$), 2-OH acetophenone ($p<0.0001$), acetophenone ($p<0.0001$), and propionic acid ($p<0.0001$) (**Figure 14A**; additional descriptive statistics available in **Table 5**). The odorants for which reliability increased following odorant exposure are the ones within the panel that elicited relatively weaker responses, as measured by

comparisons of their median evoked peak ΔF/F (**Figure 11, 12**). Median success values were not different between groups for other odorants, although comparisons of distributions differed – these values are described in **Table 5**. These data together show that early odorant exposure increases the proportion and reliability of excitatory responses in a manner not dependent on the identity of odorant used for exposure, much like the observed odor-non-specific increases in excitatory response amplitude. Rather, the reliability of response increases in an odor-specific manner relative to the initial amplitude of odor-evoked response.

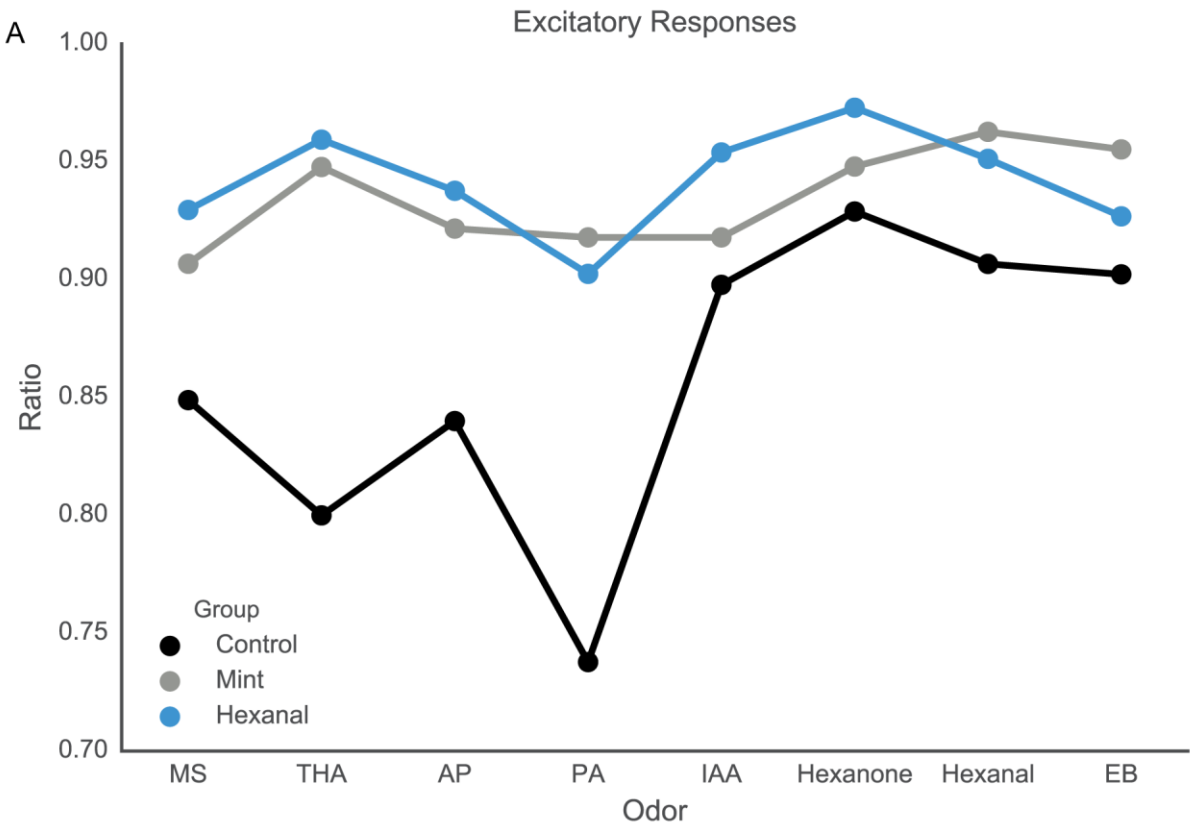
A
Excitatory Responses
1.00
0.95
0.90
0.85
0.80
0.75
0.70
Ratio
Group
Control
Mint
Hexanal
MS
THA
AP
PA
IAA
Hexanone
Hexanal
EB
Odor

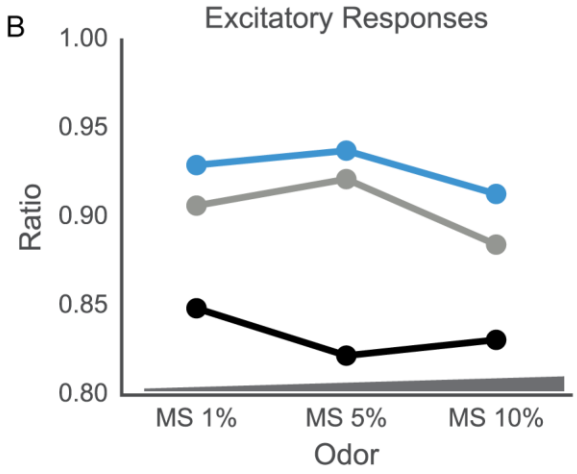
B
Excitatory Responses
1.00
0.95
0.90
0.85
0.80
Ratio
MS 1%
MS 5%
MS 10%
Odor

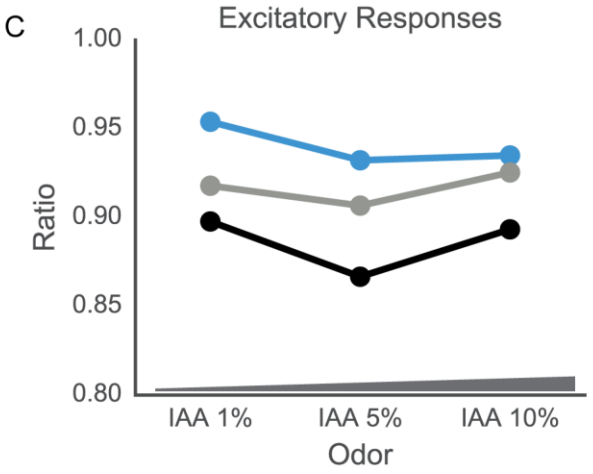
C
Excitatory Responses
1.00
0.95
0.90
0.85
0.80
Ratio
IAA 1%
IAA 5%
IAA 10%
Odor

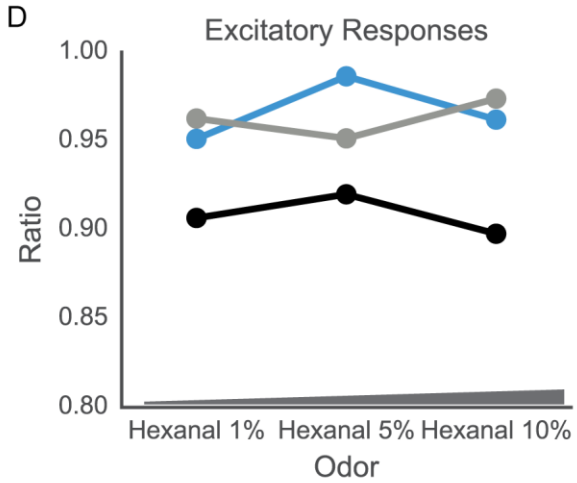
D
Excitatory Responses
1.00
0.95
0.90
0.85
0.80
Ratio
Hexanal 1%
Hexanal 5%
Hexanal 10%
Odor

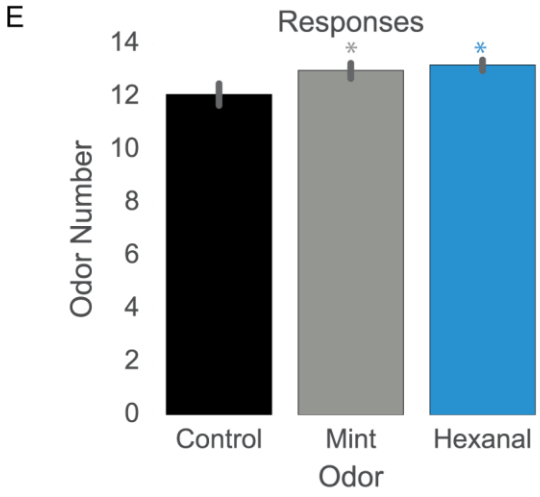
E
Responses
14
12
10
8
6
4
2
0
Odor Number
*
*
Control
Mint
Hexanal
Odor

Figure 13. Odor exposure increases number of excitatory MC responses. **A-D.** Ratio of above-threshold excitatory responses to all odor presentation trials across odorants. Odor-exposure groups had significantly higher ratio of excitatory responses as compared to control groups for odors at 1% concentration (**A.**) and multiple concentrations (**B-D.**). **E.** MCs in all groups responded to a high number of odorants (median number of odorants: Control – 13, mint-exposed - 14, hexanal-exposed - 14). Gray *: significant difference between mint-exposed and control groups; blue *: significant difference between hexanal-exposed and control groups.

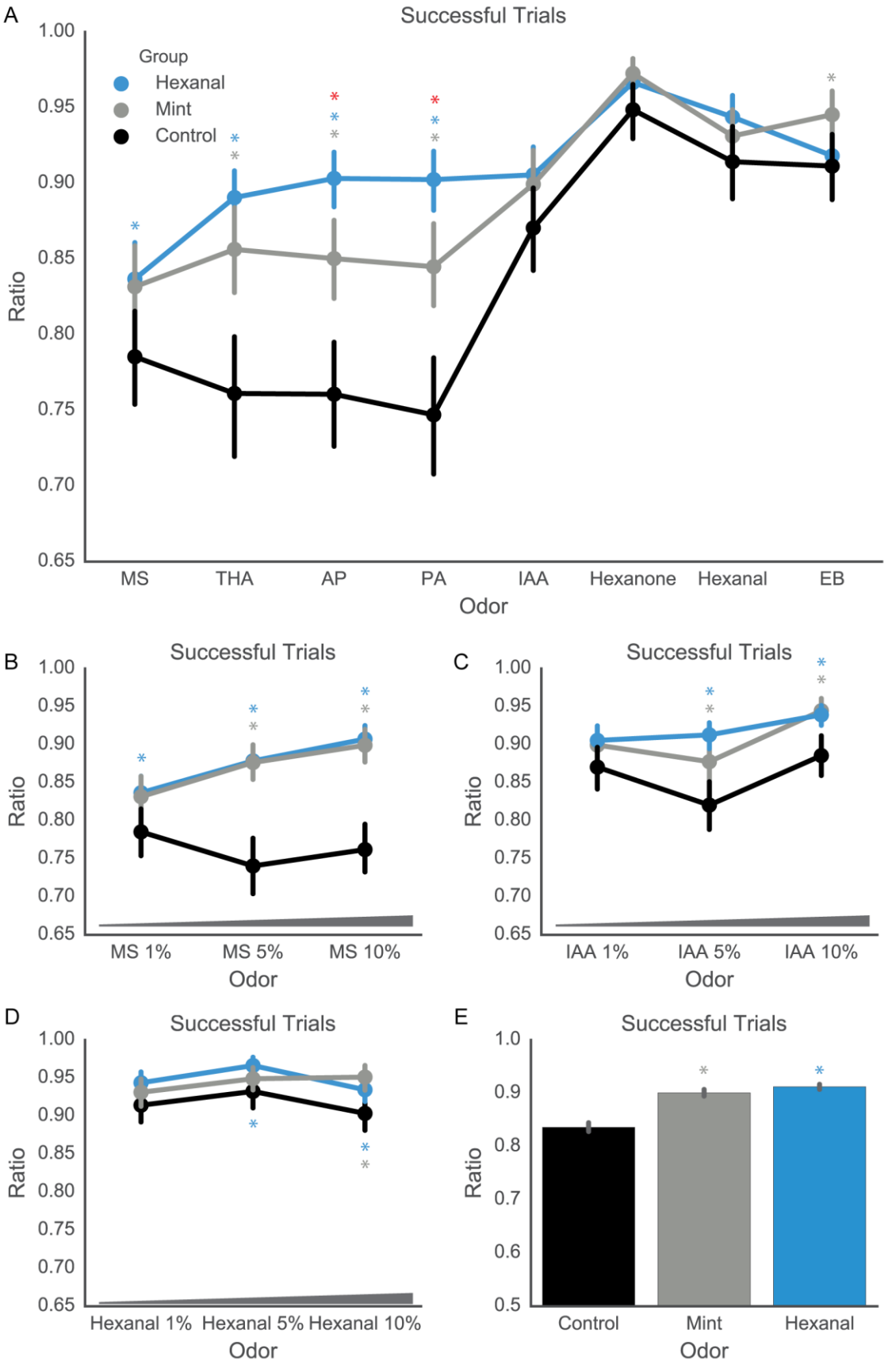
A
Successful Trials
Group
Hexanal
Mint
Control
Ratio
1.00
0.95
0.90
0.85
0.80
0.75
0.70
0.65
MS
THA
AP
PA
IAA
Hexanone
Hexanal
EB
Odor
B
Successful Trials
Ratio
MS 1%
MS 5%
MS 10%
Odor
C
Successful Trials
Ratio
IAA 1%
IAA 5%
IAA 10%
Odor
D
Successful Trials
Ratio
Hexanal 1%
Hexanal 5%
Hexanal 10%
Odor
E
Successful Trials
Ratio
1.0
0.9
0.8
0.7
0.6
0.5
Control
Mint
Hexanal
Odor

Figure 14. Odor exposure increases the rate of successful responses to odorant presentation. A-D. Ratio of successful trials above threshold (3 SD above baseline) to total trials of odorant presentation increases in odor-exposed groups across specific odorants at 1% concentration (**A.**) and multiple concentrations of methyl salicylate (**B.**) and isoamyl acetate (**C.**), but not hexanal (**D.**) **E.** Summed across all trials, odor-exposed groups had higher overall ratio of successful trials. Gray *: significant difference between mint-exposed and control groups; blue *: significant difference between hexanal-exposed and control groups; red *: significant difference between mint- and hexanal-exposed groups.

Table 4. Proportion of excitatory responses. Comparisons of proportion of excitatory odor-evoked responses from control, mint-, and hexanal-exposed groups. Data shown in **Figure 13.**

Comparison	Test	P-value	Significant	Median C	Median M	Median H
Ratio of excitatory responses				**C; N=14**	**M; N=14**	**H; N=14**
All odors	**ANOVA**	**p<0.0001**	**Yes**	**0.88**	**0.9235**	**0.9377**
All odors; C vs. M	**Tukey's**	**p<0.0001**	**Yes**	**0.88**	**0.9235**	
All odors; C vs. H	**Tukey's**	**p<0.0001**	**Yes**	**0.88**		**0.9377**
All odors; H vs. M	Tukey's	p=0.1313	No		0.9235	0.9377
Ratio of activating odorants				**C; N=225**	**M; N=268**	**H; N=369**
All groups	**Kruskal-Wallis**	**p<0.0001**	**Yes**	**13**	**14**	**14**
C vs. M	**Tukey's**	**p<0.0001**	**Yes**	**13**	**14**	
C vs. H	**Tukey's**	**p<0.0001**	**Yes**	**13**		**14**
H vs. M	Tukey's	p>0.9999	No		14	14

Table 5. Reliability of excitatory responses. Comparisons of excitatory response reliability from control, mint-, and hexanal-exposed groups. Data shown in **Figure 14.**

Comparison	Test	P-value	Median C	Median M	Median H
Ratio of Successful Trials			**C; N=225**	**M; N=268**	**H; N=369**
All odors combined; all groups	**Kruskal-Wallis**	**<0.0001**	**1**	**1**	**1**
All odors combined; C vs. M	**Dunn's**	**<0.0001**	**1**	**1**	
All odors combined; C vs. H	**Dunn's**	**<0.0001**	**1**		**1**
All odors combined; H vs. M	Dunn's	0.0836		1	1
AP; all groups	**Kruskal-Wallis**	**<0.0001**	**0.75**	**1**	**1**
AP; C vs. M	**Dunn's**	**<0.0001**	**0.75**	**1**	
AP; C vs. H	**Dunn's**	**<0.0001**	**0.75**		**1**
AP; H vs. M	**Dunn's**	**0.0029**		**1**	**1**
EB; all groups	**Kruskal-Wallis**	**0.0181**	**1**	**1**	**1**
EB; C vs. M	**Dunn's**	**0.0151**	**1**	**1**	
EB; C vs. H	Dunn's	0.5476	1		1
EB; H vs. M	Dunn's	0.2351		1	1
Hexanal 1%; all groups	Kruskal-Wallis	0.0596	1	1	1
Hexanal 1%; C vs. M	Dunn's	0.7821	1	1	
Hexanal 1%; C vs. H	Dunn's	0.0562	1		1
Hexanal 1%; H vs. M	Dunn's	0.6464		1	1
Hexanone; all groups	Kruskal-Wallis	0.1165	1	1	1
Hexanone; C vs. M	Dunn's	0.1277	1	1	
Hexanone; C vs. H	Dunn's	0.3668	1		1
Hexanone; H vs. M	Dunn's	>0.9999		1	1
IAA 1%; all groups	Kruskal-Wallis	0.0902	1	1	1
IAA 1%; C vs. M	Dunn's	0.4431	1		1
IAA 1%; C vs. H	Dunn's	0.0867	1	1	
IAA 1%; H vs. M	Dunn's	>0.9999		1	1
MS 1%; all groups	**Kruskal-Wallis**	**0.0139**	**0.75**	**1**	**1**
MS 1%; C vs. M	**Dunn's**	**0.0621**	**0.75**	**1**	
MS 1%; C vs. H	**Dunn's**	**0.0144**	**0.75**		**1**
MS 1%; H vs. M	Dunn's	>0.9999		1	1
PA; all groups	**Kruskal-Wallis**	**<0.0001**	**0.75**	**1**	**1**
PA; C vs. M	**Dunn's**	**<0.0001**	**0.75**	**1**	
PA; C vs. H	**Dunn's**	**<0.0001**	**0.75**		**1**
PA; H vs. M	**Dunn's**	**0.0019**		**1**	**1**
THA; all groups	**Kruskal-Wallis**	**<0.0001**	**0.75**	**1**	**1**
THA; C vs. M	**Dunn's**	**<0.0001**	**0.75**	**1**	

THA; C vs. H	**Dunn's**	**<0.0001**	**0.75**		**1**
THA; H vs. M	Dunn's	0.9588		1	1
MS 5%; all groups	**Kruskal-Wallis**	**<0.0001**	**0.75**	**1**	**1**
MS 5%; C vs. M	**Dunn's**	**<0.0001**	**0.75**	**1**	
MS 5%; C vs. H	**Dunn's**	**<0.0001**	**0.75**		**1**
MS 5%; H vs. M	Dunn's	>0.9999		1	1
MS 10%; all groups	**Kruskal-Wallis**	**<0.0001**	**0.75**	**1**	**1**
MS 10%; C vs. M	**Dunn's**	**<0.0001**	**0.75**	**1**	
MS 10%; C vs. H	**Dunn's**	**<0.0001**	**0.75**		**1**
MS 10%; H vs. M	Dunn's	>0.9999		1	1
Hexanal 5%; all groups	**Kruskal-Wallis**	**0.0016**	**1**	**1**	**1**
Hexanal 5%; C vs. M	Dunn's	0.4815	1	1	
Hexanal 5%; C vs. H	**Dunn's**	**0.0014**	**1**		**1**
Hexanal 5%; H vs. M	Dunn's	0.1031		1	1
Hexanal 10%; all groups	**Kruskal-Wallis**	**0.0001**	**1**	**1**	**1**
Hexanal 10%; C vs. M	**Dunn's**	**0.0001**	**1**	**1**	
Hexanal 10%; C vs. H	**Dunn's**	**0.0029**	**1**		**1**
Hexanal 10%; H vs. M	Dunn's	0.81		1	1
IAA 5%; all groups	**Kruskal-Wallis**	**<0.0001**	**1**	**1**	**1**
IAA 5%; C vs. M	**Dunn's**	**0.0026**	**1**	**1**	
IAA 5%; C vs. H	**Dunn's**	**<0.0001**	**1**		**1**
IAA 5%; H vs. M	Dunn's	0.4956		1	1
IAA 10%; all groups	**Kruskal-Wallis**	**0.0007**	**1**	**1**	**1**
IAA 10%; C vs. M	**Dunn's**	**0.0007**	**1**	**1**	
IAA 10%; C vs. H	**Dunn's**	**0.01**	**1**		**1**
IAA 10%; H vs. M	Dunn's	0.8374		1	1

3.3.5 MCs exhibit habituation following repeated acute odor trials

Previous work has demonstrated that repeated presentation of odors results in a decrease in amplitude of odor-evoked responses (Chaudhury et al., 2010; Ogg et al., 2015). Given that our odor exposure paradigm did not demonstrate this effect, we examined short term habituation in a subset of animals. In three animals, one from each group, we observed acute habituation of mitral cell response. Each of these imaging sessions took place following acquisition of MC odor-evoked responses using the complete panel of odor stimuli. Using a protocol described by Chaudhury et al., 2010, we imaged hexanal-evoked activity prior to stimulus, presented repeated blocks of short presentations of hexanal, and imaged hexanal-evoked activity 5 minutes and 30 minutes after repeated hexanal presentation (**Figure 15A**). We found prolonged decreases in odor-evoked responses 5 minutes and 30 minutes after the stimulus presentation (n=56 cells) Friedman test with Tukey's multiple comparisons test; Median decrease in amplitude as percentage of initial 'Pre' response: 37% for 5 minutes after stimulus and 35% for 30 minutes after stimulus; Pre vs. 5 min: adjusted $p<0.0001$; Pre vs. 30 min: adjusted $p<0.0001$; 5 vs. 30 min: adjusted $p>0.9999$ (**Figure 15B**). These cells demonstrate acute habituation following repeated stimulation similar to that observed in previous studies. No significant difference in habituation amplitude was observed between groups; thus, data were pooled.

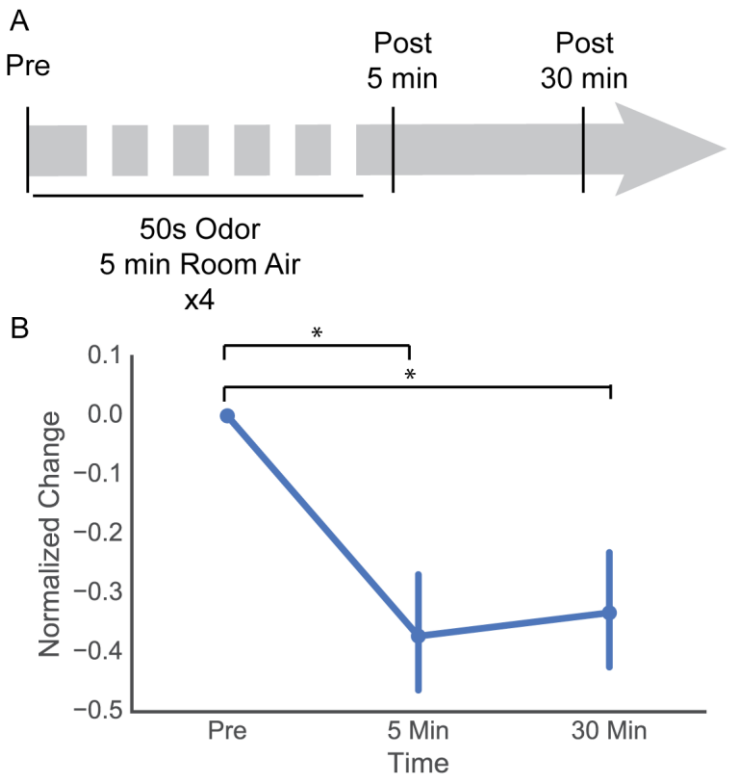

Figure 15. MCs display acute habituation following repeated short odor pulses. **A.** Odor stimulus (hexanal at 1% concentration) was presented for 50s followed by 5 minutes of room air, with stimulus repeated 4 times. MC odor-evoked response was captured prior to stimulus presentation, five minutes after final 50s odor stimulus, and 30 minutes after final 50s odor stimulus. **B.** Normalized change in odor response between pre-stimulus and 5 minutes post-stimulus or 30 minutes post-stimulus. Significant decrease in odor response was observed at both time points post stimulus. * indicates statistically significant comparison

3.4 DISCUSSION

Our data show that prenatal and early postnatal food-based odor exposure increases the amplitude, number, and reliability of excitatory MC responses *in vivo*, as measured by 2-photon calcium imaging. We observed subtle changes in the within-cell rankings of odor-evoked response amplitude, but we did not observe any changes in MC response that were specific to the conditioned odor. The mechanisms of these widespread changes are unclear but are surprising given previous work using postnatal odor enrichment (Wilson et al., 1985, 1987). Key differences between our experiments and this previous work include the timing, duration, and method of odor exposure. Using this same paradigm, it was previously observed that an increase in the number of mitral and tufted cells associated with a glomerulus known to be activated by the conditioned odor (Liu et al., 2016). The changes we report here are consistent with widespread increases in OSN input or M/TC excitability. Such changes may represent a consequence of raising mice in an enriched odor environment, but further work will be necessary to determine the mechanisms of this change and the crucial elements of the odor exposure paradigm.

3.4.1 Prenatal and early postnatal odorant exposure significantly changes excitatory odor-evoked M/TC responses in an odor-nonspecific way

The lack of clear odor-specificity in changes following odor conditioning was surprising, given previous work showing specificity in anatomical changes following prenatal and early postnatal odorant exposure (Todrank et al., 2011; Liu et al., 2016), previous work showing that a different conditioning paradigm increases lateral inhibition (Geramita and Urban, 2016), and the

observation that odor conditioning results in reduced response to conditioned but not other odors (Wilson et al., 1985). However, 2-DG maps of glomerular activation in rats (Glomerular Activity Response Archive, Michael Leon, *gara.bio.uci.edu/index.jsp)* show that both methyl salicylate and hexanal activate a number of potentially overlapping glomeruli on the dorsal OB surface, so it is possible that the widespread nature of the changes we observe in odor-evoked MC excitatory responses are due to the widespread activation of dorsal glomeruli and would not be seen in areas of the OB without glomeruli activated by either odor. Although methyl salicylate and hexanal are quite different perceptually and in odorant structure, the lack of intuitive organization by odorant in the OB precludes us from assuming that these two odorants necessarily activate very distinct sets of glomeruli. Further work is necessary to elucidate if these changes in MC response can be generalized to MCs in OB areas known to not be activated by either of these two odorants.

Rank order for specific odorants was changed following mint and hexanal odorant exposure. Because there were also significant rank differences shown between the mint- and hexanal-exposed groups, there may be relative changes in response rank specific to the identity of exposed odorant. Methyl salicylate and hexanal have different glomerular activation patterns, thus chronic odorant exposure may change the network of lateral inhibition and change odor-evoked response in overlapping but distinct ways. Use of a larger odor panel including ventral-activating odorants would help elucidate whether these changes in rank and in excitatory responses are connected to the identity of the odorant used for exposure.

3.4.2 Activation pattern similarity of odorant stimuli

In this study, most cells had observed above-threshold responses to most odorants (**Figure 13E**). This difference from the sparser MC response to odorants observed previously (Kato et al., 2012;

Blauvelt et al., 2013; Wachowiak et al., 2013; Roland et al., 2016) could be due to 1) the high sensitivity of GCaMP6s calcium indicator, 2) the choice of odorants within the stimulus panel, or 3) the use of higher odorant concentrations in our study. In *in vivo* studies of visual cortical neurons, use of GCaMP6s resulted in a fivefold higher rate of detection of responding neurons than GCaMP3, suggesting that the larger proportion of observed odor-evoked responses in our data set could be partially explained by use of a more sensitive calcium indicator (Chen et al., 2013). The choice of odorants used for chronic exposure and in the odor panel was deliberately focused on dorsal OB activating odorants in order to visualize odor-evoked responses in the cohort of cells imaged, those on the dorsal OB surface. This choice of a stimulus panel may explain why a large proportion of cells on the dorsal OB surface showed significant odor-evoked responses to many dorsally-activating odorants in the panel.

3.4.3 Prenatal and postnatal sensory enrichment

Here, we use a conditioning paradigm of constant odor exposure during both gestation and the postnatal period. Todrank et al., 2011 show that exposure during either gestation or early nursing is sufficient to significantly increase the size of activated glomeruli, while Liu et al., 2016 demonstrate that this paradigm also increases the number of M/TCs connected to a single activated glomerulus. Prenatal food-based odor exposure can produce large anatomical changes in the OB circuitry. Here we show that this paradigm also promotes non-specific changes to excitatory MC odor-evoked responses; these findings contrast with previous studies of MCs following repeated odorant exposure. However, the majority of studies analyzing experience-dependent changes to the structure and function of the OB rely on postnatal manipulations (Benson et al., 1984; Laing, 1985; Panhuber and Laing, 1987; Saghatelyan et al., 2005; Kerr and

Belluscio, 2006; Woo et al., 2006; Cavallin et al., 2010; Johnson et al., 2013; Morrison et al., 2015; Geramita and Urban, 2016). Starting exposure during gestation may trigger developmental changes distinct from those observed with postnatal odor experience.

Generalized early postnatal sensory enrichment may also explain the observed nonspecific enhanced excitatory responses. Odor deprivation during development causes significant changes to OB structure and activity. OB size, OSN activity, MC connectivity, and granule cell integration are all impacted by early nares occlusion (Benson et al., 1984; Saghatelyan et al., 2005; Cavallin et al., 2010). With regards to the anatomical effects of early postnatal chronic odor enrichment or stimulation, the consensus is less clear. A number of studies report a significant decrease in the size and density of MCs following chronic passive odor exposure (Laing, 1985; Panhuber and Laing, 1987; Woo et al., 2006; Johnson et al., 2013). However, Rosselli-Austin and Williams, 1990, used scented objects in a normal cage setting to deliver chronic odor stimulation and found that mitral and granule cell numbers actually increased following neonatal odorant exposure. In addition, numbers of adult born granule cells (Rochefort et al., 2002) and dopaminergic cells (Bonzano et al., 2014) also increase following chronic postnatal odorant exposure. All of these results suggest that richness of the sensory environment during the neonatal period can significantly modify olfactory bulb structure. Our work points to a general increase in MC excitability, as measured by the number and amplitude of excitatory odor-evoked responses. This generalized change could be due to sensory enrichment through odorant exposure during a critical period of OB development.

3.4.4 Food-associated exposure paradigm

One unique feature of this particular odor exposure paradigm is that the odorants are mixed with food. Wilson et al. 1985 used a behavioral paradigm where odorized air puffs were paired with a positive grooming stimulus and found a generalized decrease in excitatory odor-evoked events, contrary to our observations. However, a separate study using odor-food pairing showed that in the projection neurons of the moth *Manduca sexta*, pairing repeated odor exposure with food resulted in an increase in the amplitude of excitatory odor-responses (Daly et al., 2004). A similar response is observed in our results, in which we find that pairing odor with food heightens the odor-evoked excitatory responses of primary projection neurons – there may be a conserved adaptive response to the association of odor with food. Odor-exposed mice demonstrate a distinct preference for food scented with the familiar odorant (Todrank et al., 2011; Liu et al., 2016), indicating a positive odorant association following food-based exposure. The contrasting results from studies that use different odor exposure paradigms, reward-paired or passive, suggest that odor context could play an important role in determining how the circuit remodels anatomically and functionally following repeated or chronic odor exposure.

3.4.5 Conclusion

Here, we use a food-based paradigm to investigate the effects of prenatal and early postnatal odor exposure on odor-evoked responses of mitral cells. We find that following odor exposure, excitatory odor-evoked responses of MCs increase in number, amplitude, and reliability with very little stimulus specificity. It is still unclear as to whether these changes are specific to the identity of exposure odorant or the result of the generalized changes from rough environmental

manipulations such as sensory enrichment. These results highlight the complexity of and potential for experience-dependent plasticity within the olfactory bulb.

4.0 GENERAL DISCUSSION

4.1 SUMMARY OF FINDINGS

The stereotyped anatomy of the olfactory bulb is modulated by both genetics and sensory experience, during development and throughout adulthood. Both sensory deprivation and enrichment have been shown to dramatically change OB anatomy as well as odor-evoked activity. In this dissertation, we leverage the high degree of glomerular organization in the OB based on OR identity to examine how early odorant experience impacts the structure and output of the mouse OB. Here, we highlight the major and minor findings from Chapters 2 and 3.

In Chapter 2, we used a prenatal and early postnatal food-based odorant exposure paradigm known to alter glomerular morphology to examine how odorant exposure changes the number of connected primary projection neurons, the M/TCs. We used methyl salicylate, an M72 ligand, and hexanal, a non-M72 ligand, to odorize food fed to pregnant and nursing M72-IRES-GFP dams, which express GFP in M72-OR expressing OSNs. We find that this paradigm increases the volume of the M72 glomerulus following exposure of an M72 ligand (methyl salicylate) but does not change the volume of the M72 glomerulus following exposure with a non-M72 ligand (hexanal), as described previously using similar experiments by Todrank et al., 2011. In addition, odorant exposure changed food preference, as measured by amount of time spent investigating odorized or non-odorized control food. Food preference, but not glomerular

volume increases, was transient – we observed a reversal in food preference after switching previously exposed mice to control food for 30+ days, but not a reversal in glomerular volume. In addition, we found that coupling an acute odorant exposure paradigm with cFos immunohistochemistry proved to be an effective procedure by which to determine ligand activation of the genetically identified M72 glomerulus.

Using *in vivo* electroporation, a microcircuit dye-labeling technique, we labeled the post-synaptic targets of the M72 glomerulus in control mice and in odor-exposed mice. We found that 7 MCs and 3 TCs are connected to the M72 glomerulus in control animals. This number is substantially smaller than many previous estimates, which used the approximation of total glomeruli and M/TCs in the OB to determine that 20-40 M/TCs are connected to a single mouse glomerulus (Thamke et al., 1973; Benson et al., 1984; Pomeroy et al., 1990). However, more recent estimates using revised glomeruli and M/TC counts and *in vivo* electroporation reported an average of 9 MCs/glomerulus, a number closer to our findings (Richard et al., 2010; Sosulski et al., 2011). Neither of these studies analyzed the post-synaptic targets of a single genetically determined glomerulus between animals as we did in Chapter 2. Thus, here we provide the first systematic evaluation of the number of M/TCs connected to a single glomerulus.

We observed that early odorant exposure dramatically increases the number of M/TCs connected to a single activated glomerulus by 40% (MCs) and 100% (TCs). Interestingly, odorant exposure did not change the spatial distribution of connected M/TCs, indicating that glomeruli activated by exposed ligand may be competitively recruiting M/TCs away from neighboring glomeruli. These cells serve as the primary output of the OB to higher cortical areas and, through connections with inhibitory interneurons in the OB, also affect the activity and output of other glomerular modules. Thus, increasing the number of M/TCs associated with a

single glomerulus may mediate larger functional changes to the OB network. Since each odorant activates multiple glomeruli, experience-dependent changes to the M/TC composition of multiple activated glomerular module may have an even greater effect on general odorant representation in the OB.

In Chapter 3, we used the same food-based odorant exposure paradigm to assess how food-based early odorant exposure might change the functional output of the OB, specifically the odorant-evoked responses of MCs. From the work detailed in Chapter 2, we observed that this type of odorant experience has the capacity to dramatically change the structure of the M72 glomerular module by increasing the number of M72 glomerulus-associated M/TCs. Using *in vivo* 2-photon calcium imaging, we analyzed the odor-evoked responses of dorsal-OB MCs in animals following prenatal and early postnatal odorant exposure to two perceptually and molecularly distinct dorsal-OB activating odorants, methyl salicylate and hexanal. In these experiments, we used a 14-stimuli panel consisting of 9 distinct dorsal-OB activating odorants at 1% by volume concentration and 3 at 1, 5, and 10% concentrations. We found that odorant exposure changed the tuning curves of MCs in exposed animals. In addition, odorant exposure heightened dorsal OB MC activity, increasing the amplitude, reliability, and the proportion of excitatory odor-evoked MC responses. These effects were not specific to odor-evoked responses to either methyl salicylate or hexanal, the odorants used for exposure. Rather, prenatal and early postnatal odorant exposure using either odorant resulted in generalized changes to MC responses across the dorsal OB and in response to all odorants in the stimulus panel. Control, hexanal, and methyl salicylate exposed animals all demonstrated a similar decrease in odor-evoked MC responses following acute odorant habituation with hexanal, indicating that our paradigm of constant early odorant exposure does not fundamentally change mechanisms of habituation.

In this dissertation, we found that food-based prenatal and early postnatal odorant exposure significantly changes the anatomy and output of the OB. These changes may significantly impact how odorants are subsequently represented in the OB, and it is still unclear whether these potential changes to odorant representation give rise to changes in odor perception or valence. In this chapter, we discuss how these findings inform our current understanding of plasticity within the olfactory system, the impact of this type of plasticity on odorant representation, and how these anatomical and functional changes might inform behavior. Throughout, we highlight future directions and experiments that may further clarify our conclusions and lead to a better understanding of the functional implications of early odorant exposure induced changes to the OB.

4.2 CONTEXT OF THESE FINDINGS IN UNDERSTANDING SENSORY SYSTEM PLASTICITY

As we discussed in the introduction, the establishment of the OB circuit is determined by both genetics and sensory experience. In this dissertation, we focus specifically on examining how the OB changes in response to prenatal and early postnatal odorant exposure in the context of a food-based association. The changes to glomerular module anatomy and output that we describe in Chapters 2 and 3 are induced by early, lengthy odorant exposure, and in subsequent sections, we discuss how these structural modifications may provide the foundation for dramatic changes in neural processing and olfactory-guided behavior.

4.2.1 In the olfactory system

In this dissertation, we examine how the olfactory system modulates both anatomy and activity in response to early odorant experience. We used an odor exposure paradigm known to selectively increase the volume of activated glomeruli (Todrank et al., 2011) and found that early exposure significantly impacted the targeting and refinement of M/TCs to specific activated glomeruli, creating a dramatically different OB circuit. Specifically, we mixed odorants (methyl salicylate or hexanal) with food (1% odorant by volume), and fed dams odorized food throughout gestation and nursing. This type of odorant exposure takes place throughout the entirety of OB development, lasting through both prenatal and early postnatal time points. During this period, crucial components of OB structure finalize, including M72 glomerulus convergence (Mombaerts et al., 1996; Royal and Key, 1999). In addition, many maturing MCs initially extend multiple apical dendrites to multiple glomeruli until P10, at which point mature MCs have only one apical dendrite each that extends to a single glomerulus (Malun and Brunjes, 1996; Matsutani and Yamamoto, 2000; Blanchart et al., 2006). Thus, the paradigm we use throughout this dissertation provides odorant exposure throughout key early periods of OB development, impacting both glomerular convergence and M/TC maturation.

These results support previous findings showing that activity, both intrinsic neuronal activity and sensory input evoked activity, is crucial to the normal maturation of the OB circuitry. Prevention of sensory input through physical nares occlusion or disruption of normal MC or OSN activity significantly changes OB structure, namely by decreasing MC number and size, preventing normal glomerular convergence, and perturbing newborn GC and PGC survival (Meisami and Safari, 1981; Benson et al., 1984; Frazier-Cierpial and Brunjes, 1989; Corotto et al., 1994; Zheng et al., 2000; Zhao and Reed, 2001; Saghatelyan et al., 2005; Yamaguchi and

Mori, 2005; Maher et al., 2009; Johnson et al., 2013). Targeted deletion of the OCNC1 gene, which encodes a subunit of the olfactory CNG channel, in select OSN populations, renders OSNs unresponsive and disrupts glomerular convergence by increasing the number of supernumerary glomeruli and changing glomerular position on the OB surface (Zheng et al., 2000). In addition, deletion of OCNC1 decreases the survival of affected OSNs, indicating that activity is necessary for the correct incorporation of OSNs into the OB circuit (Zhao and Reed, 2001). However, this effect is not observed when genetically disrupting the function of the CNG channel in all OSNs through a null mutation of Cnca, a gene that encodes a different CNG channel subunit. Rather, rendering all rather than a subset of OSNs unresponsive to sensory input does not disrupt glomerular convergence or map development, but does slow down MC maturation and pruning of multiple MC apical dendrites. Through a form of sensory deprivation, these studies demonstrate that OSN input is important in MC maturation and glomerular targeting. We find that sensory enrichment also changes glomerular targeting by increasing the number of M/TCs associated with a single, activated glomerulus. Disrupting MC excitability through deletion of Kv1.3 channels also impairs glomerular convergence (Johnson et al., 2013), indicating that neural activity of both presynaptic OSNs and their postsynaptic targets are necessary for proper olfactory map formation.

In contrast, periodic odor enrichment was shown to decrease MC density and soma size (Johnson et al., 2013), a generalized finding that does not necessarily contradict directly with our results showing addition of M/TCs to a specific glomerular module. Our experiments did not examine global MC number or M/TC number corresponding to other, non-activated glomerular modules. Glomerular volume has been shown to change dynamically through adulthood in response to experience – olfactory fear-conditioning increases glomerulus volume and OSN

number, but these changes are reversed within 2 weeks following extinction of the fear response (Morrison et al., 2015) These striking changes are likely due to continual OSN turnover every 1-6 months and activity-dependent increases in OSN survival (Moulton, 1974; Kondo et al., 2010). However, the number of M/TCs connected to a single glomerulus is unlikely to change dynamically through adulthood, as doing so would require active removal of M/TCs or retargeting of mature M/TCs to different glomeruli. Neither of these have been reported experimentally and do not seem likely given the developmental timeline of M/TC maturation, since M/TCs refine apical dendrite targeting to a single glomerulus towards the end of the first postnatal week (Malun and Brunjes, 1996; Matsutani and Yamamoto, 2000; Blanchart et al., 2006). Thus, the observed experience-dependent increases in M/TC number corresponding to activated glomeruli are likely to be persistent anatomical changes.

Based on previous work (Wilson et al., 1985), we predicted that odor-evoked responses of M/TCs in the activated glomerular module would change following odorant exposure. However, as described in Chapter 3, we see broad changes in odor-evoked mitral cell responses in cells across the bulb. These findings contrast with Wilson et al., 1985, who found that pairing odorant exposure with a positive somatosensory stimulus in rat pups resulted in decreased excitatory activity and increased inhibitory activity of MCs. These differences may be attributable to the timing and context of our odorant exposure paradigm. Our exposure paradigm lasts through the entirety of gestation, when a large portion of OB circuitry develops, including OB targeting of specific OR-expressing OSNs and glomerular coalescence, although the latter process also extends into the first few postnatal weeks depending on OR identity (Vassar et al., 1994; Mombaerts et al., 1996). In addition, the exposure paradigm pairs odorant with food, which may cause changes in the OB not seen with simple odor exposure or through the pairing

of odorant with somatosensory stimulation. Although both are positive associative stimuli, metabolic states such as hunger, starvation, or satiety drive modulation of olfactory circuitry, ranging from hormone production and receptor expression to changes in the performance of odorant discrimination tasks (Palouzier-Paulignan et al., 2012). Thus, the increases in excitatory activity that we observe could be the consequence of nutritional status and the association of odorant stimulus with food. Alternatively, these generalized changes in MC activity may be the result of sensory enrichment, which has been shown to effect similar increases in excitatory responses in the somatosensory, visual, and auditory systems (Beaulieu and Cynader, 1990a, 1990b; Coq and Xerri, 1998; Bourgeon et al., 2004; Engineer et al., 2004).

Not all glomeruli across the dorsal OB exhibit the types of anatomical modifications that we observed in the M72 glomerulus. Specifically, glomeruli not activated by the exposure odorant will not undergo anatomical change (Todrank et al., 2011). However, changes to even a few glomerular modules may exert large effects on the highly laterally connected OB circuit and produce the changes in excitatory activity that we observe. These changes in connectivity and activity are not correlated exactly with the behavioral measure that we used (the assessment of time spent sniffing odorized or control food). We find that food preference when measured during odorant exposure correlates with experience-dependent specific increases in glomerular volume and M/TC number. This preference is transient, as food preference changes once mice are switched to unodorized food. However, as we discuss in later sections, food preference measured using sniff time is a coarse measure that reflects a transient association with the scent of the most recent food provided to the animals. If the anatomical and activity changes we observe are truly long-lasting and not transient, these may significantly change perception and

discriminability of olfactory stimulus space, the impacts of which should be assessed using more targeted behavioral assays.

4.2.2 Parallels of plasticity within the visual system

The large role of early activity and experience in shaping circuit architecture is not limited to the olfactory system – rather, other sensory systems also demonstrate a high dependence on spontaneous activity and sensory experience in establishing and maintaining normal anatomy. Large elements of visual system circuitry are established prior to sensory input, including initial topographic organization. Orientation selectivity in ferrets develops but is impaired by bilateral visual deprivation; neuronal activity during the first few postnatal weeks is crucial for normal development (Chapman and Stryker, 1993; Chapman et al., 1996). Retinal topography in mice matures prior to visual input but requires spontaneous waves of neural activity (Galli and Maffei, 1988; Meister et al., 1991; Wong et al., 1993; McLaughlin and O'Leary, 2005). Thus, spontaneous neuronal activity is a clear driver of visual system development. Similarly, maturation of OB structure and topography is dramatically impaired by silencing spontaneous OSN or M/TC activity (Zheng et al., 2000; Zhao and Reed, 2001; Johnson et al., 2013).

Both sensory deprivation and experience have dramatic effects during critical periods, developmental time windows during which circuits are highly plastic in response to sensory input. Hubel and Wiesel first described the importance of sensory input in modulating postnatal development in studies of the cat visual system. They observed massive changes in cortical organization and stimulus-evoked cortical neuron responses following monocular visual deprivation within an early developmental time window (Wiesel and Hubel, 1963; Hubel and Wiesel, 1970). As described above, the initial development of topography in the visual system

based on orientation selectivity depends on spontaneous activity and molecular guidance cues rather than on visual experience. However, visual experience is necessary for circuit maturation and maintenance (Chapman and Stryker, 1993; Chapman et al., 1999; Ko et al., 2013). It is unclear if the olfactory system demonstrates the same type of critical period as observed in the visual system, as adult-born OSNs and interneurons are continually incorporated into the olfactory bulb circuit and provide the olfactory system with a robust mechanism of plasticity throughout life. However, there may be an olfactory bulb critical period as defined by the establishment of the OB glomerular "map." The glomerular map finalizes soon after birth and manipulations such as OSN ablation do not perturb the re-formation of the initial map (Ma et al., 2014; Tsai and Barnea, 2014). In addition, our odorant exposure manipulations demonstrate that early experience can indeed shape circuit architecture, although we do not know if these changes in M/TC targeting can be induced later in life (Liu et al., 2016).

Sensory enrichment can also modify excitability of sensory systems. Studies in cat visual cortex showed that rearing animals in an enriched environment increased the number of orientation selective cells, sharpened orientation tuning of cells, and increased responsivity of cells to light stimuli (Beaulieu and Cynader, 1990a, 1990b). Such changes are observed during adulthood as well – following visual enrichment, adult rats with amblyopia demonstrated improved visual acuity and reduced inhibition/excitation balance in V1 (Baroncelli et al., 2012). Other sensory systems also demonstrate this feature, with sensory enrichment increasing excitatory responses and refinement of stimulus selectivity within the auditory and somatosensory systems (Coq and Xerri, 1998; Bourgeon et al., 2004; Engineer et al., 2004; Alwis and Rajan, 2013) This phenomenon also may be taking place in the OB, as we observe a

generalized, non-stimulus specific increase in MC excitatory response amplitude and number following odorant exposure.

4.3 ODOR REPRESENTATION

We find that odor experience modulates the connectivity and odor-evoked activity of principal projection neurons in the OB. Given the highly interconnected structure of the OB circuit, these changes may have more global effects. In this section, we focus on how increasing M/T number associated with single glomerular modules and changing mitral cell responsiveness might broadly impact odor representation in the OB.

4.3.1 Generalizability of anatomical findings

In this dissertation, we focus our anatomical studies on the structure of the M72 glomerular module. Since each odorant activates multiple glomeruli, we believe that the observed changes may also be reflected in the anatomy of all glomerular modules activated by the exposure odorant. There are no distinct features of the M72 glomerular module that lead us to believe that its development is governed by unique mechanisms. If we assume that the anatomical changes to the M72 glomerular module can be generalized to all glomeruli activated by the exposed odorant, then we conclude that the early odorant exposure paradigm could impact other glomeruli as well, specifically, all glomeruli that are also activated by methyl salicylate or any other exposure odorant. Whether the anatomical changes to the M72 glomerular module are also

observed in the same extent (40% increase in MC number, 100% increase in TC number) in other activated glomerular modules is unclear. There could be an activity-dependent effect, where glomerular modules that are activated more by methyl salicylate than the M72 glomerular module experience a greater increase in MC and TC number.

There is also significant variability in glomerular development based on OR identity. Glomerular volume, OSN number, variability in glomerulus position, timeline of glomerular coalescence, and fidelity of convergence into 2 glomeruli per OB (or lack of supernumerary glomeruli) all vary depending on OR identity (Strotmann et al., 2000; Feinstein and Mombaerts, 2004; Oka et al., 2006; Bressel et al., 2015). As a result, non-M72 glomerular modules may experience odor-exposure dependent changes of different magnitudes than we observed. However, we observe that MCs broadly across the dorsal OB demonstrate a remarkable non-odor specific increase in MC activity following odorant exposure. Thus, it is likely that more than just the M72 glomerular module are affected by this conditioning paradigm.

We may be able to assess this question by analyzing identified glomeruli with overlapping ligand sets. The M71 OR has been well-described previously and is often used to contrast with studies on the M72 OR. Both ORs are encoded in the *Olfr7* cluster on chromosome 9, have 298 of 209 amino acids in common, and correspond to dorsally located glomeruli located within 500 μm of one another on the dorsolateral OB (Feinstein and Mombaerts, 2004). An additional benefit is that there are mouse lines in which M71 or M72 OSNs also express GFP. Zhang et al., 2012 found that there are a set of odorant ligands that activate both the M71 and the M72 glomeruli and characterized the relative activation of both glomeruli by each odorant. These previous findings allow us to use the experimental paradigm described in Chapter 2 to examine whether odorant exposure elicits glomerular module changes that are correlated with initial

activation level of the target glomerulus, specifically comparing anatomical changes of the M71 and M72 glomerular modules.

4.3.2 The role of a single glomerulus

The role of a single glomerulus in odor representation is not well described. Each glomerulus functions as a unit in response to odor stimulation – while there may be variation in the amount of elicited response throughout a single glomerulus, there are no odor or concentration dependent changes to this intraglomerular variation (Wachowiak et al., 2004). Each odorant activates multiple glomeruli, and each odorants activates distinct patterns of glomeruli across the OB (Malnic et al., 1999). Perception of and discrimination between odorants thus depends on the ability to resolve different patterns of glomerular activation, including differences in activated glomerular number, identity, and amplitude (Wachowiak and Cohen, 2001; Leon and Johnson, 2003). Mice can discriminate between different enantiomers - the glomerular representations of enantiomers overlap but also differ in both the identity of glomeruli and the level of activation of each glomerulus (Rubin and Katz, 2001). These data suggest that altering the activity of a few glomeruli is sufficient to drive a change in odorant perception. However, it is unclear if changing an odorant representation by modulating activity of a single glomerulus is sufficient to change aspects of odorant perception such as odorant identity or intensity. Mice can learn to discriminate between differential activation of a single glomerulus (Smear et al., 2013), which suggests that small changes in the activity of a single glomerulus are sufficient to elicit a detectable response and behavior. Whether discrimination dependent on activity of a single glomerulus is ethologically relevant is unknown.

These findings suggest that activity of a single glomerulus provides enough detectable information for mice to modulate behavior. We observed that early odorant exposure increases the number of M/TCs connected to an activated glomerulus dramatically – a 40% increase of MCs and a 100% increase of TCs. This significantly increases the number of principal neurons connected to a single glomerulus. Although glomerular volume has been known to change dynamically due to odorant input even in adulthood, those changes are most likely possible because of the continual integration of adult-born OSNs into the circuit. However, M/TCs finalize apical dendrite targeting and pruning by the first postnatal week, indicating that any changes in glomerulus targeting will persist throughout adulthood. Thus, this permanent experience-dependent increase in M/TC number significantly increases the potential output of activated glomeruli to cortical areas such as the piriform cortex.

Sister MCs, MCs whose apical dendrites project to the same glomerulus, receive common sensory input. Sister MCs are highly correlated in odor-evoked changes in firing rate, which increases robustness of glomerular module output (Zhang et al., 2013); however, they experience odor-evoked decorrelation in response phase (Dhawale et al., 2010). These differences may be a result of variability in intrinsic and response properties (Padmanabhan and Urban, 2010; Angelo and Margrie, 2011; Angelo et al., 2012; Burton et al., 2012; Tripathy et al., 2013) or in differences in lateral inhibitory connectivity in the glomerular or granule cell layers (Aungst et al., 2003; Arevian et al., 2008; Kim et al., 2012; Gilra and Bhalla, 2015). Diversity decreases redundancy and neuronal correlation and thus provides additional ways by which more stimulus features can be encoded (Gjorgjieva et al., 2016). Indeed, simulations examining sister MC heterogeneity demonstrate that increased variability allows networks to carry more information. Variability of sister MCs is likely balanced with population size, where variability is more

meaningful to smaller populations to aid accuracy in odor representation but larger populations demonstrate more gains with increased variability in terms of the ability to encode additional information (Padmanabhan and Urban, 2010; Tripathy et al., 2013). We observe 5-10 MCs and 2-8 TCs connected to a single glomerular module depending on odorant exposure, both relatively small populations. The 40% and 100% increase in MCs and TCs, respectively, following odorant exposure may also increase the heterogeneity of sister MCs or TCs connected to activated glomeruli. This may significantly increase the impact of activated glomerular modules on the lateral inhibitory network, and may also improve perceptual decisions, such as odor discrimination (Gschwend et al., 2015). Since odorants are activate combinations of glomeruli, changing the impact of even a single glomerulus may have broad ranging effects through increased OB output, increased diversity of the M/TC population, or changing lateral inhibition of other glomerular modules.

4.3.3 Impact of these changes on lateral inhibition

Lateral inhibition is an important mechanism used to modulate M/TC output (Laurent, 1999; Friedrich and Laurent, 2001). As in other sensory systems, lateral inhibition functions to mediate contrast enhancement and enhance the ability to discriminate between distinct sensory representations. In the OB, M/TCs do not form synapses with one another but rather are functionally coupled through granule and periglomerular cells; this lateral inhibition is critical to components of olfactory processing such as M/TC synchrony, inter-glomerular communication, and odorant discrimination (Price and Powell, 1970; Jahr and Nicoll, 1980; Stopfer et al., 1997; Shepherd et al., 2007; Koulakov and Rinberg, 2011; Lepousez and Lledo, 2013; Nunez-Parra et al., 2013). However, the structure of lateral inhibition in the OB is not analogous to the classical

center-surround model observed in other sensory systems. Rather, anatomical evidence suggests that each M/TC connects sparsely with columns of GCs broadly across the OB (Willhite et al., 2006). The spatially distributed lateral inhibitory network allows for interglomerular inhibition across a broad spatial range, not limited to impacting only neighboring glomeruli in a classical center-surround network (Cleland and Sethupathy, 2006; Arevian et al., 2008; Kim et al., 2012). This feature of the lateral inhibitory network reflects the lack of simple chemotopy in the OB. Since odorants activate spatially dispersed sets of glomeruli (Davison and Katz, 2007), center-surround inhibition as observed in the visual system is less relevant – extended distributed lateral inhibitory networks allow for interaction between glomeruli whose receptive fields overlap but are not within close spatial proximity.

We observe that following early odorant exposure using a single odorant, the number of M/TCs associated with an activated glomerulus increases and there is a generalized increase in excitatory odor-evoked MC response number and amplitude. These changes in anatomy and activity may have significant effects on the impact of activated glomeruli on the lateral inhibitory network. Exposure using a different conditioning paradigm demonstrated that early exposure increased the strength of lateral inhibition from a glomerulus activated by the conditioning odorant (Geramita and Urban, 2016). There, authors odorized nursing dams and examined inhibition onto M/TCs in resulting litters. Interestingly, they found that odorant exposure only increased lateral inhibition onto TCs and observed no change in the strength of lateral inhibition onto MCs. These findings contrast with our observations of increased number of both MCs and TCs – one might predict that increasing the numbers of both populations would increase interneuron activation and subsequent inhibition of both MCs and TCs of other glomeruli. In addition, we observe increases in MC excitatory activity following odorant exposure – this

increase in both M/TC number and MC activity could result in increased inhibition of TCs through recruitment of larger populations of GCs. However, it is unclear why MCs do not receive increased inhibition as well. One potential explanation could be that since TCs and MCs form inhibitory connections with distinct GC populations in the OB, odor exposure may differentially affect inhibition onto M/TCs.

4.3.4 Support for two distinct output pathways

In Chapter 2, we find that odorant exposure differentially affects mitral and tufted cell number, with a 40% increase in mitral cell number vs. a 100% increase in tufted cell number following prenatal and early postnatal odorant exposure. Although both cell types provide excitatory output from the OB to a large range of cortical areas, differences in connectivity and activity suggest that MCs and TCs mediate two distinct pathways of information processing. TCs are distributed throughout the superficial external plexiform layer (EPL), receiving inhibitory input from superficial GCs, and project primarily to anterior areas of olfactory cortex (Haberly and Price, 1977; Igarashi et al., 2012; Geramita and Urban, 2017). MCs make up a uniform layer 1-2 cell bodies thick directly below the EPL, with lateral dendrites extending radially and contacting primarily deep GCs (Mori et al., 1983; Orona et al., 1984). MCs project more broadly across olfactory cortical areas, to both anterior and posterior areas, although to regions spatially distinct from regions that TCs project to (Igarashi et al., 2012). Tracing studies demonstrate that tufted cells send more axons to the olfactory tubercle, while mitral cells project more to piriform cortex (Nagayama et al., 2010). These anatomical differences indicate that although sister MCs and TCs receive similar input from the same population of OSNs, they convey information to different olfactory cortical areas and thus may process odorant information in distinct ways.

MCs and TCs in fact do encode olfactory information differently. MCs respond to higher odor concentrations and respond to relatively lower firing rates in comparison to TCs (Nagayama et al., 2004; Igarashi et al., 2012; Kikuta et al., 2013). MCs fire preferentially during the inhalation phase of the sniff cycle, while TCs fire during the exhalation phase, a difference mediated by inhibitory networks that shift MC response (Fukunaga et al., 2012; Geramita and Urban, 2017). These cell populations also exhibit intrinsic differences – TCs are more excitable and receive stronger OSN input than MCs (Gire et al., 2012; Burton and Urban, 2014). These differences in odor-evoked response timing and strength allow MCs and TCs to encode different features of odorant stimuli and modulate behavior. Simulations show that due to differences in lateral inhibitory connections, MCs are likely to aid in discrimination between odorant stimuli at high concentrations, while TCs aid in discrimination between odorants at low concentrations (Geramita et al., 2016).

Our anatomical work suggests that experience differentially modulates glomerular targeting of mitral and tufted cells during development. By increasing the tufted cell population considerably more than the mitral cell population, the resultant absolute numbers of MC and TCs connected to a single glomerulus become more similar. Indeed, we observe that the ratios of TCs to MCs increases significantly following odorant exposure, from 0.43 ± 0.04 to 0.66 ± 0.03. Thus, not only do we observe a general increase in output to both pathways, but the pathways become more similarly consequential as described by absolute number following early experience. Interestingly, early postnatal odorant experience results in increased interglomerular lateral inhibition onto TCs, but not MCs (Geramita et al., 2016), indicating a different modulatory role of experience-dependent inhibition onto tufted cells potentially due to the greater relative increase in TCs. In Chapter 2, we find that odor exposure increases MC

excitatory responses; further work is necessary to understand whether this food-based odor exposure paradigm also changes the excitatory responses of TCs. Given the finding that odor exposure enhances lateral inhibition onto tufted cells, we predict that TCs will exhibit a decrease in excitatory responses and response amplitude.

4.4 IMPLICATIONS FOR BEHAVIOR

Many different types of odorant exposure paradigms change OB anatomy, OB function, and performance on behavior tasks. In our studies, we find that early odorant exposure using a food-based paradigm changes the structure of an activated glomerular module, heightens mitral cell responses across the dorsal OB, and transiently influences food preference as measured by a simple sniffing task. Here, we consider how this early food-based odorant exposure might influence odor behavior, focusing on odor perception, discrimination, and preference.

4.4.1 Perception

The links between perception, molecular identity and physicochemical properties of odorants, and neural representation in the OB are not well understood. Groups have used each of these odorant descriptors to organize and predict neural responses. A rough chemotopy exists across the OB, with select regions of glomeruli activated by odorants with different carbon chain lengths or functional groups (Belluscio and Katz, 2001; Meister and Bonhoeffer, 2001). However, this organization breaks down at the level of the glomerulus – neighboring glomeruli do not possess similar or related odor-evoked tuning curves, suggesting that the OB does not

possess a continuous chemotopy based on basic molecular features (Soucy et al., 2009). Enantiomers, molecules that are identical with the exception of chirality, elicit distinct smells that humans and rodents can clearly discriminate between (Laska and Teubner, 1999; Rubin and Katz, 2001). Enantiomers also produce different but overlapping neural representations in terms of glomerular activation maps in the OB. This suggests that molecular formula, either based on carbon chain length or functional group, is not sufficient to describe or predict activation patterns. More complex descriptors of odorant space may be more effective, as the Sobel group used over 1600 physicochemical descriptors of odorants to describe odorant stimulus space and predict neural representations with much better success than methods using simpler molecular descriptors (Haddad et al., 2008).

In addition to physicochemical descriptors (Haddad et al., 2008), odorants can be characterized and organized by elicited perception. Indeed, several groups have created methods by which to predict and organize odorants using data from human perception studies, which examine subject reported data to create descriptors and predictions of perception (Bushdid et al., 2014; Keller and Vosshall, 2016; Keller et al., 2017). Perception is difficult to describe because of its qualitative nature, but general categories of descriptive language have been established. Odorants can be categorized using descriptors such as “sweet” or “flowery” and can also be described based on intensity and hedonic value (Keller and Vosshall, 2016). Specific molecular characteristics have been linked with perceptual qualities. For example, molecules with sulfur atoms tend to smell unpleasant (Keller and Vosshall, 2016).

Odorant concentration and molecular structure may play a role in determining the hedonic valence of odorants. Perceived pleasantness is correlated with molecular complexity and size and may be able to be predicted based on physicochemical properties (Khan et al., 2007;

Zarzo, 2011; Keller et al., 2017). Specific odorant molecules elicit very different odor perceptions at different concentration levels – a study on human odorant perception found that certain odorants were quite pleasant at low concentrations but quickly became noxious at high concentrations (Doty, 1975). They found that reported odor intensity correlated with actual odor concentration, but there was significant variability between test odorants in the relationship between intensity and pleasantness. That is, humans, in this case, college students, can assess relative odor intensity reliably regardless of odor identity. Quality of odorant is not correlated as neatly with odor intensity but rather depends on the odorant in question. Increases in concentration increases glomerular response, both in amplitude of single glomerular response as well as number of OSNs and glomeruli activated (Sato et al., 1994; Johnson and Leon, 2000; Wachowiak et al., 2004). Thus, changing concentration of an odorant stimulus changes the OB glomerular representation of the odorant as well as the perception, indicating that perhaps ordering glomerular activation patterns based on perception may lead to a better understanding of how to organize olfactory stimulus space. Establishing methods by which to predict perceptual qualities of odorants and link these to physiochemical descriptors and neural representation in the OB would provide the field with important tools by which to study how circuit-level mechanisms like glomerular activation give rise to olfactory perception.

Our results in both Chapters 2 and 3 have interesting potential implications on perception. Perception is ultimately determined by the glomerular activation pattern that results from an odorant stimulus, yet the exact same odorant can elicit numerous different perceptions in qualitative description, perceived intensity, and hedonic valence depending on stimulus concentration (Doty, 1975; Khan et al., 2007; Haddad et al., 2008; Sela and Sobel, 2010; Keller et al., 2017). This suggests that changing excitability or responsiveness of the neural circuits that

represent odorants may be sufficient to change perception. We find that food-based odorant exposure increases the number of output neurons from activated glomeruli and produces a generalized heightening of odor-evoked mitral cell responses. These changes may serve to modulate perception or improve the capacity of the OB to detect the exposed odorant.

It is not clear if the changes we observe are specific to glomerular modules activated by the odorant used for early exposure. However, our data show relatively wide-spread changes in activity across the dorsal OB, which has the potential to affect perception of a wide range of dorsally activating odorants, potentially in a manner similar to that observed when increasing odorant concentration, a manipulation that also results in increased numbers of odor-evoked mitral cell responses via an increased number of activated glomeruli (Johnson and Leon, 2000). Because of the odorant-dependent link between pleasantness and increased odorant intensity, in this case we would predict that odorant exposure would increase the perceived pleasantness of the exposure odorant, as measured by odorant preference tests. Unfortunately, while we observe exposed mice spending more time sniffing and exploring odorized food, the exact perceptual changes experienced by mice are impossible to assess. From the experience of humans and discussion by Khan et al., 2007, many foods have noxious odors, the hedonic valence of which changes following a positive dining experience, suggesting that familiarity and association with a positive reinforcing stimulus has the capacity to change elements of perception. While the ethological relevance of hexanal and methyl salicylate to mice is unknown (the two odorants used for odorant exposure in Chapters 2 and 3), a similar perceptual change mediated by associative experience may be reflected in the changes in odor-evoked MC responses.

4.4.2 Odor discrimination

Discrimination depends on the ability to resolve distinct patterns of glomerular activation. Mice are remarkably capable at detecting small differences in glomerular activation patterns (Rubin and Katz, 2001) and are even able to detect amplitude differences in the optogenetic activation of a single glomerulus (Smear et al., 2013). However, the latter discrimination task becomes much more difficult during presentation of background odorants that are also ligands for the targeted glomerulus (Smear et al., 2013). However, presentation of background odorants that were not ligands for the targeted glomerulus did not disrupt detection of amplitude differences within the single glomerulus, indicating that mice can focus on a single glomerulus and identify differences in neural representation at a very fine level. Interestingly, large manipulations do not always impair odor detection or discrimination tasks. Up to 79% of the rat OB can be lesioned before changing error rates on these types of tasks (Lu and Slotnick, 1998). However, changing OR expression such that 95% of OSNs express a single OR impairs performance on some discrimination tasks, while preserving detection (Fleischmann et al., 2008). These monoclonal mice, which express the M71 OR on 95% of OSNs, cannot detect acetophenone, a strong M71 ligand, but can detect odorants presented on a background of acetophenone. Acetophenone activates the majority of glomeruli in the monoclonal mouse, yet the slight changes in glomerular activation evoked by an additional odorant are sufficient for perception. These studies suggest that mice can use minimal changes in sensory input to guide perceptual decisions, which is further supported by the finding that mice can clearly use sensory input from a single glomerulus to drive behavior (Smear et al., 2013).

Increasing the number of M/TCs connected to activated glomeruli may serve to strengthen output of those glomeruli and thus significantly changing the role of affected

glomeruli in odorant representation. This increase may also mediate increased interglomerular lateral inhibition, thus increasing contrast in odor representation (Abraham et al., 2010; Nunes and Kuner, 2015; Geramita and Urban, 2016) and providing meaningful improvements in discriminations involving affected glomeruli. The additional M/TCs may also increase heterogeneity of sister M/TC populations, thus providing increased capacity to encode information for affected glomerular modules. Decorrelation is important for odor discrimination learning (Gschwend et al., 2015) – thus, early odorant exposure could also mediate improved performance at odor discrimination for exposed odorants through an increase in M/TC decorrelation via increased sister M/TC diversity and number.

In Chapter 3, we observe that early odorant exposure causes a generalized increase in excitatory MC responses, a finding seemingly at odds with Chapter 2, where we find an activation-specific increase in M/TC number associated with single glomeruli. The mechanisms behind this non-specific increase in MC activity are unclear, but may reflect either the context of odorant exposure or a generalized change due to environmental enrichment. Early postnatal odorant exposure using a non-food based paradigm increases lateral inhibition onto TCs but not MCs, a finding which may help explain why we do not observe decreased MC excitatory activity following odorant exposure. It is unclear if this type of generalized increase in MC responses will impact odorant discrimination. It is likely that given the ability of mice to detect and discriminate odorants with only a fraction of the number and diversity of glomeruli in normal OBs, discrimination will not be impaired by a generalized increase in MC activity but rather enhanced. Sensory enrichment increases responsiveness of neurons and sharpens representations of stimuli in auditory, visual, and somatosensory cortical areas (Beaulieu and Cynader, 1990a,

1990b; Coq and Xerri, 1998; Bourgeon et al., 2004; Engineer et al., 2004) – a similar process could be occurring in the OB following sensory enrichment via early odorant exposure.

4.4.3 Odor preference

The odor exposure paradigm used throughout this thesis pairs exposure odorants with food. In Chapter 2 and from Todrank et al., 2011, we find that a behavioral assay to roughly measure food preference is a useful metric by which to assess efficacy of odorant conditioning. Here, we use "preference" to describe an experimental outcome. In our study, we placed mice in a circular chamber with a control food pellet on one side and an odorized food pellet on the other side. We characterized the odorant of the pellet that mice spent more time investigating as the "preferred" odorant. Our definition of preference is thus quite limited, as we do not know if this investigative behavior can be replicated during a choice between pure odorants unassociated with the food mixture. Thus, using this measurement, we are unable to assess the extent of odorant preference, only the presence or absence of a preference for scented or unscented food. A more complex behavioral assay is necessary to study how this odorant exposure paradigm might change perception or preference for pure odorants.

Immediately following odorant exposure with either hexanal or methyl salicylate, mice spend more time investigating food odorized with the scent used for exposure, as measured by sniff time. Associative odor preference can be learned quite early, as demonstrated by numerous studies in rat pups (Gregory and Pfaff, 1971; Johanson and Hall, 1979, 1982; Morrison et al., 2013; Fontaine et al., 2014; Yuan et al., 2014). 1-3 day old neonatal rats can learn to associate previously repulsive odorants with milk stimuli for up to 24 hours, demonstrating that food-based odor preference can be learned very early in life (Johanson and Hall, 1979, 1982).

However, we observe that if odorant exposure is stopped and mice are subsequently fed with control-scented food, mice spend more time investigating control-scented food. This change in behavior demonstrates that the odorant preference measurement most likely reflects a learned association between food and scent – this association is paired with the most recent food stimulus. These changes in food preference accompany anatomical modifications to activated glomerular modules following early food-based odorant exposure. Because food preference reflects the most recent food source, these observed changes in glomerular module anatomy (increases in glomerular volume and M/TC number) are not the sole driving force behind behavioral changes. Rather, circuits outside of the OB may also be important in mediating behavior such as odor preference. Projections from the MOB target diverse cortical areas including anterior piriform cortex, the amygdala, and the olfactory tubercle (Sosulski et al., 2011). These areas have been shown to be important in odor learning, especially in the association of odorants with attractive or aversive behaviors (Morrison et al., 2013). Learned representations of neural activity in the piriform cortex is sufficient to drive aversive or appetitive behavior (Choi et al., 2011). The lateral nucleus of the amygdala is also important in odorant-induced behavior – dopamine mediated circuits increase neural excitability within this region following foot-shock conditioning (Rosenkranz and Grace, 2002). In addition, the olfactory tubercle demonstrates segmented topography relevant to odor valence – odorants associated with positive cues activated the anteromedial OT, while odorants associated with negative cues activated the lateral OT (Murata et al., 2015). The exact mechanisms by which salience and valence are associated with olfactory stimuli are unclear, but attractive and aversive behaviors are likely to be modulated in olfactory areas downstream of the OB. Cortical feedback projections from these higher regions to the OB provide input onto GCs (Laaris et al., 2007) and

thus modulate contextual M/TC activity, such as changes in M/TC firing during task performance (Kay and Laurent, 1999; Rinberg et al., 2006; Fuentes et al., 2008).

4.5 CONCLUSION

As in other sensory systems, the olfactory system is highly responsive to sensory experience during development. Deprivation disrupts normal circuit development and maintenance, while enrichment also modifies anatomy and activity. In this dissertation, we focus on how early odorant exposure modifies the OB. Specifically, we find that early food-based odorant exposure increases the number of M/TCs associated with a single activated glomerular module and causes a widespread increase in the number and amplitude of excitatory odor-evoked responses of MCs across the dorsal OB. We observe that these changes are accompanied by a transient preference for odorized food. These substantial and long-lasting modifications to the OB may significantly modify other networks in the OB, especially impacting the lateral inhibitory network and thus broadly changing odorant representation. While the exact behavioral impacts of these changes are unknown, our results provide insight into potential mechanisms by which sensory experience may modulate olfactory perception and behavior.

BIBLIOGRAPHY

Abraham NM, Egger V, Shimshek DR, Renden R, Fukunaga I, Sprengel R, Seeburg PH, Klugmann M, Margrie TW, Schaefer AT, Kuner T (2010) Synaptic inhibition in the olfactory bulb accelerates odor discrimination in mice. Neuron 65:399–411.

Allison AC, Warwick RT (1949) Quantitative observations on the olfactory system of the rabbit. Brain 72:186–197.

Alwis DS, Rajan R (2013) Environmental enrichment causes a global potentiation of neuronal responses across stimulus complexity and lamina of sensory cortex. Front Cell Neurosci 7:124.

Angelo K, Margrie TW (2011) Population diversity and function of hyperpolarization-activated current in olfactory bulb mitral cells. Sci Rep 1:50.

Angelo K, Rancz EA, Pimentel D, Hundahl C, Hannibal J, Fleischmann A, Pichler B, Margrie TW (2012) A biophysical signature of network affiliation and sensory processing in mitral cells. Nature 488:375–378.

Arevian AC, Kapoor V, Urban NN (2008) Activity-dependent gating of lateral inhibition in the mouse olfactory bulb. Nat Neurosci 11:80–87.

Arneodo EM, Penikis KB, Rabinowitz N, Cichy A, Zhang J, Bozza TC, Rinberg D (2017) Stimulus dependent diversity and sterotypy in the output of an olfactory functional unit. bioRxiv Available at: http://www.biorxiv.org/content/biorxiv/early/2017/05/03/133561.full.pdf [Accessed May 8, 2017].

Arruda D, Publio R, Roque AC (2013) The Periglomerular Cell of the Olfactory Bulb and its Role in Controlling Mitral Cell Spiking: A Computational Model Cymbalyuk G, ed. PLoS ONE 8:e56148.

Astic L, Saucier D, Holley A (1987) Topographical relationships between olfactory receptor cells and glomerular foci in the rat olfactory bulb. Brain Res 424:144–152.

Aungst JL, Heyward PM, Puche AC, Karnup SV, Hayar A, Szabo G, Shipley MT (2003) Centre–surround inhibition among olfactory bulb glomeruli. Nature 426:623–629.

Bailey MS, Puche AC, Shipley MT (1999) Development of the olfactory bulb: Evidence for glia-neuron interactions in glomerular formation. J Comp Neurol 415:423–448.

Baroncelli L, Bonaccorsi J, Milanese M, Bonifacino T, Giribaldi F, Manno I, Cenni MC, Berardi N, Bonanno G, Maffei L, Sale A (2012) Enriched experience and recovery from amblyopia in adult rats: Impact of motor, social and sensory components. Neuropharmacology 62:2388–2397.

Bastien-Dionne P-O, David LS, Parent A, Saghatelyan A (2010) Role of sensory activity on chemospecific populations of interneurons in the adult olfactory bulb. J Comp Neurol 518:1847–1861.

Beaulieu C, Cynader M (1990a) Effect of the richness of the environment on neurons in cat visual cortex. II. Spatial and temporal frequency characteristics. Brain Res Dev Brain Res 53:82–88.

Beaulieu C, Cynader M (1990b) Effect of the richness of the environment on neurons in cat visual cortex. I. Receptive field properties. Brain Res Dev Brain Res 53:71–81.

Belluscio L, Katz LC (2001) Symmetry, Stereotypy, and Topography of Odorant Representations in Mouse Olfactory Bulbs. J Neurosci 21:2113–2122.

Benson TE, Ryugo DK, Hinds JW (1984) Effects of sensory deprivation on the developing mouse olfactory system: a light and electron microscopic, morphometric analysis. J Neurosci 4:638–653.

Biju KC, Marks DR, Mast TG, Fadool DA (2008) Deletion of voltage-gated channel affects glomerular refinement and odorant receptor expression in the mouse olfactory system. J Comp Neurol 506:161–179.

Bischofberger J, Jonas P (1997) Action potential propagation into the presynaptic dendrites of rat mitral cells. J Physiol 504:359–365.

Blanchart A, De Carlos JA, López-Mascaraque L (2006) Time frame of mitral cell development in the mice olfactory bulb. J Comp Neurol 496:529–543.

Blauvelt DG, Sato TF, Wienisch M, Murthy VN (2013) Distinct spatiotemporal activity in principal neurons of the mouse olfactory bulb in anesthetized and awake states. Front Neural Circuits 7 Available at: http://www.ncbi.nlm.nih.gov/pmc/articles/PMC3610170/ [Accessed September 18, 2013].

Bonzano S, Bovetti S, Fasolo A, Peretto P, De Marchis S (2014) Odour enrichment increases adult-born dopaminergic neurons in the mouse olfactory bulb. Eur J Neurosci 40:3450–3457.

Bourgeon S, Xerri C, Coq J-O (2004) Abilities in tactile discrimination of textures in adult rats exposed to enriched or impoverished environments. Behav Brain Res 153:217–231.

Bovetti S, Veyrac A, Peretto P, Fasolo A, De Marchis S (2009) Olfactory Enrichment Influences Adult Neurogenesis Modulating GAD67 and Plasticity-Related Molecules Expression in Newborn Cells of the Olfactory Bulb. PLoS ONE 4:e6359.

Boyd AM, Sturgill JF, Poo C, Isaacson JS (2012) Cortical Feedback Control of Olfactory Bulb Circuits. Neuron 76:1161–1174.

Bozza T, Feinstein P, Zheng C, Mombaerts P (2002) Odorant Receptor Expression Defines Functional Units in the Mouse Olfactory System. J Neurosci 22:3033–3043.

Bressel OC, Khan M, Mombaerts P (2015) Linear correlation between the number of olfactory sensory neurons expressing a given mouse odorant receptor gene and the total volume of the corresponding glomeruli in the olfactory bulb. J Comp Neurol:n/a-n/a.

Buck L, Axel R (1991) A novel multigene family may encode odorant receptors: A molecular basis for odor recognition. Cell 65:175–187.

Buonviso N, Chaput M (1999) Olfactory experience decreases responsiveness of the olfactory bulb in the adult rat. Neuroscience 95:325–332.

Burton SD, Ermentrout GB, Urban NN (2012) Intrinsic heterogeneity in oscillatory dynamics limits correlation-induced neural synchronization. J Neurophysiol 108:2115–2133.

Burton SD, LaRocca G, Liu A, Cheetham CEJ, Urban NN (2016) Olfactory bulb deep short-axon cells mediate widespread inhibition of tufted cell apical dendrites. J Neurosci Available at: http://www.jneurosci.org/cgi/doi/10.1523/JNEUROSCI.2880-16.2016 [Accessed January 22, 2017].

Burton SD, Urban NN (2014) Greater excitability and firing irregularity of tufted cells underlies distinct afferent-evoked activity of olfactory bulb mitral and tufted cells: Intrinsic cellular differences drive parallel processing in olfaction. J Physiol 592:2097–2118.

Bushdid C, Magnasco MO, Vosshall LB, Keller A (2014) Humans can Discriminate more than one Trillion Olfactory Stimuli. Science 343:1370.

Caggiano M, Kauer JS, Hunter DD (1994) Globose basal cells are neuronal progenitors in the olfactory epithelium: a lineage analysis using a replication-incompetent retrovirus. Neuron 13:339–352.

Carleton A, Petreanu LT, Lansford R, Alvarez-Buylla A, Lledo P-M (2003) Becoming a new neuron in the adult olfactory bulb. Nat Neurosci 6:507–518.

Cavallin MA, Powell K, Biju KC, Fadool DA (2010) State-Dependent Sculpting of Olfactory Sensory Neurons Attributed to Sensory Enrichment, Odor Deprivation, and Aging. Neurosci Lett 483:90–95.

Chapman B, Gödecke I, Bonhoeffer T (1999) Development of Orientation Preference in the Mammalian Visual Cortex. J Neurobiol 41:18–24.

Chapman B, Stryker MP (1993) Development of orientation selectivity in ferret visual cortex and effects of deprivation. J Neurosci 13:5251–5262.

Chapman B, Stryker MP, Bonhoeffer T (1996) Development of orientation preference maps in ferret primary visual cortex. J Neurosci 16:6443–6453.

Chaudhury D, Manella L, Arellanos A, Escanilla O, Cleland TA, Linster C (2010) Olfactory bulb habituation to odor stimuli. Behav Neurosci 124:490–499.

Chen T-W, Wardill TJ, Sun Y, Pulver SR, Renninger SL, Baohan A, Schreiter ER, Kerr RA, Orger MB, Jayaraman V, Looger LL, Svoboda K, Kim DS (2013) Ultrasensitive fluorescent proteins for imaging neuronal activity. Nature 499:295–300.

Chen WR, Midtgaard J, Shepherd GM (1997) Forward and Backward Propagation of Dendritic Impulses and Their Synaptic Control in Mitral Cells. Science 278:463–467.

Chen WR, Shepherd GM (2005) The olfactory glomerulus: A cortical module with specific functions. J Neurocytol 34:353–360.

Chen WR, Xiong W, Shepherd GM (2000) Analysis of Relations between NMDA Receptors and GABA Release at Olfactory Bulb Reciprocal Synapses. Neuron 25:625–633.

Cho JH, Prince JEA, Cutforth T, Cloutier J-F (2011) The Pattern of Glomerular Map Formation Defines Responsiveness to Aversive Odorants in Mice. J Neurosci 31:7920–7926.

Choi GB, Stettler DD, Kallman BR, Bhaskar ST, Fleischmann A, Axel R (2011) Driving Opposing Behaviors with Ensembles of Piriform Neurons. Cell 146:1004–1015.

Churchland PS, Ramachandran VS, Sejnowski TJ (1994) A critique of pure vision. Large-Scale Neuronal Theor Brain:23–60.

Cleland TA, Sethupathy P (2006) Non-topographical contrast enhancement in the olfactory bulb. BMC Neurosci 7:7.

Coq JO, Xerri C (1998) Environmental enrichment alters organizational features of the forepaw representation in the primary somatosensory cortex of adult rats. Exp Brain Res 121:191–204.

Corotto FS, Henegar JR, Maruniak JA (1994) Odor deprivation leads to reduced neurogenesis and reduced neuronal survival in the olfactory bulb of the adult mouse. Neuroscience 61:739–744.

Daly KC, Christensen TA, Lei H, Smith BH, Hildebrand JG (2004) Learning modulates the ensemble representations for odors in primary olfactory networks. Proc Natl Acad Sci U S A 101:10476–10481.

Davison IG, Katz LC (2007) Sparse and Selective Odor Coding by Mitral/Tufted Neurons in the Main Olfactory Bulb. J Neurosci 27:2091–2101.

De Saint Jan D, Hirnet D, Westbrook GL, Charpak S (2009) External tufted cells drive the output of olfactory bulb glomeruli. J Neurosci Off J Soc Neurosci 29:2043–2052.

Debarbieux F, Audinat E, Charpak S (2003) Action Potential Propagation in Dendrites of Rat Mitral Cells In Vivo. J Neurosci 23:5553–5560.

Decharms RC, Zador A (2000) Neural representation and the cortical code. Annu Rev Neurosci 23:613–647.

Dhawale AK, Hagiwara A, Bhalla US, Murthy VN, Albeanu DF (2010) Non-redundant odor coding by sister mitral cells revealed by light addressable glomeruli in the mouse. Nat Neurosci 13:1404–1412.

Dias BG, Ressler KJ (2014) Parental olfactory experience influences behavior and neural structure in subsequent generations. Nat Neurosci 17:89–96.

Dietz SB, Markopoulos F, Murthy VN (2011) Postnatal development of dendrodendritic inhibition in the Mammalian olfactory bulb. Front Cell Neurosci 5:10.

Doty RL (1975) An examination of relationships between the pleasantness, intensity, and concentration of 10 odorous stimuli. Atten Percept Psychophys 17:492–496.

Doucette W, Restrepo D (2008) Profound context-dependent plasticity of mitral cell responses in olfactory bulb. PLoS Biol 6:e258.

Eerdunfu, Ihara N, Ligao B, Ikegaya Y, Takeuchi H (2017) Differential timing of neurogenesis underlies dorsal-ventral topographic projection of olfactory sensory neurons. Neural Develop 12 Available at: http://neuraldevelopment.biomedcentral.com/articles/10.1186/s13064-017-0079-0 [Accessed March 23, 2017].

Egger V, Svoboda K, Mainen ZF (2003) Mechanisms of Lateral Inhibition in the Olfactory Bulb: Efficiency and Modulation of Spike-Evoked Calcium Influx into Granule Cells. J Neurosci 23:7551–7558.

Egger V, Urban NN (2006) Dynamic connectivity in the mitral cell–granule cell microcircuit. Semin Cell Dev Biol 17:424–432.

Engineer ND, percaccio CR, Pandya PK, Moucha R, Rathbun DL, Kilgard MP (2004) Environmental Enrichment Improves Response Strength, Threshold, Selectivity, and Latency of Auditory Cortex Neurons. J Neurophysiol 92:73–82.

Fadool DA, Levitan IB (1998) Modulation of Olfactory Bulb Neuron Potassium Current by Tyrosine Phosphorylation. J Neurosci 18:6126–6137.

Fadool DA, Tucker K, Perkins R, Fasciani G, Thompson RN, Parsons AD, Overton JM, Koni PA, Flavell RA, Kaczmarek LK (2004) Kv1.3 Channel Gene-Targeted Deletion Produces

"Super-Smeller Mice" with Altered Glomeruli, Interacting Scaffolding Proteins, and Biophysics. Neuron 41:389.

Falk N, Lösl M, Schröder N, Gießl A (2015) Specialized Cilia in Mammalian Sensory Systems. Cells 4:500–519.

Feinstein P, Bozza T, Rodriguez I, Vassalli A, Mombaerts P (2004) Axon guidance of mouse olfactory sensory neurons by odorant receptors and the β2 adrenergic receptor. Cell 117:833–846.

Feinstein P, Mombaerts P (2004) A Contextual Model for Axonal Sorting into Glomeruli in the Mouse Olfactory System. Cell 117:817–831.

Fleischmann A, Shykind BM, Sosulski DL, Franks KM, Glinka ME, Mei DF, Sun Y, Kirkland J, Mendelsohn M, Albers MW, Axel R (2008) Mice with a "Monoclonal Nose": Perturbations in an Olfactory Map Impair Odor Discrimination. Neuron 60:1068–1081.

Fletcher ML (2012) Olfactory aversive conditioning alters olfactory bulb mitral/tufted cell glomerular odor responses. Front Syst Neurosci 6 Available at: http://journal.frontiersin.org/article/10.3389/fnsys.2012.00016/abstract [Accessed November 18, 2016].

Fontaine CJ, Mukherjee B, Morrison GL, Yuan Q (2014) A Lateralized Odor Learning Model in Neonatal Rats for Dissecting Neural Circuitry Underpinning Memory Formation. J Vis Exp JoVE Available at: https://www-ncbi-nlm-nih-gov.pitt.idm.oclc.org/pmc/articles/PMC4827974/ [Accessed May 14, 2017].

Frazier-Cierpial L, Brunjes PC (1989) Early postnatal cellular proliferation and survival in the olfactory bulb and rostral migratory stream of normal and unilaterally odor-deprived rats. J Comp Neurol 289:481–492.

Friedrich RW, Laurent G (2001) Dynamic Optimization of Odor Representations by Slow Temporal Patterning of Mitral Cell Activity. Science 291:889–894.

Fuentes RA, Aguilar MI, Aylwin ML, Maldonado PE (2008) Neuronal Activity of Mitral-Tufted Cells in Awake Rats During Passive and Active Odorant Stimulation. J Neurophysiol 100:422–430.

Fukunaga I, Berning M, Kollo M, Schmaltz A, Schaefer AT (2012) Two Distinct Channels of Olfactory Bulb Output. Neuron 75:320–329.

Galli L, Maffei L (1988) Spontaneous impulse activity of rat retinal ganglion cells in prenatal life. Science 242:90–91.

Geramita M, Urban NN (2016) Postnatal Odor Exposure Increases the Strength of Interglomerular Lateral Inhibition onto Olfactory Bulb Tufted Cells. J Neurosci 36:12321–12327.

Geramita M, Urban NN (2017) Differences in Glomerular-Layer-Mediated Feedforward Inhibition onto Mitral and Tufted Cells Lead to Distinct Modes of Intensity Coding. J Neurosci 37:1428–1438.

Geramita MA, Burton SD, Urban NN (2016) Distinct lateral inhibitory circuits drive parallel processing of sensory information in the mammalian olfactory bulb. Elife 5:e16039.

Gilra A, Bhalla US (2015) Bulbar Microcircuit Model Predicts Connectivity and Roles of Interneurons in Odor Coding. PLoS ONE 10:e0098045.

Gire DH, Franks KM, Zak JD, Tanaka KF, Whitesell JD, Mulligan AA, Hen R, Schoppa NE (2012) Mitral cells in the olfactory bulb are mainly excited through a multistep signaling path. J Neurosci Off J Soc Neurosci 32:2964–2975.

Gjorgjieva J, Drion G, Marder E (2016) Computational Implications of Biophysical Diversity and Multiple Timescales in Neurons and Synapses for Circuit Performance. Curr Opin Neurobiol 37:44.

Gogos JA, Osborne J, Nemes A, Mendelsohn M, Axel R (2000) Genetic ablation and restoration of the olfactory topographic map. Cell 103:609–620.

Gregory EH, Pfaff DW (1971) Development of olfactory-guided behavior in infant rats. Physiol Behav 6:573–576.

Gschwend O, Abraham NM, Lagier S, Begnaud F, Rodriguez I, Carleton A (2015) Neuronal pattern separation in the olfactory bulb improves odor discrimination learning. Nat Neurosci advance online publication Available at: http://www.nature.com/neuro/journal/vaop/ncurrent/full/nn.4089.html [Accessed August 26, 2015].

Gussing F, Bohm S (2004) NQO1 activity in the main and the accessory olfactory systems correlates with the zonal topography of projection maps. Eur J Neurosci 19:2511–2518.

Haberly LB, Price JL (1977) The axonal projection patterns of the mitral and tufted cells of the olfactory bulb in the rat. Brain Res 129:152–157.

Haddad R, Khan R, Takahashi YK, Mori K, Harel D, Sobel N (2008) A metric for odorant comparison. Nat Methods 5:425–429.

Hallem EA, Carlson JR (2006) Coding of Odors by a Receptor Repertoire. Cell 125:143–160.

Hayar A, Karnup S, Ennis M, Shipley MT (2004) External Tufted Cells: A Major Excitatory Element That Coordinates Glomerular Activity. J Neurosci 24:6676–6685.

He J, Tian H, Lee AC, Ma M (2012) Postnatal experience modulates functional properties of mouse olfactory sensory neurons. Eur J Neurosci 36:2452–2460.

Hinds J (1973) Mitral cell development in the mouse olfactory bulb: reorientation of the perikaryon and maturation of the axon initial segment. J Comp Neurol 151:281–305.

Hinds JW, Hinds PL (1976) Synapse formation in the mouse olfactory bulb. II. Morphogenesis. J Comp Neurol 169:41–61.

Hovis KR, Padmanabhan K, Urban NN (2010) A simple method of in vitro electroporation allows visualization, recording, and calcium imaging of local neuronal circuits. J Neurosci Methods 191:1–10.

Hubel DH, Wiesel TN (1970) The period of susceptibility to the physiological effects of unilateral eye closure in kittens. J Physiol 206:419–436.

Igarashi KM, Ieki N, An M, Yamaguchi Y, Nagayama S, Kobayakawa K, Kobayakawa R, Tanifuji M, Sakano H, Chen WR, Mori K (2012) Parallel Mitral and Tufted Cell Pathways Route Distinct Odor Information to Different Targets in the Olfactory Cortex. J Neurosci 32:7970–7985.

Imai T, yamakazi T, Kobayakawa R, Kobayakawa K, Abe T, Suzuki M, Sakano H (2009) Pre-target axon sorting establishes the neural map topography. Science 325:585–590.

Imamura K, Mataga N, Mori K (1992) Coding of odor molecules by mitral/tufted cells in rabbit olfactory bulb. I. Aliphatic compounds. J Neurophysiol 68:1986–2002.

Jahr CE, Nicoll RA (1980) Dendrodendritic inhibition: demonstration with intracellular recording. Science 207:1473–1475.

Jiang Y, Gong NN, Hu XS, Ni MJ, Pasi R, Matsunami H (2015) Molecular profiling of activated olfactory neurons identifies odorant receptors for odors in vivo. Nat Neurosci 18:1446–1454.

Johanson IB, Hall WG (1979) Appetitive learning in 1-day-old rat pups. Science 205:419–421.

Johanson IB, Hall WG (1982) Appetitive conditioning in neonatal rats: Conditioned orientation to a novel odor. Dev Psychobiol 15:379–397.

Johnson BA, Leon M (2000) Modular representations of odorants in the glomerular layer of the rat olfactory bulb and the effects of stimulus concentration. J Comp Neurol 422:496–509.

Johnson BA, Leon M (2007) Chemotopic Odorant Coding in a Mammalian Olfactory System. J Comp Neurol 503:1–34.

Johnson BA, Woo CC, Leon M (1998) Spatial coding of odorant features in the glomerular layer of the rat olfactory bulb. J Comp Neurol 393:457–471.

Johnson MA, Tsai L, Roy DS, Valenzuela DH, Mosley C, Magklara A, Lomvardas S, Liberles SD, Barnea G (2012) Neurons expressing trace amine-associated receptors project to

discrete glomeruli and constitute an olfactory subsystem. Proc Natl Acad Sci 109:13410–13415.

Johnson MC, Biju KC, Hoffman J, Fadool DA (2013) Odor Enrichment Sculpts the Abundance of Olfactory Bulb Mitral Cells. Neurosci Lett 0:173–178.

Kato HK, Chu MW, Isaacson JS, Komiyama T (2012) Dynamic Sensory Representations in the Olfactory Bulb: Modulation by Wakefulness and Experience. Neuron 76:962–975.

Katoh K, Koshimoto H, Tani A, Mori K (1993) Coding of odor molecules by mitral/tufted cells in rabbit olfactory bulb. II. Aromatic compounds. J Neurophysiol 70:2161–2175.

Kay LM, Laurent G (1999) Odor- and context-dependent modulation of mitral cell activity in behaving rats. Nat Neurosci 2:1003–1009.

Ke M-T, Fujimoto S, Imai T (2013) SeeDB: a simple and morphology-preserving optical clearing agent for neuronal circuit reconstruction. Nat Neurosci 16:1154–1161.

Keller A, Gerkin RC, Guan Y, Dhurandhar A, Turu G, Szalai B, Mainland JD, Ihara Y, Yu CW, Wolfinger R, Vens C, Schietgat L, De Grave K, Norel R, DREAM Olfaction Prediction Consortium, Stolovitzky G, Cecchi GA, Vosshall LB, Meyer P (2017) Predicting human olfactory perception from chemical features of odor molecules. Science:eaal2014.

Keller A, Vosshall LB (2016) Olfactory perception of chemically diverse molecules. BMC Neurosci 17 Available at: http://bmcneurosci.biomedcentral.com/articles/10.1186/s12868-016-0287-2 [Accessed April 24, 2017].

Kerr MA, Belluscio L (2006) Olfactory experience accelerates glomerular refinement in the mammalian olfactory bulb. Nat Neurosci 9:484–486.

Khan RM, Luk C-H, Flinker A, Aggarwal A, Lapid H, Haddad R, Sobel N (2007) Predicting Odor Pleasantness from Odorant Structure: Pleasantness as a Reflection of the Physical World. J Neurosci 27:10015–10023.

Kikuta S, Fletcher ML, Homma R, Yamasoba T, Nagayama S (2013) Odorant Response Properties of Individual Neurons in an Olfactory Glomerular Module. Neuron 77:1122–1135.

Kim DH, Chang AY, McTavish TS, Patel HK, Willhite DC (2012) Center-surround vs. distance-independent lateral connectivity in the olfactory bulb. Front Neural Circuits 6:34.

Kim H, Greer CA (2000) The emergence of compartmental organization in olfactory bulb glomeruli during postnatal development. J Comp Neurol 422:297–311.

Ko H, Cossell L, Baragli C, Antolik J, Clopath C, Hofer SB, Mrsic-Flogel TD (2013) The emergence of functional microcircuits in visual cortex. Nature 496:96–100.

Komiyama T, Luo L (2006) Development of wiring specificity in the olfactory system. Curr Opin Neurobiol 16:67–73.

Kondo K, Suzukawa K, Sakamoto T, Watanabe K, Kanaya K, Ushio M, Yamaguchi T, Nibu K-I, Kaga K, Yamasoba T (2010) Age-related changes in cell dynamics of the postnatal mouse olfactory neuroepithelium: Cell proliferation, neuronal differentiation, and cell death. J Comp Neurol 518:1962–1975.

Kosaka K, Hama K, Nagatsu I, Wu J-Y, Ottersen OP, Storm-Mathisen J, Kosaka T (1987) Postnatal development of neurons containing both catecholaminergic and GABAergic traits in the rat main olfactory bulb. Brain Res 403:355–360.

Kosaka T, Kosaka K (2011) "Interneurons" in the olfactory bulb revisited. Neurosci Res 69:93–99.

Koulakov AA, Rinberg D (2011) Sparse incomplete representations: a potential role of olfactory granule cells. Neuron 72:124–136.

Laaris N, Puche A, Ennis M (2007) Complementary Postsynaptic Activity Patterns Elicited in Olfactory Bulb by Stimulation of Mitral/Tufted and Centrifugal Fiber Inputs to Granule Cells. J Neurophysiol 97:296–306.

Laing DG (1985) Prolonged exposure to an odor or deodorized air alters the size of mitral cells in the olfactory bulb. Brain Res 336:81–87.

Laska M, Teubner P (1999) Olfactory discrimination ability of human subjects for ten pairs of enantiomers. Chem Senses 24:161–170.

Laurent G (1999) A Systems Perspective on Early Olfactory Coding. Science 286:723–728.

Leon M, Johnson BA (2003) Olfactory coding in the mammalian olfactory bulb. Brain Res Brain Res Rev 42:23–32.

Lepousez G, Lledo P-M (2013) Odor Discrimination Requires Proper Olfactory Fast Oscillations in Awake Mice. Neuron 80:1010–1024.

Leung CT, Coulombe PA, Reed RR (2007) Contribution of olfactory neural stem cells to tissue maintenance and regeneration. Nat Neurosci 10:720–726.

Liberles SD, Buck LB (2006) A second class of chemosensory receptors in the olfactory epithelium. Nature 442:645–650.

Lin DM, Wang F, Lowe G, Gold GH, Axel R, Ngai J, Brunet L (2000) Formation of precise connections in the olfactory bulb occurs in the absence of odorant-evoked neuronal activity. Neuron 26:69–80.

Liu A, Savya S, Urban NN (2016) Early Odorant Exposure Increases the Number of Mitral and Tufted Cells Associated with a Single Glomerulus. J Neurosci 36:11646–11653.

Liu S, Plachez C, Shao Z, Puche A, Shipley MT (2013) Olfactory Bulb Short Axon Cell Release of GABA and Dopamine Produces a Temporally Biphasic Inhibition-Excitation Response in External Tufted Cells. J Neurosci 33:2916–2926.

Lois C, Alvarez-Buylla A (1994) Long-Distance Neuronal Migration in the Adult Mammalian Brain. Science 264:1145–1148.

Lu X-C, Slotnick BM (1998) Olfaction in rats with extensive lesions of the olfactory bulbs: implications for odor coding. Neuroscience 84:849–866.

Luskin MB (1993) Restricted proliferation and migration of postnatally generated neurons derived from the forebrain subventricular zone. Neuron 11:173–189.

Ma L, Wu Y, Qiu Q, Scheerer H, Moran A, Yu CR (2014) A Developmental Switch of Axon Targeting in the Continuously Regenerating Mouse Olfactory System. Science 344:194–197.

Maher BJ, McGinley MJ, Westbrook GL (2009) Experience-dependent maturation of the glomerular microcircuit. Proc Natl Acad Sci 106:16865–16870.

Malnic B, Hirono J, Sato T, Buck LB (1999) Combinatorial receptor codes for odors. Cell 96:713–723.

Malun D, Brunjes PC (1996) Development of olfactory glomeruli: temporal and spatial interactions between olfactory receptor axons and mitral cells in opossums and rats. J Comp Neurol 368:1–16.

Markopoulos F, Rokni D, Gire DH, Murthy VN (2012) Functional Properties of Cortical Feedback Projections to the Olfactory Bulb. Neuron 76:1175–1188.

Matsutani S, Yamamoto N (2000) Differentiation of mitral cell dendrites in the developing main olfactory bulbs of normal and naris-occluded rats. J Comp Neurol 418:402–410.

McLaughlin T, O'Leary DDM (2005) Molecular Gradients and Development of Retinotopic Maps. Annu Rev Neurosci 28:327–355.

Meisami E, Safari L (1981) A quantitative study of the effects of early unilateral olfactory deprivation on the number and distribution of mitral and tufted cells and of glomeruli in the rat olfactory bulb. Brain Res 221:81–107.

Meister M (2015) On the dimensionality of odor space. eLife 4:e07865.

Meister M, Bonhoeffer T (2001) Tuning and Topography in an Odor Map on the Rat Olfactory Bulb. J Neurosci 21:1351–1360.

Meister M, Wong RO, Baylor DA, Shatz CJ (1991) Synchronous bursts of action potentials in ganglion cells of the developing mammalian retina. Science 252:939–943.

Menco BP (1984) Ciliated and microvillous structures of rat olfactory and nasal respiratory epithelia. A study using ultra-rapid cryo-fixation followed by freeze-substitution or freeze-etching. Cell Tissue Res 235:225–241.

Migliore M, Shepherd GM (2008) Dendritic action potentials connect distributed dendrodendritic microcircuits. J Comput Neurosci 24:207–221.

Miyamichi K, Serizawa S, Kimura HM, Sakano H (2005) Continuous and Overlapping Expression Domains of Odorant Receptor Genes in the Olfactory Epithelium Determine the Dorsal/Ventral Positioning of Glomeruli in the Olfactory Bulb. J Neurosci 25:3586–3592.

Mombaerts P (1996) Targeting olfaction. Curr Opin Neurobiol 6:481–486.

Mombaerts P, Wang F, Dulac C, Chao SK, Nemes A, Mendelsohn M, Edmondson J, Axel R (1996) Visualizing an Olfactory Sensory Map. Cell 87:675–686.

Mori K, Kishi K, Ojima H (1983) Distribution of dendrites of mitral, displaced mitral, tufted, and granule cells in the rabbit olfactory bulb. J Comp Neurol 219:339–355.

Morrison FG, Dias BG, Ressler KJ (2015) Extinction reverses olfactory fear-conditioned increases in neuron number and glomerular size. Proc Natl Acad Sci 112:12846–12851.

Morrison GL, Fontaine CJ, Harley CW, Yuan Q (2013) A role for the anterior piriform cortex in early odor preference learning: evidence for multiple olfactory learning structures in the rat pup. J Neurophysiol 110:141–152.

Moulton DG (1974) Dynamics of Cell Populations in the Olfactory Epithelium. Ann N Y Acad Sci 237:52–61.

Murata K, Kanno M, Ieki N, Mori K, Yamaguchi M (2015) Mapping of Learned Odor-Induced Motivated Behaviors in the Mouse Olfactory Tubercle. J Neurosci 35:10581–10599.

Nagayama S, Enerva A, Fletcher ML, Masurkar AV, Igarashi KM, Mori K, Chen WR (2010) Differential Axonal Projection of Mitral and Tufted Cells in the Mouse Main Olfactory System. Front Neural Circuits 4 Available at: http://www.ncbi.nlm.nih.gov/pmc/articles/PMC2952457/ [Accessed February 26, 2015].

Nagayama S, Takahashi YK, Yoshihara Y, Mori K (2004) Mitral and Tufted Cells Differ in the Decoding Manner of Odor Maps in the Rat Olfactory Bulb. J Neurophysiol 91:2532–2540.

Nagayama S, Zeng S, Xiong W, Fletcher ML, Masurkar AV, Davis DJ, Pieribone VA, Chen WR (2007) In Vivo Simultaneous Tracing and Ca2+ Imaging of Local Neuronal Circuits. Neuron 53:789–803.

Najac M, Diez AS, Kumar A, Benito N, Charpak S, Jan DDS (2015) Intraglomerular Lateral Inhibition Promotes Spike Timing Variability in Principal Neurons of the Olfactory Bulb. J Neurosci 35:4319–4331.

Nunes D, Kuner T (2015) Disinhibition of olfactory bulb granule cells accelerates odour discrimination in mice. Nat Commun 6:8950.

Nunez-Parra A, Maurer RK, Krahe K, Smith RS, Araneda RC (2013) Disruption of centrifugal inhibition to olfactory bulb granule cells impairs olfactory discrimination. Proc Natl Acad Sci 110:14777–14782.

Ogg MC, Bendahamane M, Fletcher ML (2015) Habituation of glomerular responses in the olfactory bulb following prolonged odor stimulation reflects reduced peripheral input. Front Mol Neurosci:53.

Oka Y, Katada S, Omura M, Suwa M, Yoshihara Y, Touhara K (2006) Odorant Receptor Map in the Mouse Olfactory Bulb: In Vivo Sensitivity and Specificity of Receptor-Defined Glomeruli. Neuron 52:857–869.

Orona E, Rainer EC, Scott JW (1984) Dendritic and axonal organization of mitral and tufted cells in the rat olfactory bulb. J Comp Neurol 226:346–356.

Oswald A-M, Urban NN (2012) There and Back Again: The Corticobulbar Loop. Neuron 76:1045–1047.

Padmanabhan K, Osakada F, Tarabrina A, Kizer E, Callaway EM, Gage FH, Sejnowski TJ (2016) Diverse Representations of Olfactory Information in Centrifugal Feedback Projections. J Neurosci 36:7535–7545.

Padmanabhan K, Urban NN (2010) Intrinsic biophysical diversity decorrelates neuronal firing while increasing information content. Nat Neurosci 13:1276–1282.

Palouzier-Paulignan B, Lacroix M-C, Aime P, Baly C, Caillol M, Congar P, Julliard AK, Tucker K, Fadool DA (2012) Olfaction Under Metabolic Influences. Chem Senses 37:769–797.

Panhuber H, Laing DG (1987) The size of mitral cells is altered when rats are exposed to an odor from their day of birth. Dev Brain Res 431:133–140.

Panhuber H, Laing DG, Willcox ME, Eagleson GK, Pittman EA (1985) The distribution of the size and number of mitral cells in the olfactory bulb of the rat. J Anat 140:297–308.

Pinching AJ, Powell TPS (1971) The Neuropil of the Glomeruli of the Olfactory Bulb. J Cell Sci 9:347–377.

Pomeroy SL, LaMantia AS, Purves D (1990) Postnatal construction of neural circuitry in the mouse olfactory bulb. J Neurosci 10:1952–1966.

Potter SM, Zheng C, Koos DS, Feinstein P, Fraser SE, Mombaerts P (2001) Structure and Emergence of Specific Olfactory Glomeruli in the Mouse. J Neurosci 21:9713–9723.

Price JL, Powell TPS (1970) The Mitral and Short Axon Cells of the Olfactory Bulb. J Cell Sci 7:631–651.

Ressler KJ, Sullivan SL, Buck LB (1993) A zonal organization of odorant receptor gene expression in the olfactory epithelium. Cell 73:597–609.

Ressler KJ, Sullivan SL, Buck LB (1994) Information coding in the olfactory system: evidence for a stereotyped and highly organized epitope map in the olfactory bulb. Cell 79:1245–1255.

Richard MB, Taylor SR, Greer CA (2010) Age-induced disruption of selective olfactory bulb synaptic circuits. Proc Natl Acad Sci 107:15613–15618.

Rinberg D, Koulakov A, Gelperin A (2006) Sparse Odor Coding in Awake Behaving Mice. J Neurosci 26:8857–8865.

Rochefort C, Gheusi G, Vincent J-D, Lledo P-M (2002) Enriched odor exposure increases the number of newborn neurons in the adult olfactory bulb and improves odor memory. J Neurosci 22:2679–2689.

Rodríguez FB, Huerta R, Aylwin M de la L (2013) Neural Sensitivity to Odorants in Deprived and Normal Olfactory Bulbs. PLoS ONE 8 Available at: http://www.ncbi.nlm.nih.gov/pmc/articles/PMC3620332/ [Accessed April 6, 2015].

Roland B, Jordan R, Sosulski DL, Diodato A, Fukunaga I, Wickersham I, Franks KM, Schaefer AT, Fleischmann A (2016) Massive normalization of olfactory bulb output in mice with a "monoclonal nose." eLife 5:e16335.

Rosenkranz JA, Grace AA (2002) Dopamine-mediated modulation of odour-evoked amygdala potentials during pavlovian conditioning. Nature 417:282–287.

Rosselli-Austin L, Williams J (1990) Enriched neonatal odor exposure leads to increased numbers of olfactory bulb mitral and granule cells. Dev Brain Res 51:135–137.

Royal SJ, Key B (1999) Development of P2 Olfactory Glomeruli in P2-Internal Ribosome Entry Site-Tau-LacZ Transgenic Mice. J Neurosci 19:9856–9864.

Royet J-P, Distel H, Hudson R, Gervais R (1998) A re-estimation of the number of glomeruli and mitral cells in the olfactory bulb of rabbit. Brain Res 788:35–42.

Rubin BD, Katz LC (2001) Spatial coding of enantiomers in the rat olfactory bulb. Nat Neurosci 4:355–356.

Saghatelyan A, Roux P, Migliore M, Rochefort C, Desmaisons D, Charneau P, Shepherd GM, Lledo P-M (2005) Activity-Dependent Adjustments of the Inhibitory Network in the Olfactory Bulb following Early Postnatal Deprivation. Neuron 46:103–116.

Sato T, Hirono J, Tonoike M, Takebayashi M (1994) Tuning specificities to aliphatic odorants in mouse olfactory receptor neurons and their local distribution. J Neurophysiol 72:2980–2989.

Sawada M, Kaneko N, Inada H, Wake H, Kato Y, Yanagawa Y, Kobayashi K, Nemoto T, Nabekura J, Sawamoto K (2011) Sensory Input Regulates Spatial and Subtype-Specific Patterns of Neuronal Turnover in the Adult Olfactory Bulb. J Neurosci 31:11587–11596.

Schaefer ML, Finger TE, Restrepo D (2001) Variability of position of the P2 glomerulus within a map of the mouse olfactory bulb. J Comp Neurol 436:351–362.

Schwob JE, Jang W, Holbrook EH, Lin B, Herrick DB, Peterson JN, Hewitt Coleman J (2017) Stem and progenitor cells of the mammalian olfactory epithelium: Taking poietic license: Stem and progenitor cells of the Mammalian OE. J Comp Neurol 525:1034–1054.

Sela L, Sobel N (2010) Human olfaction: a constant state of change-blindness. Exp Brain Res Exp Hirnforsch Exp Cerebrale 205:13–29.

Shepherd GM, Chen WR, Willhite D, Migliore M, Greer CA (2007) The olfactory granule cell: From classical enigma to central role in olfactory processing. Brain Res Rev 55:373–382.

Smear M, Resulaj A, Zhang J, Bozza T, Rinberg D (2013) Multiple perceptible signals from a single olfactory glomerulus. Nat Neurosci 16:1687–1691.

Sosulski DL, Lissitsyna MV, Cutforth T, Axel R, Datta SR (2011) Distinct Representations of Olfactory Information in Different Cortical Centers. Nature 472:213–216.

Soucy ER, Albeanu DF, Fantana AL, Murthy VN, Meister M (2009) Precision and diversity in an odor map on the olfactory bulb. Nat Neurosci 12:210–220.

Stettler DD, Axel R (2009) Representations of Odor in the Piriform Cortex. Neuron 63:854–864.

Stopfer M, Bhagavan S, Smith BH, Laurent G (1997) Impaired odour discrimination on desynchronization of odour-encoding neural assemblies. Nature 390:70–74.

Strotmann J, Conzelmann S, Beck A, Feinstein P, Breer H, Mombaerts P (2000) Local Permutations in the Glomerular Array of the Mouse Olfactory Bulb. J Neurosci 20:6927–6938.

Strotmann J, Wanner I, Helfrich T, Beck A, Breer H (1994) Rostro-caudal patterning of receptor-expressing olfactory neurones in the rat nasal cavity. Cell Tissue Res 278:11–20.

Thamke B, Schulz E, Schönheit B (1973) [Neurohistological studies on the olfactory bulb of the adult white laboratory rat (Rattus norvegicus, forma alba)]. J Für Hirnforsch 14:435–449.

Todrank J, Heth G, Restrepo D (2011) Effects of in utero odorant exposure on neuroanatomical development of the olfactory bulb and odour preferences. Proc R Soc B Biol Sci 278:1949–1955.

Treloar HB, Feinstein P, Mombaerts P, Greer CA (2002) Specificity of Glomerular Targeting by Olfactory Sensory Axons. J Neurosci 22:2469–2477.

Tripathy SJ, Padmanabhan K, Gerkin RC, Urban NN (2013) Intermediate intrinsic diversity enhances neural population coding. Proc Natl Acad Sci 110:8248–8253.

Tsai L, Barnea G (2014) A critical period defined by axon-targeting mechanisms in the murine olfactory bulb. Science 344:197.

Urban NN (2002) Lateral inhibition in the olfactory bulb and in olfaction. Physiol Behav 77:607–612.

Urban NN, Sakmann B (2002) Reciprocal intraglomerular excitation and intra- and interglomerular lateral inhibition between mouse olfactory bulb mitral cells. J Physiol 542:355–367.

Valle-Leija P, Blanco-Hernández E, Drucker-Colín R, Gutiérrez-Ospina G, Vidaltamayo R (2012) Supernumerary Formation of Olfactory Glomeruli Induced by Chronic Odorant Exposure: A Constructivist Expression of Neural Plasticity. PLoS ONE 7:e35358.

Vassar R, Chao SK, Sitcheran R, Nun˜ez JM, Vosshall LB, Axel R (1994) Topographic organization of sensory projections to the olfactory bulb. Cell 79:981–991.

Vassar R, Ngai J, Axel R (1993) Spatial segregation of odorant receptor expression in the mammalian olfactory epithelium. Cell 74:309–318.

Wachowiak M, Cohen LB (2001) Representation of Odorants by Receptor Neuron Input to the Mouse Olfactory Bulb. Neuron 32:723–735.

Wachowiak M, Cohen LB (2003) Correspondence Between Odorant-Evoked Patterns of Receptor Neuron Input and Intrinsic Optical Signals in the Mouse Olfactory Bulb. J Neurophysiol 89:1623–1639.

Wachowiak M, Denk W, Friedrich RW (2004) Functional organization of sensory input to the olfactory bulb glomerulus analyzed by two-photon calcium imaging. Proc Natl Acad Sci U S A 101:9097–9102.

Wachowiak M, Economo MN, Díaz-Quesada M, Brunert D, Wesson DW, White JA, Rothermel M (2013) Optical Dissection of Odor Information Processing In Vivo Using GCaMPs Expressed in Specified Cell Types of the Olfactory Bulb. J Neurosci 33:5285–5300.

Wang F, Nemes A, Mendelsohn M, Axel R (1998) Odorant Receptors Govern the Formation of a Precise Topographic Map. Cell 93:47–60.

Wiesel TN, Hubel DH (1963) Single-Cell Responses in Striate Cortex of Kittens Deprived of Vision in One Eye. J Neurophysiol 26:1003–1017.

Willhite DC, Nguyen KT, Masurkar AV, Greer CA, Shepherd GM, Chen WR (2006) Viral tracing identifies distributed columnar organization in the olfactory bulb. Proc Natl Acad Sci 103:12592–12597.

Wilson DA, Rennaker RL (2010) Cortical Activity Evoked by Odors. In: The Neurobiology of Olfaction (Menini A, ed) Frontiers in Neuroscience. Boca Raton (FL): CRC Press. Available at: http://www.ncbi.nlm.nih.gov/books/NBK55970/ [Accessed April 7, 2015].

Wilson DA, Sullivan RM, Leon M (1985) Odor familiarity alters mitral cell response in the olfactory bulb of neonatal rats. Brain Res 354:314–317.

Wilson DA, Sullivan RM, Leon M (1987) Single-unit analysis of postnatal olfactory learning: modified olfactory bulb output response patterns to learned attractive odors. J Neurosci 7:3154–3162.

Wong ROL, Meister M, Shatz CJ (1993) Transient period of correlated bursting activity during development of the mammalian retina. Neuron 11:923–938.

Woo CC, Coopersmith R, Leon M (1987) Localized changes in olfactory bulb morphology associated with early olfactory learning. J Comp Neurol 263:113–125.

Woo CC, Hingco EE, Taylor GE, Leon M (2006) Exposure to a broad range of odorants decreases cell mortality in the olfactory bulb. Neuroreport 17:817.

Xie SY, Feinstein P, Mombaerts P (2000) Characterization of a cluster comprising ~100 odorant receptor genes in mouse. Mamm Genome 11:1070–1078.

Xiong W, Chen WR (2002) Dynamic Gating of Spike Propagation in the Mitral Cell Lateral Dendrites. Neuron 34:115–126.

Yamaguchi M, Mori K (2005) Critical period for sensory experience-dependent survival of newly generated granule cells in the adult mouse olfactory bulb. Proc Natl Acad Sci U S A 102:9697.

Yoshihara Y, Kawasaki M, Tamada A, Fujita H, Hayashi H, Kagamiyama H, Mori K (1997) OCAM: a new member of the neural cell adhesion molecule family related to zone-to-zone projection of olfactory and vomeronasal axons. J Neurosci 17:5830–5842.

Yu CR, Power J, Barnea G, O'Donnell S, Brown HE, Osborne J, Axel R, Gogos JA (2004) Spontaneous neural activity is required for the establishment and maintenance of the olfactory sensory map. Neuron 42:553–566.

Yuan Q, Shakhawat AMD, Harley CW (2014) Mechanisms Underlying Early Odor Preference Learning in Rats. In: Progress in Brain Research, pp 115–156. Elsevier. Available at:

http://linkinghub.elsevier.com/retrieve/pii/B978044463350700005X [Accessed May 4, 2017].

Zapiec B, Mombaerts P (2015) Multiplex assessment of the positions of odorant receptor-specific glomeruli in the mouse olfactory bulb by serial two-photon tomography. Proc Natl Acad Sci 112:E5873–E5882.

Zarzo M (2011) Hedonic Judgments of Chemical Compounds Are Correlated with Molecular Size. Sensors 11:3667–3686.

Zhang D, Li Y, Wu S, Rasch MJ (2013) Design principles of the sparse coding network and the role of "sister cells" in the olfactory system of Drosophila. Front Comput Neurosci 7 Available at: http://journal.frontiersin.org/article/10.3389/fncom.2013.00141/abstract [Accessed April 29, 2017].

Zhang J, Huang G, Dewan A, Feinstein P, Bozza T (2012) Uncoupling stimulus specificity and glomerular position in the mouse olfactory system. Mol Cell Neurosci 51:79–88.

Zhao H, Reed RR (2001) X inactivation of the OCNC1 channel gene reveals a role for activity-dependent competition in the olfactory system. Cell 104:651–660.

Zheng C, Feinstein P, Bozza T, Rodriguez I, Mombaerts P (2000) Peripheral Olfactory Projections Are Differentially Affected in Mice Deficient in a Cyclic Nucleotide-Gated Channel Subunit. Neuron 26:81–91.